

Institut für Hydrologie
Albert-Ludwigs-Universität Freiburg

Bernadette Prömse

Tracerhydrological Investigations in a Forest Plot



Diplomarbeit unter der Leitung von
Prof. Dr. M. Weiler
Freiburg, August 2008

Institut für Hydrologie
Albert-Ludwigs-Universität Freiburg

Bernadette Prömse

Tracerhydrological Investigations in a Forest Plot

Referent: Prof. Dr. M. Weiler

Koreferent: Dr. J. Lange

Diplomarbeit unter der Leitung von
Prof. Dr. M. Weiler
Freiburg, August 2008

Contents

List of Figures	iii
List of Figures in the Appendix	vi
List of Tables	vi
List of Abbreviations	vii
 Summary	 ix
Zusammenfassung	xi
1 Introduction	1
1.1 Motivation	1
1.2 State of the Art.....	3
1.2.1 Pesticide Mitigation Systems	3
1.2.2 Interflow and Preferential Flow.....	5
2 Methodology.....	9
2.1 Fluorescent Dye Tracers.....	9
2.1.1 Uranine	9
2.1.2 Sulforhodamine B.....	10
2.1.3 Analysis and Interpretation of Dye Tracing	11
2.2 Salt Tracers	14
2.3 The Herbicide Isoproturon	15
2.4 Estimation of the hydraulic conductivity	16
3 Study Site.....	19
3.1 Climate	23
3.2 Geology	23
3.3 Soil.....	24
3.4 Hydrology.....	28
3.5 Conclusion.....	32
4 Experimental Design	33
4.1 Subsurface Flow Experiment	35
4.2 Wetting front experiment	38
4.3 Multi-Tracer Experiment.....	41

5	Results.....	45
5.1	Subsurface Flow Experiment results.....	45
5.1.1	Profile probe.....	45
5.1.2	Piezometers	46
5.1.3	Discussion	48
5.1.4	Conclusion	50
5.2	Wetting front results.....	51
5.2.1	FDR probes	51
5.2.2	ECH ₂ O probes.....	53
5.2.3	Piezometers	55
5.2.4	Discussion	57
5.2.5	Conclusion	58
5.3	Tracer Experiment Results.....	59
5.3.1	Dye Tracer.....	59
5.3.1.1	Analysis.....	59
5.3.1.2	Breakthrough curves	61
5.3.1.3	Mathematical Modelling using the Dispersion Model.....	65
5.3.1.4	Discussion	66
5.3.2	Isoproturon.....	69
5.3.2.1	Results.....	69
5.3.2.2	Discussion	72
5.3.3	Electric Conductivity, Anions and Cations.....	74
5.3.3.1	Results.....	74
5.3.3.2	Discussion	79
5.3.4	Discussion and Conclusion	81
6	Conclusion and Outlook.....	85
	Bibliography	89
	Appendix.....	99

List of Figures

Figure 1.1: Schematic of a forest buffer system including the runoff components surface flow, subsurface flow and groundwater flow (LOWRANCE 1998).....	4
Figure 1.2: Flow paths for the movement of water through a shallow forest soil (BEVEN & GERMANN 1982, after MOSLEY 1982).....	6
Figure 2.1: Fluorescence intensity vs. pH. U=Uranine, E=Eosin, RB=Rhodamin B, RG=Amidorhodamine G, RWT=Rhodamine WT, P=Pyranine, N=Sodium-Naphtionat (KÄSS 1998).....	10
Figure 2.2: Setup principle of a modern spectrofluorimeter where L = light source, Sf = fixed slit, Sv = movable slit, MA = excitation monochromator, MF = fluorescence monochromator, K = sample cuvette, Pk = photomultiplier, R = reference ray receiver, S = analog exit to recorder, D = digital exit to printer, PC = data processing and storage, A = exit to digital or analog display (KÄSS 1998).....	11
Figure 2.3: Synchroscan for UA and SRB	12
Figure 3.1: Location of Study Site (marked red) (URL2)	19
Figure 3.2: Research watershed (CEMAGREF)	20
Figure 3.3: Left: Location of the forested plot and the artificial wetland in the watershed; Right: Design of the two buffer zones (ARTWET 2008)	20
Figure 3.4: Left: Both systems closed. Right: Both systems open. (Green: inlet forest. Dark blue: inlet wetland) (CEMAGREF).....	21
Figure 3.5: General functioning of the forest plot during the experimental period. Due to low flow conditions only part of the plot was investigated.....	22
Figure 3.6: Temperature and precipitation of Tours-Parcay-Meslay, based on the period 1971-2000 (METEOFRANCE 2008)	23
Figure 3.7: Geological map of research area (BRGM 2008, modified).....	24
Figure 3.8: Left: Soil auger sample. Middle: Clay-with-flints on the field. Right: Soil profile (photo from CEMAGREF).....	25
Figure 3.9: Soil Texture Triangle of the forest soil at different depths.....	26

Figure 3.10: Rainfall, runoff, cumulative rainfall and cumulated runoff during the winter season 2007/2008. The experimental period is marked in the red rectangle (Data by CEMAGREF)	28
Figure 3.11: Double mass curve for the cumulated runoff versus cumulated rainfall during the period 08.09.2007-21.05.2008. The change in slope represents the different drainage stages (Data by CEMAGREF).....	30
Figure 3.12: Rainfall and runoff during the experimental period	31
Figure 4.1: Experiment schedule during the experimental period of 03.03.2008-11.03.2008	33
Figure 4.2: Location of the different measurement devices in the forest plot	34
Figure 4.3: Conceptual model of the expected hydrological conditions of the piezometer experiment.....	35
Figure 4.4: Location of the piezometers during the first experiment.....	36
Figure 4.5: Experimental setup of the piezometers and the dammed up water	37
Figure 4.6: Experimental setup of the piezometers P1, P2 and P3	38
Figure 4.7: Arrangement of the “Theta field” composed of 14 FDR probes.....	39
Figure 4.8: Installation of the FDR probes and one of the two data loggers.	39
Figure 4.9: Arrangement of the three ECH ₂ O profiles with 5 moisture probes each for profile 1 and 2, and 4 probes for profile 3.	40
Figure 4.10: Filter fluorimeter ("Fluo") installed in the outlet ditch of the forest. The automatic sampler "FO" took samples through the little tube fixed in the PVC pipe, where the EC was also recorded (black cable). Low flow conditions obvious.	42
Figure 4.11: Injection of the tracer cocktail.....	43
Figure 5.1: Results of the section probe device	46
Figure 5.2: Electric conductivity in each piezometer recorded by the divers.....	47
Figure 5.3: Water table in the piezometers.	48
Figure 5.4: Soil moisture recorded by the FDR probes	52
Figure 5.5: ArcView image showing the elevation distribution of the experimental plot. Dots represent the FDR probes.....	52
Figure 5.6: Profile 1, soil moisture recorded by the ECH ₂ Os.....	53

Figure 5.7: Profile 2, soil moisture recorded by the ECH ₂ O _s	54
Figure 5.8: ArcView image showing the elevation of the ECH ₂ O devices (red: Profile 1; blue: Profile 2).....	55
Figure 5.9: Electric conductivity (EC) recorded by the divers in the piezometers 1, 2 and 3..	56
Figure 5.10: Water tables recorded by the divers in the piezometers P1, P2 and P3	56
Figure 5.11: ArcView image showing the elevation of the piezometers	57
Figure 5.12: Comparison of synchroscans of unfiltered and filtered samples	60
Figure 5.13: UA and SRB breakthrough curves at “forest outlet” (“FO”).....	62
Figure 5.14: Tracer recovery curves for SRB and UA	62
Figure 5.15: SRB and UA breakthrough curves at “forest middle” (“FM”)	63
Figure 5.16: UA and SRB breakthrough curves compared to the UA and SRB breakthrough curves recorded by the filter fluorimeter (“Fluo”).....	64
Figure 5.17: Correlation between the continuous data (“Fluo data”) and the laboratory results (“PE data”). Storm event excluded.	65
Figure 5.18: Simulated breakthrough curves using the dispersion model.....	66
Figure 5.19: Tracer breakthrough curves (curve A: ideal tracer; curve B: reversible sorption) (LEIBUNDGUT ET AL. unpublished)	68
Figure 5.20: SRB residues in the inlet ditch still on March, 10th prior the storm event.....	69
Figure 5.21: UA, SRB and IPU breakthrough curves at “FO”	71
Figure 5.22: UA, SRB and IPU breakthrough curves at “FM”	71
Figure 5.23: Sorbed concentration versus time observed in batch experiments (WORRALL ET AL. 1997).....	72
Figure 5.24: Electric conductivity at “FM” and “FO”.	74
Figure 5.25: Anion analysis of selected “FO” samples	76
Figure 5.26: Anion analysis of selected “FM” samples.....	76
Figure 5.27: Result of cation analysis of selected FO samples	78
Figure 5.28: Tracer recoveries at “FO”	81
Figure 5.29: Tracer recoveries for “FM”	81

Figure 5.30: Locations forest outlet ("FO") and forest middle ("FM") on March, 10th, after the rainfall event.	84
---	----

List of Figures in the Appendix

Figure A 1: The inlet ditch of the forest plot prior injection and after injection of the tracer cocktail.	99
Figure A 2: Surface flow in the forest plot after the storm event.	100
Figure A 3: Surface flow in the forest plot.	101
Figure A 4: Surface flow on the adjacent field and at the outlet of the forest.	102
Figure A 5: Functioning of the forest plot in July 2008 (CEMAGREF).	102

List of Tables

Table 3.1: Soil analysis of forest sample (data from CEMAGREF)	25
Table 3.2: Saturated hydraulic conductivities at different depths.....	26
Table 4.1: Piezometer locations in m distance from the inlet and the dam	37
Table 5.1: Subsurface velocities based on electric conductivity detection in "PE" and "PH".	49
Table 5.2: Flow velocities. according to the two kf-estimation-methods.....	49
Table 5.3: Velocities of the wetting front at the FDR probes according to their time of first reaction.....	51
Table 5.4: Maximum velocities at Profile 1.....	53
Table 5.5: Maximum velocities at Profile 2.....	54
Table 5.6: Recoveries of dye tracers depending on the runoff data and the experimental period	67
Table 5.7: Recoveries of IPU depending on the runoff data and the experimental period.....	70

List of Abbreviations

API	Antecedent precipitation index
CEC	Cation exchange capacity [cmol/kg]
EC	Electric conductivity [$\mu\text{S}/\text{cm}$]
ET	Evapotranspiration [mm]
“FM”	Automatic sampler station “forest middle”
“FO”	Automatic sampler station “forest outlet”
F _{OC}	Fraction of organic carbon [%]
IHF	Institute of Hydrology, University of Freiburg
IPU	Isoproturon
K _d	Partition constant
k _f	Hydraulic conductivity
K _{OC}	Soil organic carbon coefficient
P	Precipitation [mm]
“P[no.]”	Device [no.]
Q _{in}	runoff measured at the inlet (L/s)
Q _{out}	runoff measured at the outlet (L/s)
R	Recovery rate [%]
R _t	Retardation factor
ΔS	Change in storage [mm]
SRB	Sulforhodamine B
UA	Uranine
WFD	Water Framework Directive

Acknowledgements

I would like to thank the following people:

Prof. Dr. Markus Weiler for making this work possible and Dr. Jens Lange for the supervision of this thesis; Julien Tournebize, Elodie Passeport, and Cédric Chaumont from the Cemagref Antony for all their support during the field experiments and their help and discussions afterwards; Sonja Jankowsky and Tobias Schütz for helping in the field, the precious discussions and important suggestions; Emil Blattmann for his commitment during the experiments and for the support with the measurement devices.

My family for their all-round support as well as their care, and last but not least all my dearest friends for their encouragement, assistance and helpful conversations.

Summary

Many studies have been conducted concerning the pesticide mitigation efficiency of artificial wetlands, grass strips or riparian buffer zones but the focus on hardwood forests is new. In the framework of recent legislative concepts such as the European Water Framework Directive improvements in water quality are required, enforcing the establishment of mitigation systems.

Within the EU project ARTwet, Cemagref Antony monitors two end-of-field buffer zones at Bray, Indre-et-Loire, France. The two buffer zones, an artificial wetland and a forest plot, are located at the outlet of a 42 ha agriculturally used watershed. The heavy soil is classified a Luvisol with high clay contents (26-37%); hence the watershed is drained by an artificial drainage system. The drained water contributes to a main ditch leading to the buffer zones which can be regulated by PVC elbow inlet tubes. The farmer himself is in charge to open them after pesticide application.

In this study tracerhydrological investigations have been carried out in a 1% sloped forest plot (530 m²) during 03.03.2008-11.03.2008. Altogether, three experiments were performed. The first two experiments focussed on runoff processes in the forest plot, especially interflow. Interflow has been reported as an important runoff component transporting chemicals, e.g. the pesticide Isoproturon (NG & CLEGG 1997). It is usually observed at hillslope scale. So far, little literature exists about its velocities.

For the first plot scale experiment, several piezometers were installed and NaCl labelled water was injected in the forest inlet ditch. CTD divers recorded the electric conductivity and the water table in the piezometers. Only two of the piezometers provided evaluable data as their use in clayey soil is difficult. Calculated subsurface flow velocities range about $5 \cdot 10^{-6}$ m/s, whereas hydraulic conductivity estimations via grain size distribution indicate velocities of 10^{-8} m/s, but there is no clear evidence for preferential flow.

In further investigations the use of soil moisture probes and again piezometers spread over 71 m did not lead to better results. High velocities in the order of 10^{-3} - 10^{-2} m/s were assumed to be surface flow. The forest plot was not visited prior the experimental period and it turned out that this site does not suit for interflow observations, unfortunately. There does not exist a distinct interface between humus and clay layer as assumed.

Finally, a multi-tracer approach was conducted using 2 g Uranine, 5 g Sulforhodamine B and 50 g Isoproturon. Besides the dye tracers and the pesticide, 3 kg potassium nitrate was

accidentally injected instead of the conservative tracer bromide. Actually, a conservative tracer should be usually used to complement dye tracer experiments.

Even though peak concentrations of the dyes were already observed 2 hours after injection, calculations lead to low recovery rates which are 33.1% for UA, 39% for SRB and 42.4% for IPU. Additionally, NO_3 , SO_4 , Cl as well as the cations K, Ca, Mg and Na were analyzed. Although the tracer experiment lasted 4 days, there were still amounts of tracer in the forest plot and flushing during a storm event on March, 10th, was observed.

The mean residence time of 6.6 hours calculated by using the 1D-dispersion model is probably too short to allow adsorption processes and uptake by plants or micro organisms. Thus, arrangements should be made to extend the residence time in the forest plot.

Keywords: forest plot, multi-tracer experiment, interflow, pesticide mitigation, piezometer, Isoproturon

Zusammenfassung

Zahlreiche Studien belegen die Pestizidreduzierung durch künstliche Feuchtflächen, Grasstreifen und Uferzonen, wohingegen die Betrachtung von Waldgebieten neu ist. Im Zuge aktueller Gesetzesvorgaben wie der EU Wasserrahmenrichtlinie müssen Verbesserungen in der Wasserqualität vorgenommen werden. Das erfordert auch die Entwicklung von Systemen, die zu einer Verminderung von Schadstoffen führen.

Im Rahmen des EU Projektes ARTwet untersucht Cemagref Antony zwei solcher Systeme in Bray, Indre-et-Loire, Frankreich. Die beiden Pufferzonen, eine künstliche Feuchtfläche und ein Waldstück, befinden sich am Ende eines 42 ha großen landwirtschaftlich genutzten Einzugsgebietes. Der schwere Boden ist mit seinen hohen Tonanteilen (26-37%) als Luvisol zu klassifizieren, weshalb das Gebiet künstlich drainiert wird. Dieses Drainagesystem führt das Wasser in einen Graben, von dem es aus in die Pufferzonen geleitet werden kann. Der Landwirt ist für das Öffnen der PVC Einlassrohre, die die Wasserzufuhr in die Systeme regulieren, nach der Anwendung von Pestiziden verantwortlich.

In dieser Studie wurden tracer-hydrologische Untersuchungen im Zeitraum vom 03.03.2008-11.03.2008 in dem 530 m² großen Waldstück mit 1% Neigung durchgeführt.

Insgesamt wurden drei verschiedene Experimente ausgeführt, wobei sich die ersten beiden vor allem auf die Untersuchung von abflussbildenden Prozessen, insbesondere Interflow, richteten. In der Literatur findet sich Interflow als wichtige Abflusskomponente, die Substanzen wie auch das Pestizid Isoproturon transportieren kann (NG & CLEGG 1997). Obwohl Interflow häufig in der Hangskala beobachtet wird, ist über seine Fließgeschwindigkeiten nur wenig bekannt.

Im ersten Versuch wurden mehrere Piezometerrohre installiert und Salz als Tracer im Waldeinlass eingespeist. CTD Diver in den Rohren zeichneten Leitfähigkeits- und Wasserstandsdaten auf. Nur zwei der Piezometerrohre lieferten auswertbare Daten, da sich ihre Benutzung in tonigen Böden als schwierig erwies. Berechnungen der unterirdischen Fließgeschwindigkeiten ergaben $5 \cdot 10^{-6}$ m/s, wohingegen hydraulische Leitfähigkeitsschätzungen Fließgeschwindigkeiten von 10^{-8} m/s ergaben. Es konnte jedoch nicht eindeutig bewiesen werden, dass präferentielles Fließen der Grund für diese höheren Geschwindigkeiten ist.

Des Weiteren wurden Messgeräte zur Messung der Bodenfeuchte und wiederum Piezometerrohre benutzt, um die gesamte Fließstrecke von 71 m zu untersuchen. Aber auch hier führten die erhobenen Daten nicht zu eindeutigen Ergebnissen. Fließgeschwindigkeiten

von 10^{-3} - 10^{-2} m/s sind dem Oberflächenabfluss zuzuordnen. Das Waldgebiet wurde vor den Experimenten nicht eingehend untersucht und es stellte sich heraus, dass es keinen geeigneten Ort für Interflow Beobachtungen darstellt. Eine eindeutige Grenzfläche zwischen Humus und Tonschicht, auf der Interflow möglich gewesen wäre, konnte nicht festgestellt werden.

Letztlich wurde ein Multi-Tracer-Versuch mit 2 g Uranin, 5 g Sulforhodamin B und 50 g Isoproturon durchgeführt. Anstelle des konservativen Tracers Bromid wurden versehentlich 3 kg Kaliumnitrat eingespeist. Konservative Tracer liefern bei der Anwendung von Fluoreszenztracern wichtige ergänzende Informationen.

Obwohl maximale Konzentrationen bereits 2 Stunden nach Tracereinspeisung am Waldauslass gemessen wurden, ergaben Berechnungen der Rückerhalte nur Werte von 33.1% für UA, 39% für SRB und 42.4% für IPU. Zusätzlich wurden einige Proben neben NO_3 , SO_4 , Cl. auch auf die Kationen K, Ca, Mg und Na hin analysiert. Obwohl der Tracerversuch 4 Tage dauerte, waren immer noch Tracerrückstände im Einlassgraben sichtbar, die erst durch ein Unwetter am 10. März ausgewaschen wurden.

Mit Hilfe des Dispersionsmodells wurde eine mittlere Verweilzeit von 6.6 Stunden berechnet. Hinsichtlich erwünschter Adsorptionsprozesse und Aufnahmemechanismen durch Pflanzen und Mikroorganismen sollten Maßnahmen zur Verlängerung der Verweilzeit vorgenommen werden.

1 Introduction

Pesticides are used all over the world to improve plant growth and agricultural cultivation. This leads to pollution of soil, surface and ground water which involves a serious risk to the environment and also to human health. Therefore, the increase of production and application of chemicals has converted the problem of environmental pollution into national and international issues.

To meet the Water Framework Directive 2000/60/EC improvements in water quality are required. Establishing biological treatment systems resulting in mitigation of pesticides is the objective of the EU-Life project ArtWET (Mitigation of pesticides pollution and phytoremediation in Artificial WETland ecosystems).

As a part of this project, Cemagref Antony (France) runs an experimental field site consisting of two buffer zones at Bray, Indre-et-Loire, France. The two systems, an artificial wetland and a forested plot, are located at the outlet of a 42 ha agricultural catchment where various pesticides are applied each year. Due to soil properties, fields are usually artificially drained in this area and pesticides are found in drainage and surface water.

In order to assess the pesticide mitigation efficiency of the forested plot a multi tracer experiment using NaCl, Uranine, Sulforhodamine B, Nitrate and the pesticide Isoproturon was carried out in March 2008.

1.1 Motivation

As reported by the European Parliament (2008), more than 220,000 tons of pesticides are annually applied over Europe. Therefore, the European Commission calls for guidelines for the application of pesticides and the investigation of mitigation strategies.

The Water Framework Directive (WFD) has been initiated for the European Union to improve water quality. In its “List of Priority Substances” (Annex X) several pesticides including Isoproturon are classified as priority substances. According to the WFD the total concentration of all pesticides in water should not exceed 0.5 µg/L, and 0.1 µg/L for each single pesticide. As reported by SCHULZ (2004) it becomes evident that the established water quality guideline has been exceeded in multiple instances.

ArtWET gives priority to the development of pesticide mitigation systems applicable in the European Union and will provide technical guidance on reducing the risk of pesticide

pollution. Various buffer systems next to agricultural fields have been built or discovered and their research is still in progress. The scientific aim is to understand and assess potential effects under field conditions. Thus, there is a need for further experimental studies conducted in natural surface waters which are affected by normal farming practices (SCHULZ 2004).

Therefore, Cemagref Antony investigates the two end-of-field buffer zones on the experimental site at Bray, Indre-et-Loire, where the forested zone apparently presents an ideal site to study runoff components transporting agricultural pollutants into stream water.

Thus, the objective of this study is to:

- investigate hydrological runoff processes in the forest plot
- determine the pesticide mitigation efficiency of the forested buffer system

The results will be compared to those derived from the adjacent artificial wetland by Cemagref Antony.

Therefore, the experiments during March 2008 at Bray were designed to:

- distinguish between different flow paths, especially regarding interflow on the interface between humus and clay layer and its velocity
- estimate the pesticide retention capacity of the forested plot

Dye tracers have been used for more than a century and turned into a versatile tool in hydrological investigations. For instance, flow connections, flow paths, residence times, hydrodynamic dispersion as well as chemical leaching can be determined with the help of tracers. Although many are commercially available, only few of them are suitable for hydrological investigations. Uranine and Sulforhodamine B have emerged as useful tracers as they are readily detected at low concentrations, simple to quantify and inexpensive (e.g. WGSHS 2003, KÄSS 1998, MON 2004). Thus, they have been chosen for this study to investigate flow paths and their recovery rates and residence times lead to a better understanding of the mitigation efficiency of the forest plot. Additionally, the pesticide Isoproturon has been applied to observe its behaviour in the forested buffer zone, and the salt NaCl was injected as it can be easily detected via electric conductivity. Bromide was supposed to be used as a conservative tracer, but nitrate has been accidentally applied instead. The results will help to improve the functioning of the forest plot regarding pesticide mitigation, the timing and efficiency of pesticide application as leaching into water supplies should be prevented.

1.2 State of the Art

1.2.1 Pesticide Mitigation Systems

Lots of work has been done to understand transportation and mitigation of pesticide input. Pesticide pollution of surface water can appear as point source pollution such as farmyard runoff or non point source pollution resulting from agricultural applications on fields via runoff/erosion or through spray drift (DABROWSKI ET AL. 2005, REICHENBERGER ET AL. 2007, SCHULZ ET AL. 2003, SCHULZ 2004).

Factors influencing the mitigation of pesticides in buffer zones are mainly adsorption on the soil (WAUCHOPE ET AL. 2002) and sedimentation (LOWRANCE 1998). The positive influence of certain vegetation on mitigation (*phytoremediation*) of different pollutant is also studied (e.g. BOULDIN ET AL. 2006, MOORE ET AL. 2006, BURKEN & SCHNOOR 1996) as well as the influence of beneficial micro organisms (e.g. ISSA ET AL. 1997).

Especially artificial wetlands gained attention being an inexpensive and efficient method as treatment systems (e.g. HAMMER 1992, HAARSTAD & BRASKERUD 2005, SUDO ET AL. 2006). Not only constructed wetlands are often described as a risk mitigation strategy and their ecological importance as ecotones between land and water is undisputed (SCHULZ 2004, LOWRANCE 1998). Also other buffer zones such as vegetated ditches (e.g. BOULDIN ET AL. 2004) or vegetated streams (e.g. DABROWSKI ET AL. 2006) as well as vegetated strips among fields, field margins and riparian zones have been investigated (SCHULZ 2004). Even microcosms were established (e.g. BOULDIN ET AL. 2005, FRIESEN-PANKRATZ ET AL. 2003, MCKINLAY & KASPEREK 1999) as a pesticide mitigation possibility, whereas scaling is a problem as their transfer to wetland functioning remains difficult.

Another efficient mitigation possibility are grass buffer strips. ARORA ET AL. (1996) observed the retention of the pesticide Atrazine in a brome grass strip ranging from 11% to 100% depending on the infiltration capacity.

So far, forest plots have not been intensively investigated, but several studies in riparian forest buffers were conducted (LOWRANCE & SHERIDAN 2005, LOWRANCE ET AL. 1997, LOWRANCE ET AL. 1984). Riparian forest buffers act as nutrient filters resulting from biotic processes and their function in detaining sediments and sediment-borne pollutants is reported (LOWRANCE 1998). But very little is known about their effectiveness for the control of pesticide transport (VELLIDIS ET AL. 2002). Herbicide concentrations and loads in surface runoff can be reduced significantly during transit through the riparian buffer system (ANBUMOZHI ET AL. 2005,

VELLIDIS ET AL. 2002). VELLIDIS ET AL. (2002) also observed interactions between surface runoff and shallow groundwater in herbicide transport.

LOWRANCE AND SHERIDAN (2005) compared a grass strip to a managed forest and an unmanaged forest and found out that the largest percentage in reduction of the incoming nutrient load (65%) took place in the grass buffer zone because of large decrease in flow. They recommend the combination of grass buffer and managed forest as an effective system. The effect of a restored forested riparian wetland buffer system was investigated regarding the surface and subsurface transport of nitrogen, phosphorus as well as of herbicides from agricultural production sites with an overall nitrate removal and retention of 78% (VELLIDIS ET AL. 2003)

LOWRANCE (1998) reports guidelines where three-zone riparian forest buffer systems have been established (Figure 1.1). The figure also presents the different runoff components leading to pesticide transport: surface runoff, subsurface flow and ground water flow.

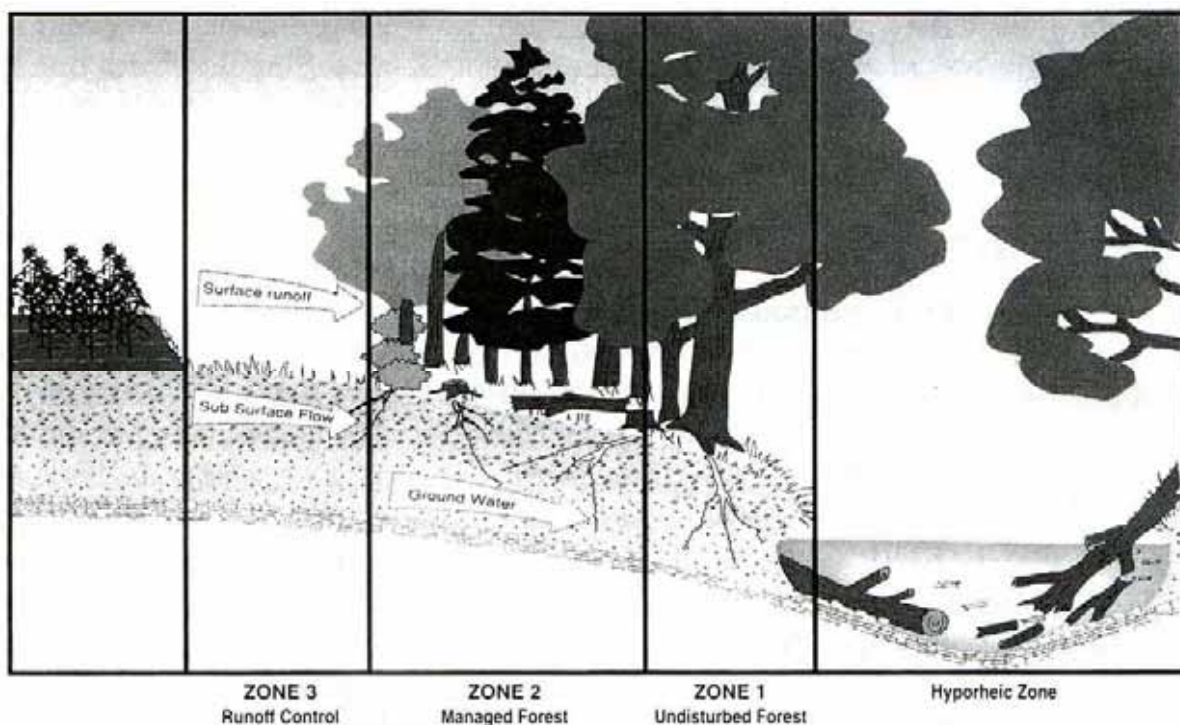


Figure 1.1: Schematic of a forest buffer system including the runoff components surface flow, subsurface flow and groundwater flow (LOWRANCE 1998).

According to SCHULZ (2004) surface runoff due to rainfall events has attracted the most attention regarding edge-of-field losses. Losses are greatest during rainstorms after pesticide application.

Numerous studies try to develop rules of thumb and parameters (e.g. effective wetland length, vegetation) for the construction of buffer zones regarding pesticide mitigation (e.g. ROUSSEAU ET AL. 2004, HAMMER 1992) and designing models is still tried to predict pesticide transport (e.g. ROUSSEAU ET AL. 2004). Some general trends are beginning to emerge, but as prediction remains uncertain site-specific valuations are needed.

Recommendable reviews over numerous studies are given by SCHULZ (2004) and REICHENBERGER ET AL. (2007).

1.2.2 Interflow and Preferential Flow

Water that infiltrates a sloping soil surface and moves as a lateral subsurface flow is called interflow (NG & CLEGG 1997, AHUJA & ROSS 1983, LEHMANN & AHUJA 1985). It can occur in surface horizons of high permeability underlain by horizons of much lower permeability (LEHMANN & AHUJA 1985), e.g. in A soil horizons, agricultural tilled soils or forest litter (FREEZE & CHERRY 1979) and depends on soil slope, leakiness of restricting layers, layer thickness and its hydraulic conductivity as well as the hydraulic conductivity of the underlying base material (LEHMANN & AHUJA 1985, AHUJA & ROSS 1983). Its high potential in transporting chemicals is not new as interflow has been reported as an important runoff component (NG & CLEGG 1997, LEHMANN & AHUJA 1985, LEITE 1985). A common method to determine interflow as a runoff component is observation on excavated soil blocks (DEEKS ET AL. 2008, HORNBERGER ET AL. 1991, LEHMANN & AHUJA 1985).

LEITE (1985) observed the highest interflow volume of 53% of rainfall on an Alfisol slope of Southern Bahia, Brazil, and average 14% of annual rainfall resulting in interflow being an important process in leaching nutrients and fertilizers. LEHMANN & AHUJA (1985) reported that 11.2% of rainfall was interflow on a 6-8% slope.

Also preferential flow has been reported as an important mechanism for the transport of pollutants in deeper soil layers, ground and surface water (DÖRFLER ET AL. 2006, ZEHE & FLÜHLER 2001, RENAUD ET AL. 2004, HARRIS ET AL. 1994). DÖRFLER ET AL. (2006) reported rapid transport of Isoproturon (IPU) and its degradation products due to preferential flow. Preferential flow can be caused by various types of macropores due to bioturbation e.g. of earthworms, shrinkage cracks or fissures (BEVEN & GERMAN 1982).

ZEHE & FLÜHLER (2001) investigated macropores causing the rapid transport of surface applied IPU. Preferential flow occurred in deep penetrating earthworm burrows and resulted in a fast breakthrough of Isoproturon. They concluded that a high affinity for sorption to clay or organic matter would no longer guarantee a low mobility of pesticides in soil and that process models have to be improved by including this transport.

Also FEYEN ET AL. (1999) carried out tracer experiments to study transport through flow paths such as macropores.

Figure 1.2 presents the different flow paths water can take in soil. The main processes are surface flow (1.), interflow (2.), preferential flow (3., 6.) i.e. macropore flow through fissures or cracks, and baseflow (7.).

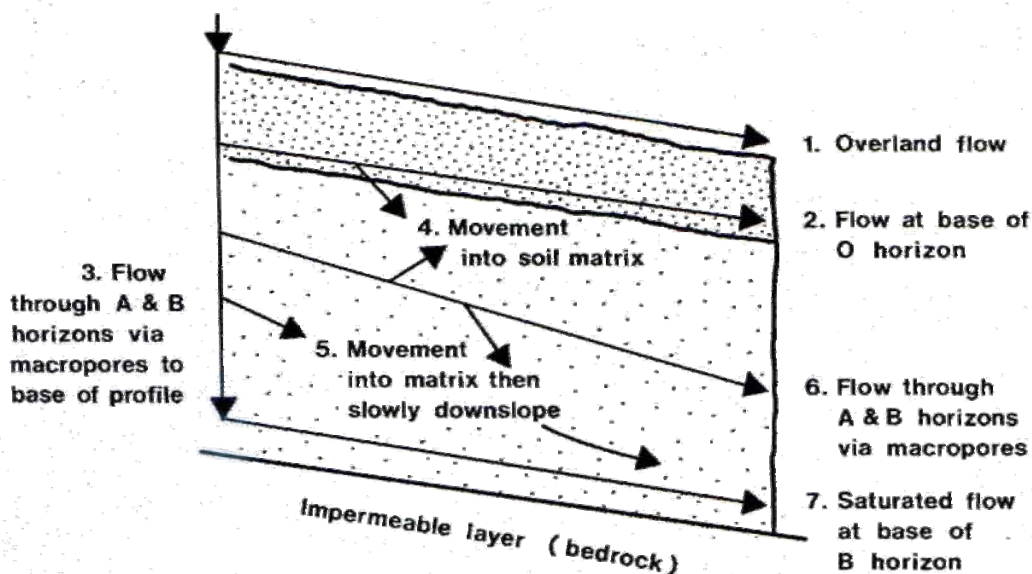


Figure 1.2: Flow paths for the movement of water through a shallow forest soil (BEVEN & GERMANN 1982, after MOSLEY 1982)

Even though some work has been done to observe interflow very little is known about its velocities.

MOSLEY (1982) measured subsurface flow velocities on a steep slope (55-70%) in a shallow soil (1 m) overlying impermeable gravels. The mean velocity of interflow was 0.3 cm/s, (maximum velocity up to 2 cm/s), depending on the antecedent precipitation index (API) and 40% of the input water contributed to subsurface flow. LEHMANN & AHUJA (1985) reported velocities ranging from 0.05 to 0.5 cm/hr on isolated experimental field plots (6-8% slope).

Since the catchment-scale nutrient and pollutant transport is still poorly understood (HYER ET AL. 2001) there is a need to know pathways, rates and sources areas of interflow to control

water pollution (AHUJA & ROSS 1983). Hence there is a prospect for controlling the transport of chemicals in interflow.

2 Methodology

2.1 Fluorescent Dye Tracers

Tracing technique is an important tool for hydrological investigations. There is a wide range of available tracers each with different characteristics, but only few meet the requirements of a hydrogeologic tracer (WGSHS 2003). Dealing with surface and subsurface flow, the applied tracers should fulfil selection criteria such as good water solubility, low adsorption and must be toxicologically harmless.

For these reasons Uranine and Sulforhodamine B were selected as dye tracers in this study. The description of the chosen dye tracers given below follows KÄSS (1998).

2.1.1 Uranine

The fluorescein-anion has the strongest fluorescence properties of all known dye tracers. Its use as a tracer has been known for over a hundred years. The most common applied fluorescein is the sodium fluorescein, also called Uranine.

Uranine ($C_{20}H_{10}Na_2O_5$, abbreviation UA) is highly water soluble (>600 g/L, 20°C) and fluoresces best in solution. Its colour varies depending on concentration between red, yellow-green and green with a maximum of fluorescence at 512 nm.

At concentrations lower than $10\text{ }\mu\text{g/L}$, Uranine is no longer visible, but is still detectable in concentrations as low as $0.002\text{ }\mu\text{g/L}$ with modern spectrofluorimeters.

The intensity of the fluorescence decreases in consequence of its individual light absorption and due to retrograde dissociation at very high concentrations exceeding $10,000\text{ }\mu\text{g/L}$.

The fluorescence intensity is strongly pH-dependent. Uranine has its maximum fluorescence at pH-values over 8.5. At a pH of 7 (neutrality point), the fluorescence intensity is only 80% of the maximum intensity (Figure 2.1). Fluorescence loss is reversible, and high intensities can be restored by alkalinisation.

Uranine is less sorptive and a soil organic carbon sorption coefficient (K_{OC}) of between 69-89 has been reported by LI & ALCANTARA-LICUDINE (1999).

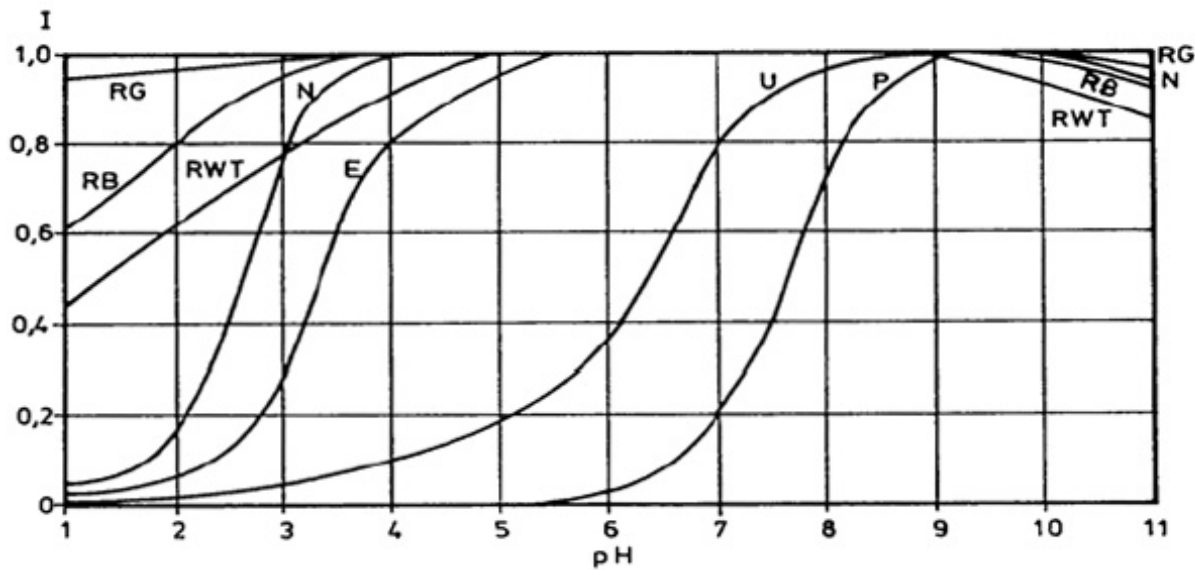


Figure 2.1: Fluorescence intensity vs. pH. U=Uranine, E=Eosin, RB=Rhodamin B, RG=Amidorhodamine G, RWT=Rhodamine WT, P=Pyranine, N=Sodium-Naphtionat (Käss 1998)

Dissolved Uranine is irreversibly destroyed by light. Its half-life depends on concentration, temperature and light intensity and is approximately 11 h under daylight conditions (LEIBUNDGUT ET AL., unpublished). Therefore the use of Uranine for surface experiments is restricted.

Uranine has its fluorescence maximum at 512 nm and its extinction maximum at about 491 nm, depending on pH, the instruments and the spectral sensitivity distribution of the multiplier.

2.1.2 Sulforhodamine B

Sulforhodamine B ($C_{27}H_{29}N_2NaO_7S_2$, abbreviation SRB) is less soluble than Uranine (10 g/L at 20°C). The extinction maximum is at 564 nm and the fluorescence maximum at 583 nm. The fact that these values are different for Uranine allows the use of both tracers in the same experiment.

The detection limit of SRB is about 0.01 µg/L (WERNLI 2003). In general, the rhodamines are not as pH sensitive as other dye tracers, therefore fluorescence has its maximum at pH values between 3.5 and 9.

SRB is not as sensitive to photochemical decay as UA. Its half-life is about 820 h (>34 days), which is 75-times higher than UA. In general, dye tracers with excitation maxima above 500 nm are less photosensitive (LEIBUNDGUT ET AL, unpublished).

Due to adsorption processes the retardation factor R_t (migration distance of substance divided by migration distance of solvent front) is about 1.4 and substrates rich in clay and organic matter increase tracer losses (WGSHS 2003).

2.1.3 Analysis and Interpretation of Dye Tracing

For the quantitative analysis of dye tracers, spectrofluorimeters with two monochromators are used. This is due to the fact that dye tracer concentrations and emission intensities are linearly proportional over a range of several orders of magnitude and their correlation can easily be determined by calibration prior to sampling. The setup principle of a modern spectrofluorimeter is shown in Figure 2.2.

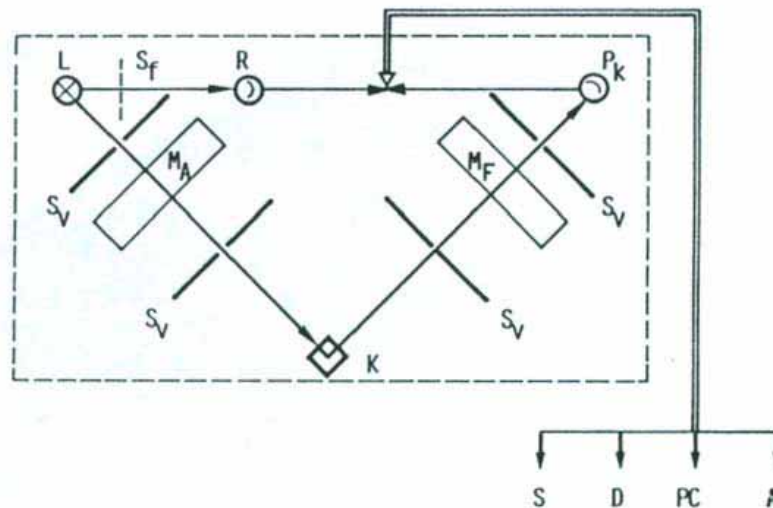


Figure 2.2: Setup principle of a modern spectrofluorimeter where L = light source, S_f = fixed slit, S_v = movable slit, MA = excitation monochromator, MF = fluorescence monochromator, K = sample cuvette, P_k = photomultiplier, R = reference ray receiver, S = analog exit to recorder, D = digital exit to printer, PC = data processing and storage, A = exit to digital or analog display (Käss 1998)

The principle of this measurement technique is that fluorescent substances are excited best by a specific wavelength (excitation wavelength) and emit light at a lower energy level and thus at longer wavelength (fluorescence wavelength).

The advantage of the spectrofluorimeter with two monochromators is that both excitation and fluorescence spectra are recorded and both the excitation and emission wavelength can be selected as well as the speed of the spectral change (nm/min). If the difference ($\Delta\lambda$) between fluorescence and excitation wavelength is kept constant and both monochromators scan

simultaneously, the method is called *synchroscan* (Figure 2.3). This is especially useful when measuring samples containing two different fluorescent dyes simultaneously.

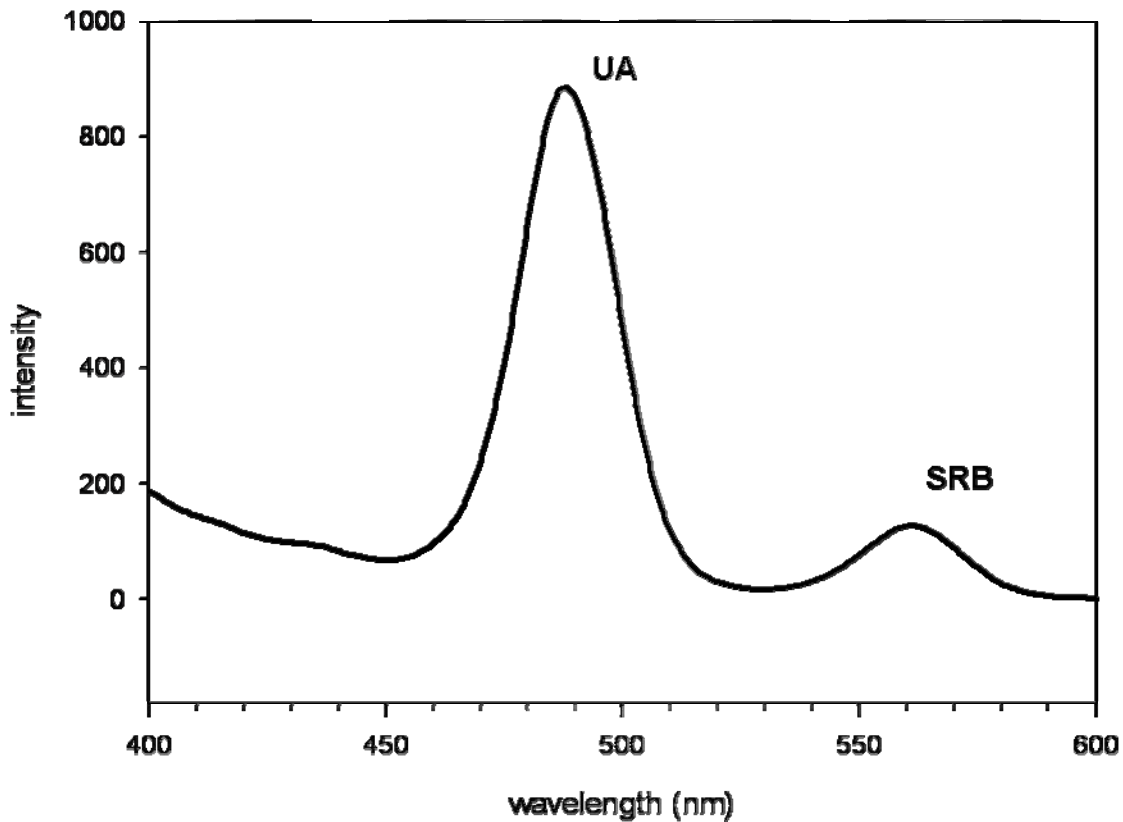


Figure 2.3: Synchroscan for UA and SRB

Therefore, Uranine can be used along with Sulforhodamine B as they do not have the same extinction and fluorescence maxima, but similar values for $\Delta\lambda$ of approximately 25 nm.

In this study, samples have been analyzed for UA and SRB concentrations by a *Perkin Elmer* LS 50 B Luminescence Spectrometer using the described synchroscan method with $\Delta\lambda=25$ nm. This value was determined by preliminary simple emission and excitation scans for each tracer. The fluorescence peaks were observed at 512 nm for UA (excitation wavelength 490 nm,) and 582 nm for SRB (excitation wavelength 553 nm), resulting in $\Delta\lambda$ of 22 nm and 29 nm, respectively.

For interpretation of tracer experiments the breakthrough curve at the monitoring site obtains the basic information.

In order to describe convection as well as longitudinal and transversal dispersion, the movement of water can be expressed by the 3-D transport equation. Under boundary conditions which are valid for column or combined pumping-tracer experiments,

approximations can be made which yield a 1D solution of the transport equation according to MALOSZEWSKI (1994).

In this study the 1-D dispersion model is applicable since tracer concentrations were recorded at only one single location implying no spatial distribution.

MALOSZEWSKI (1994) gives the following solution for the 1-D case:

$$C(x,t) = \frac{M}{Q} \cdot \frac{x}{\sqrt{4\pi D_L t^3}} \exp\left[-\frac{(x-vt)^2}{4D_L t}\right] \quad (2.1)$$

where $C(x,t)$ =tracer concentration at the distance x and at the time t , M =mass of tracer injected, Q =volumetric flow rate, D_L =longitudinal dispersion coefficient, v =velocity.

The mean transit time of water (t_0) is defined by

$$t_0 = \frac{x}{v}. \quad (2.2)$$

For the 1-D case this equals to

$$t_0 = \frac{V}{Q} \quad (2.3)$$

with V being the volume of mobile water. By introducing the dispersion parameter P_D

$$P_D = \frac{D_L}{v \cdot x} \quad (2.4)$$

we obtain

$$C(t) = \frac{M}{Qt_0} \frac{1}{\sqrt{4\pi P_D (t/t_0)^3}} \exp\left[-\frac{(1-t/t_0)^2}{4P_D t/t_0}\right] \quad (2.5)$$

whereas the dispersion parameter P_D and the mean transit time t_0 are the fitting parameters. The dispersion parameter P_D describes the proportion of dispersion (D_L) to convection ($v \cdot x$). At small P_D , convection is the dominant process. Otherwise, dispersion should be considered in modelling approaches.

The application of the 1-D dispersion model requires steady state conditions which were not obtained in this study. Therefore, the variable flow rate Q can be rearranged to

$$C(t) \cdot Q(t) = \frac{M}{t_0} \frac{1}{\sqrt{4\pi P_D (t/t_0)^3}} \exp\left[-\frac{(1-t/t_0)^2}{4P_D t/t_0}\right] \quad (2.6)$$

where the product $C(t) \cdot Q(t)$ describes the mass flux at the time t .

The theoretical tracer recovery R (%) obtained in the outflow from the whole system can be calculated by

$$R = Q \cdot \int_0^{\infty} C(t) dt . \quad (2.7)$$

Rearranging due to unsteady state conditions yields

$$R = \int_0^{\infty} C(t) \cdot Q(t) dt . \quad (2.8)$$

As mentioned above, Uranine is sensitive to photo degradation and if longer-term experiments are carried out one should consider the following term:

$$I(t) = I_0 \cdot e^{(-kt)} \quad (2.9)$$

with $I(t)$ =fluorescence after irradiation time t , I_0 =fluorescence at irradiation time $t=0$, and k =degradation coefficient (LEIBUNDGUT ET AL. unpublished).

Assuming the half-life of Uranine by LEIBUNDGUT ET AL. (unpublished) of 11h yield

$$k = \frac{\ln 2}{T_{1/2}} = 1.75 \cdot 10^{-5} \text{ [1/s]} \quad (2.10)$$

which can be then inserted in (2.9).

2.2 Salt Tracers

Salts belong to the classical tracers and are occasionally used to complement dye tracers. Sodium chloride (NaCl) and potassium bromide (KBr) are commonly used for this purpose.

Usually, the anion of the salt is used as a tracer, whereas the cation is subject to sorption and exchange processes in the subsurface. The exchange capacity of the cation depends on its charge and size. For example, Ca^{2+} and Mg^{2+} are preferentially exchanged. Anions underlie no or negligible exchange and thus remain mobile (KÄSS 1998).

Due to high geogenic and sometimes anthropogenic background values, high injection volumes might be required (WGSHS 2003).

Both NaCl and bromide are highly soluble with a solubility 357 g/l and 850 g/l (at 10°C), respectively.

Detection of NaCl can usually be done by measuring the electric conductivity (EC), where as a rule of thumb 1 mg/l dissolved solids approximately equals to 2 $\mu\text{S/cm}$ (URL1). Additionally, each ion should be measured by ion chromatography. For KBr, the Br^- ion can be measured by using an ion selective electrode.

If concentrations are high, the increase in density can result in salt retention. KÄSS (1998) advises to use no more than 3 g/l of chloride concentration in the injected solution to avoid sinking of the tracer.

2.3 The Herbicide Isoproturon

Isoproturon ($C_{12}H_{18}N_2O$, abbreviation IPU) is classified as a priority substance in the WFD (Annex X).

Among the phenylurea family, IPU acts as a pre-emerge or post-emerge herbicide which is used to control annual grasses and weeds in wheat, barley and rye, whereat the main uptake is via roots (FEURTET-MAZEL ET AL. 1996) resulting in translocation and inhibition of the photosynthetic electron transport.

IPU is classified as *harmful* (Xn) and *dangerous for the environment* (N) as it is toxic to aquatic organisms and may cause long-term adverse effects in the aquatic environment (ESIS 2008).

FEURTET-MAZEL ET AL. (1996) report critical doses of IPU for some non-target species, e.g. aquatic plants. Waterweed (*elodea densa*) shows growth inhibition for IPU concentrations close to 10 µg/l.

The solubility of the herbicide is low, 65 mg/l at 22°C, but it is more mobile than other pesticides (NEMETH-KONDA ET AL. 2002). Its half-life ranges between 6 and 28 days (ERTLI ET AL. 2004).

2.4 Estimation of the hydraulic conductivity

Several approaches have been proposed to predict the saturated hydraulic conductivity using easy to measure soil properties such as grain size distribution.

A good overview of several pedo-transfer-functions, their validity and accuracy is given by TIETJE & HENNINGS (1996). The two main evaluation methods are:

- a) Estimation of the hydraulic conductivity by regression statistics from input variables such as clay, sand, organic matter content and bulk density (e.g. COSBY ET AL. 1984, SAXTON ET AL. 1986).
- b) Derivation of a physico-empirical relationship between grain size distribution and conductivity (e.g. BLOEMEN (1980)).

There exist other methods using a physical concept, but they are no longer accurate once applied to different soils. The estimation accuracy of hydraulic properties can be improved considerably for example by measuring water retention (VAN GENUCHTEN ET AL., 1989), a type of input data not routinely determined by soil surveys. The Hazen method includes the effective grain size as input data, but its applicability is limited to sandy sediments (FETTER 2001).

The soil data available for this study are the grain size distribution and organic matter content, therefore methods by COSBY ET AL. (1984) and SAXTON ET AL. (1986) have been chosen to estimate the hydraulic conductivity (k_f):

COSBY ET AL. (1984):

$$k_f = 60.96 \cdot 10^{(-0.6+0.0126s-0.0064c)} \quad [\text{cm/d}] \quad (2.11)$$

SAXTON ET AL. (1986):

$$k_f = 2.778 \cdot 10^{-6} \cdot \exp \left[12.012 - 7.55 \cdot 10^{-2} \cdot s + \frac{-3.895 + 3.671 \cdot 10^{-2} \cdot s - 0.1103 \cdot c + 8.7546 \cdot 10^{-4} \cdot c^2}{0.332 - 7.251 \cdot 10^{-4} \cdot s + 0.1276 \cdot \log_{10}(c)} \right] \quad [\text{m/s}] \quad (2.12)$$

where s =sand content (%) and c =clay content (%), according to their classification (sand 50-2000 μm , clay <2 μm).

According to TIETJE & HENNINGS (1996), the geometric mean error ratio calculated for the SAXTON ET AL. (1986) method applied on different soils is almost one, but predictions are in general deteriorating with increasing clay content due to possible additional effects (e.g.

shrinking and swelling). Overall, prediction of the saturated hydraulic conductivity using a pedo-transfer function remains rather inaccurate.

3 Study Site

The study site “Bray” is located in the department Indre-et-Loire in France, approximately 63 km south east of the City Tours (Central France) and 25 km east of Loches, and belongs to the community of Villedomain. A general map of France and the rough location of the study site is shown in Figure 3.1. It is situated about 99 m above sea level, latitude $1^{\circ}17'4''$ E and longitude $47^{\circ}3'50''$ N.



Figure 3.1: Location of Study Site (marked red) (URL2)

The catchment covers about 42 ha agricultural area where various pesticides are applied. Crops are mainly cereals, in typical rotation of colza, winter wheat, and barley. Due to the clayey soil, fields in this area are usually artificially drained at 90 cm depth with a 10 m drain spacing (ARTWET 2008).

Figure 3.2 shows that the watershed is draining into a main ditch which contributes to the natural creek “Le Calais”. At the end of this ditch, there are two buffer zones, an artificial

wetland and a forested area (Figure 3.3), which belong to the property of the farmer Bernard Crépin. These buffer zones were studied during the field experiments in March 2008.

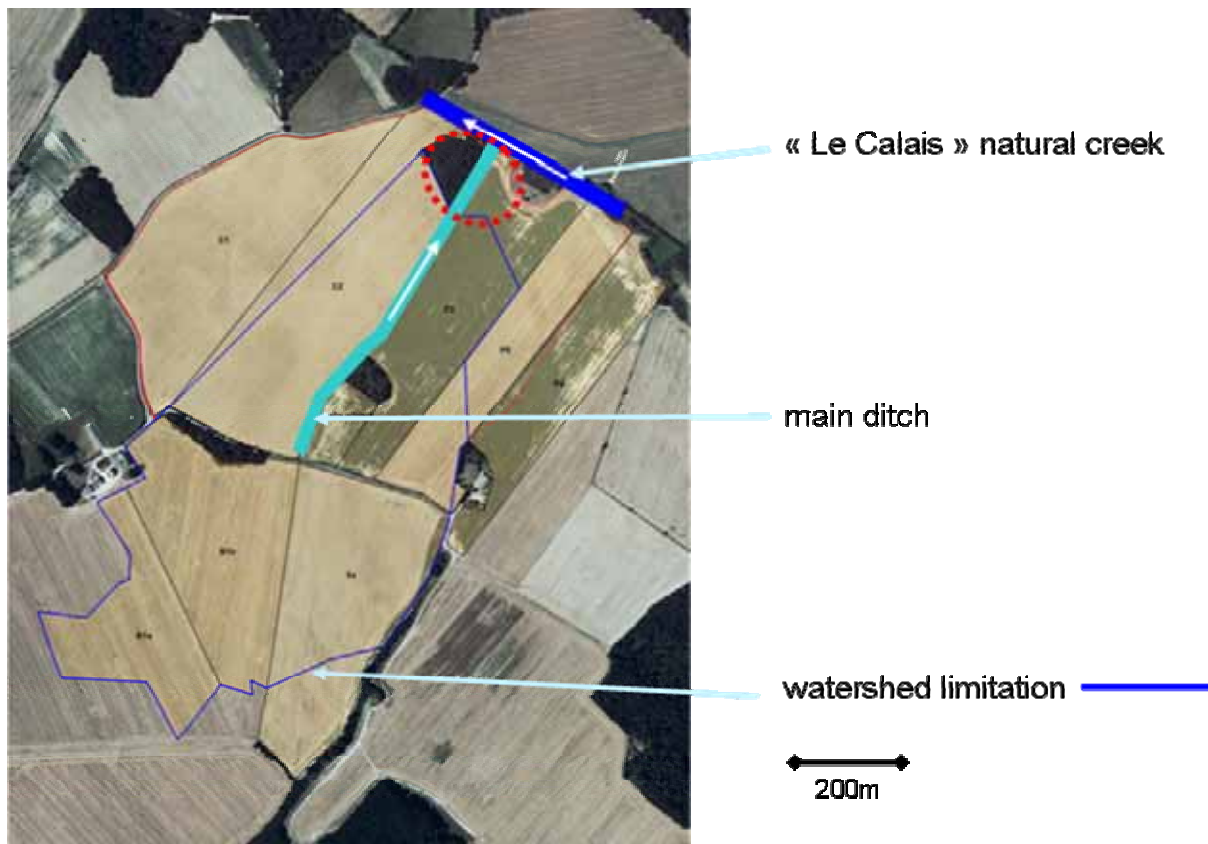


Figure 3.2: Research watershed (CEMAGREF)

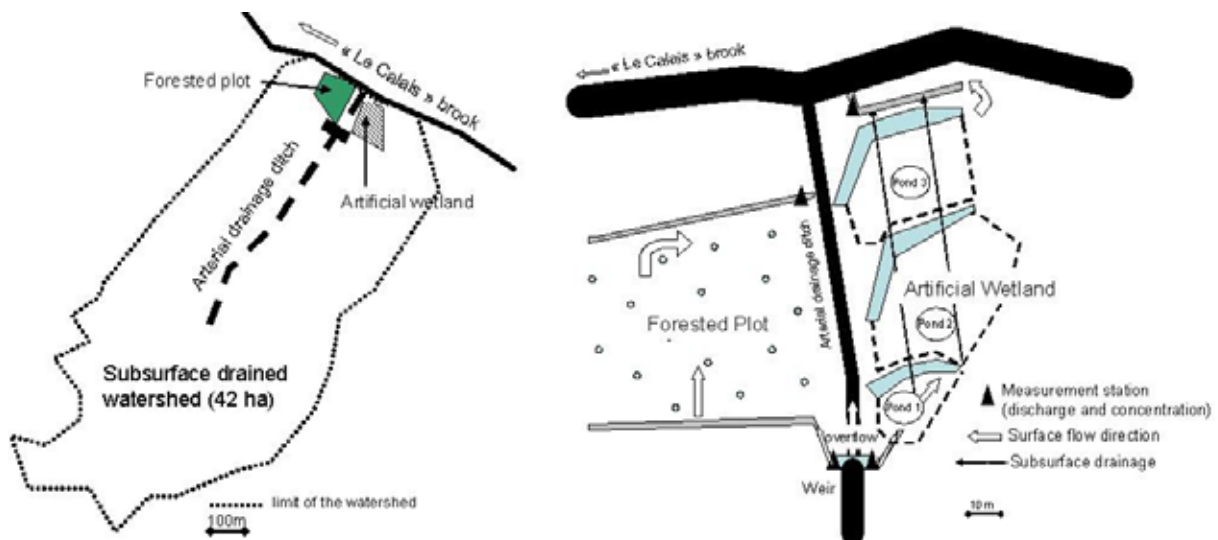


Figure 3.3: Left: Location of the forested plot and the artificial wetland in the watershed; Right: Design of the two buffer zones (ARTWET 2008)

The forest plot contains approximately 1690 m² with a slope of about 1%, covered by common oak (*Quercus robur*). As the experiments were not carried out during the vegetation period, there was almost no soil cover. The application of drainage systems is younger than the forest plot for which reason the forest is not drained even though the whole catchment is drained. The artificial wetland consists of three compartments with a total surface of 1280 m² and it was recently expanded. Therefore, no vegetation could be found in the wetland either. Tracer experiments were carried out in both buffer zones, but the focus of this paper is on the forest plot, only. Therefore, the artificial wetland is not described in this thesis.

The two systems can be regulated by opening/closing of the PVC elbow inlet tubes (Figure 3.4) but not all water can be treated by both systems. Residual water contributes directly to the creek “Le Calais” and its discharge is measured by a V-notch weir in the main ditch using the following formula

$$Q = (1.5 \cdot h^{2.45}) \cdot 1000 \quad [\text{L/s}] \quad (3.1)$$

where h is the height of the water table in the weir expressed in meters.

The farmer applies periodically pesticides and fertilizer which are found in the drainage due to the fast runoff response and the low filter capacity of the soil. He is in charge of opening the inlet tubes after pesticide application. As reported in HARRIS ET AL. (1994), the first drainflow after application is most important for the transport of such substances.

One month prior to application, the buffer zones are closed to be able to revitalize before the next opening. The overall application dates are September until November for the winter crops, February until March for spring cultivation and sometimes also between April and May. The exact dates and amounts of the applied chemicals are known and reported by the farmer.



Figure 3.4: Left: Both systems closed. Right: Both systems open. (Green: inlet forest. Dark blue: inlet wetland) (CEMAGREF)

When the forest inlet tube is open, water from the main ditch enters the forest through another inlet ditch, flows through the forest area and after approximately 71 m into the outlet ditch, which contributes to the main ditch again (Figure 3.5). The tubes can be covered if the water table rises above the inlet tubes.

Cemagref Antony runs the study site and installed several measurement devices in 2006. In the forest plot, the runoff is measured continuously by electromagnetic flowmeters (*MGFLO 8000 DN100/DN200*) at the inlet as well as at the outlet of the plot.

There are further two piezometers where the water level can be detected manually. At the outlet cumulative samples for weekly IPU analysis are usually taken by an automatic sampler. Precipitation is recorded by a tipping bucket rain gauge at the site.

Additional measurement devices which were necessary for the experiments will be described later on.

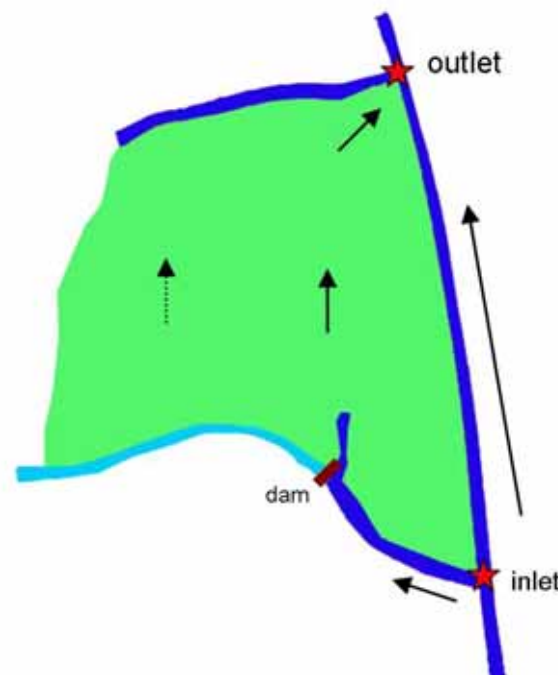


Figure 3.5: General functioning of the forest plot during the experimental period. Due to low flow conditions only part of the plot was investigated

Trenches were recently dug by Cemagref to distribute the water to the forest plot. The design is similar to the functioning of a sewage field. But as clay is nearly impermeable and parts of the forest soil are compacted and without any humus on top, the ditches lead to surface flow.

3.1 Climate

According to the Koeppen classification the climate of the study area is a typical maritime temperate or oceanic climate (*Cfb – uniform precipitation distribution*), which usually occurs on the western sides of continents between the latitudes of 45° and 55°. Therefore summers are temperate and winters are mild, with rain all over the year (Figure 3.6).

METEOFRANCE (2008) gives values of 11.1°C for the annual mean temperature and 650-700 mm/year precipitation for the department Indre et Loire, whereas ARTWET 2008 describes the climate as semi-oceanic with an average annual mean temperature of 12.2°C, total precipitation of 694 mm/year and a potential evapotranspiration of 772 mm/year (ARTWET 2008).

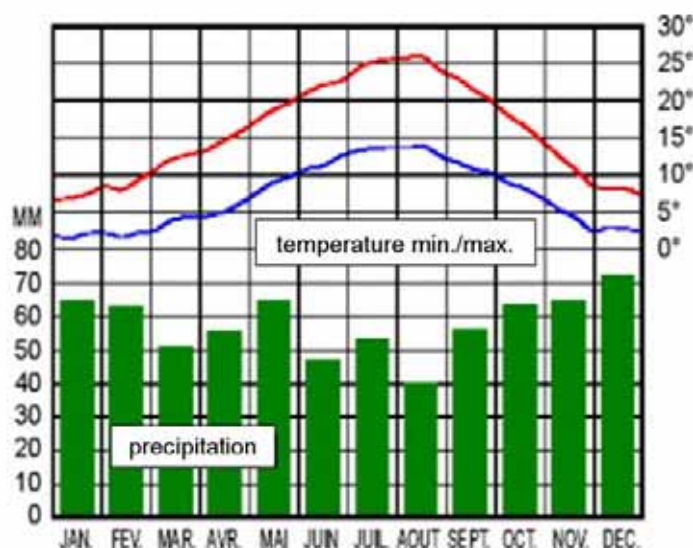


Figure 3.6: Temperature and precipitation of Tours-Parcay-Meslay, based on the period 1971-2000 (METEOFRANCE 2008)

3.2 Geology

The region is located in a basin which is filled by lacustrine formations of the upper Eocene (ALCAYDÉ ET AL. 1990). The study site is bedded between the Loire/Cher valley and the Indre valley, with its alluvial plains, on a limestone plateau of the upper Cretaceous (BRGM 2008). Figure 3.7 shows a geological map where the study site location is marked with a red dot. According to POMEROL (1980) the area is dominated by the clay-with-flints (Figure 3.8), a plateau of clay and flints which is formed when chalk chemically weathers on the surface. Yellow tuff of the upper Turonian marbled by fossils can also be found.

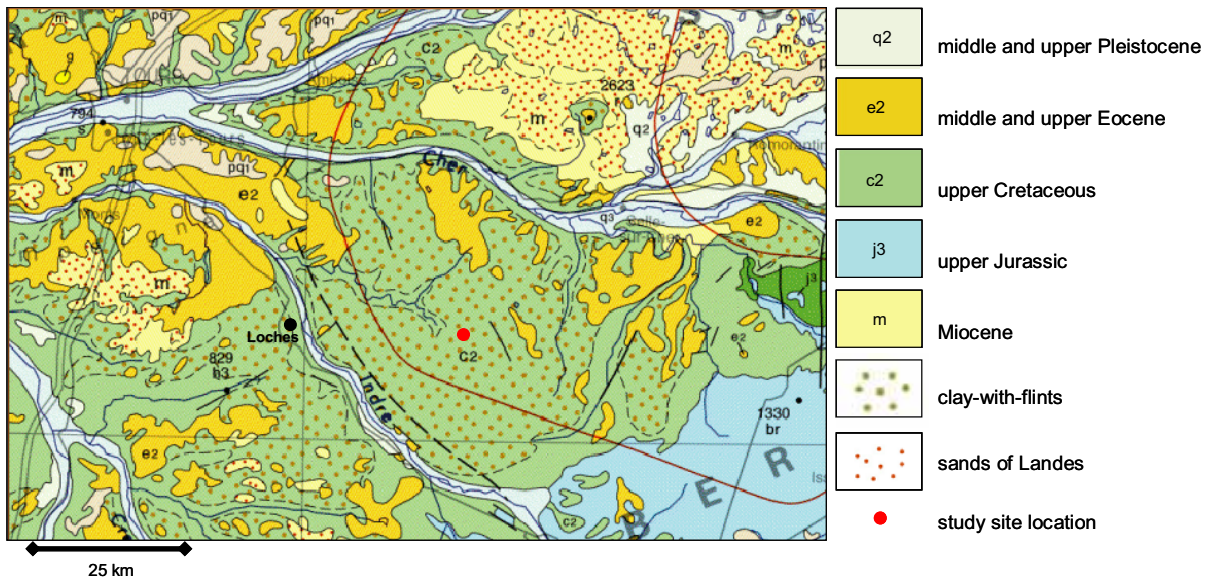


Figure 3.7: Geological map of research area (BRGM 2008, modified)

3.3 Soil

The “Gâtine de Loches-Montrésor” is a monotone landscape of forest, fields and heavy soils which are less fertile. Soils are hydromorphic due to the shallow layer of accumulated Senonian siliceous clay. Layers of silt can be found where vegetation prevents erosion (ALCAYDÉ ET AL. 1990). Due to the high clay content, artificial subsurface drainage is necessary to enhance agricultural use.

According to the FAO, the soil in the study area is an oximorphic Luvisol occurring predominantly in the temperate zone. Luvisols are slightly acid soils with a horizon of accumulated clay enhancing gleysation. High cation exchange capacities are characteristic.

The soil in the forest plot has a thin O horizon consisting of litter and oak leaves. Beneath this decomposition layer, the amount of humus decreases whereas the amount of clay increases. The soil auger sample in Figure 3.8 displays the pedological situation of the forest plot representing the upper 50 cm. Beneath the litter (L) is only a small Ah horizon fading in the mineral Bt horizon. Initially, the soil was expected to exhibit a sharp interface between an humus and a clay layer. However, the right picture in Figure 3.8 shows that the soil is not composed of a distinguishable humus horizon overlaying a mineral horizon.

Figure 3.9 shows the in Table 3.1 listed grain size distribution of the samples taken at different depth in the forest plot according to the FAO classification system. The texture triangle indicates that the soil is clay loam except the upper sample (0-20 cm), which is loam. The high clay content is responsible for the low permeability of the soil which implies the drainage system mentioned above.



Figure 3.8: Left: Soil auger sample. Middle: Clay-with-flints on the field. Right: Soil profile (photo from CEMAGREF)

Table 3.1: Soil analysis of forest sample (data from CEMAGREF)

Depth:	0-20 cm	20-30	30-45	45-65
Clay (<2 μ m)	260 g/kg	305 g/kg	366 g/kg	329 g/kg
Silt, fine (2-20 μ m)	271 g/kg	218 g/kg	199 g/kg	155 g/kg
Silt, coarse (20-50 μ m)	225 g/kg	180 g/kg	180 g/kg	122 g/kg
Sand, fine (50-200 μ m)	89 g/kg	88 g/kg	78 g/kg	74 g/kg
Sand, coarse(200-2000 μ m)	155 g/kg	209 g/kg	177 g/kg	320 g/kg
Nitrogen (N), total	3.28 g/kg	0.709 g/kg	0.378 g/kg	0.303 g/kg
C/N	14.4	11.5	9.15	9.28
Organinc Carbon (C)	47.1 g/kg	8.14 g/kg	3.46 g/kg	2.81 g/kg
Organic material	81.6 g/kg	14.1 g/kg	5.98 g/kg	4.86 g/kg
CEC (cmol/kg)	23.6	17.0	19.3	17.7
Clay (%)	26.0	30.5	36.6	32.9
Silt (%)	49.6	39.8	37.9	27.7
Sand (%)	24.4	29.7	25.5	39.4
Texture	loam	clay loam	clay loam	clay loam
F _{oc} (%)	4.71	0.814	0.346	0.281

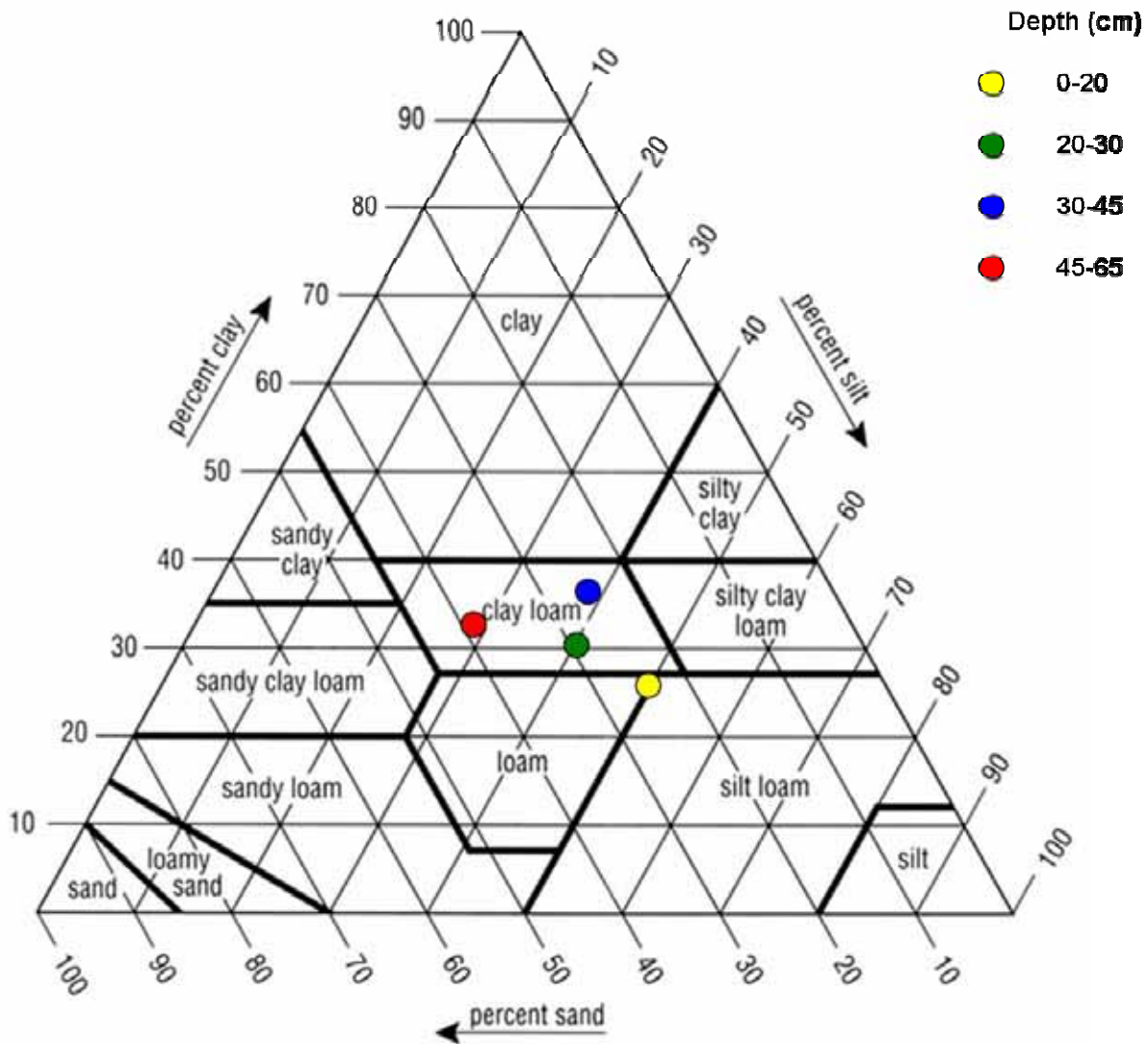


Figure 3.9: Soil Texture Triangle of the forest soil at different depths

Table 3.2 shows the saturated hydraulic conductivities calculated according to SAXTON ET AL. (1986) and COSBY ET AL. (1984). The range of values is similar and there are no big differences in hydraulic conductivity between the different depths. Even though there is less clay content in the upper 20 cm, this horizon is not more permeable than the others.

Table 3.2: Saturated hydraulic conductivities at different depths

Depth (cm)	k_f (SAXTON ET AL. 1986) [m/s]	k_f (COSBY ET AL. 1984) [m/s]	Clay content [%]
0-20	$1.70 \cdot 10^{-6}$	$2.45 \cdot 10^{-6}$	26.0
20-30	$1.08 \cdot 10^{-6}$	$2.68 \cdot 10^{-6}$	30.5
30-45	$0.79 \cdot 10^{-6}$	$2.17 \cdot 10^{-6}$	36.6
45-60	$0.77 \cdot 10^{-6}$	$3.42 \cdot 10^{-6}$	32.9

By calculating the geometric mean according to FETTER (2001) one obtains an average hydraulic conductivity of $1.03 \cdot 10^{-6}$ m/s for the Saxton-Method and $2.64 \cdot 10^{-6}$ m/s for the Cosby-Method, which is both about in the same order of magnitude.

SPITZ & MORENO (1996) summarized hydrogeologic parameters from several studies and report hydraulic conductivities for clay in the range of 10^{-10} m/s. According to their summary, the porosity of clayey soil can be estimated to be about 40%. APPELO & POSTMA (2005) proposes porosities between 30-65% and hydraulic conductivities of $1.2 \cdot 10^{-10}$ - $1.2 \cdot 10^{-5}$ m/s.

3.4 Hydrology

Even though rainfall is uniform distributed over the whole year, the main runoff season is winter. During summer, the water table drops due to evapotranspiration and is lowest at the end of summer. In autumn, rainfall starts to exceed evapotranspiration and the water table rises and the shallow groundwater reaches the drainage system. This is when the drainage season starts (LUCIANI 2007).

During the winter period 2007/2008, the average daily rainfall was 2.4 mm. But throughout February, there was generally less rainfall than average, including the first days of the experimental period which was in March (03.03.2008-11.03.2008). Figure 3.10 shows the cumulative rainfall for the period 08.09.2007-21.05.2008. It can be seen that there was almost no rain in February 2008. Rainfall was only 38.7 mm which is 62% of the long-term mean for February.

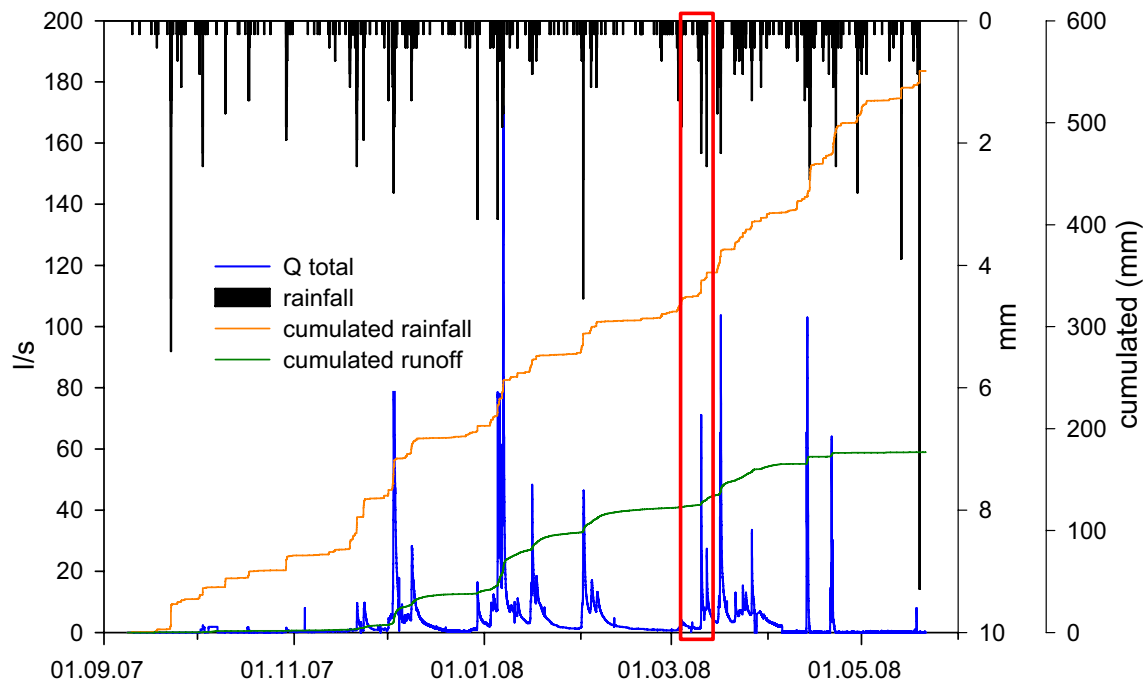


Figure 3.10: Rainfall, runoff, cumulative rainfall and cumulated runoff during the winter season 2007/2008. The experimental period is marked in the red rectangle (Data by CEMAGREF)

As evapotranspiration is lowest in winter the main runoff season started in December 2007 and was highest in January 2008 with a maximum peak of 172.14 L/s on January, 7th 2008. Runoff was remarkably low during February which is the reason why the experiment was postponed to March.

The arithmetic mean for the period of 08.09.2007-21.05.2008 is 6.74 l/s with a variation coefficient of 1.28. Applying the water balance equation which is

$$P = R + ET + \Delta S \quad [\text{mm}] \quad (3.2)$$

with P =precipitation, R =runoff, ET =evapotranspiration and ΔS =changes in storage, for this period one obtains

$$551 = 177 + 374 \quad [\text{mm}] \quad (3.3)$$

whereas 374 mm is the sum of ET and ΔS which equals 68%. These values lead to an average runoff coefficient of 32.1%.

The application of the double mass curve of the cumulated runoff versus cumulated rainfall (Figure 3.11) allows the distinction of different drainage periods. Drainage starts in summer until end of autumn, which is the period of highest groundwater recharge. Intensive drainage is observed during winter until the beginning of spring when the groundwater table reaches the drainage system. The change to the period of ending drainage, lasting from about spring until the beginning of summer, is not as distinct as the first change in slope (LUCIANI 2007). The slope represents the magnitude of runoff coefficient varying from 6% in the beginning, increasing to 67% for the intense drainage and finally decreasing to 23% for the end of drainage.

The behaviour of these drainage stages was the same last year if compared to calculations by LUCIANI (2007), where the intense drainage started 07.12.2006 also with a runoff coefficient of 67% until 17.03.2007.

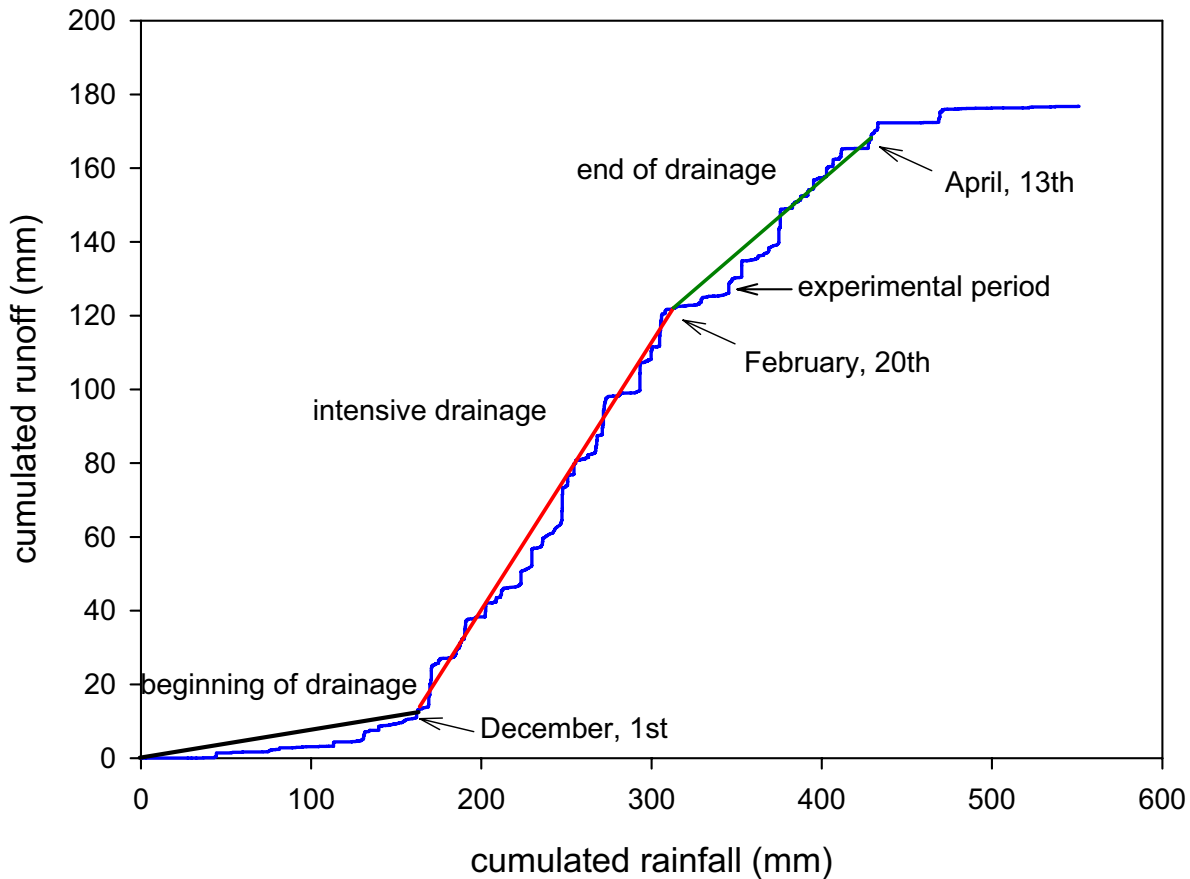


Figure 3.11: Double mass curve for the cumulated runoff versus cumulated rainfall during the period 08.09.2007-21.05.2008. The change in slope represents the different drainage stages (Data by CEMAGREF)

Figure 3.12 shows rainfall and runoff during the experimental period in detail. The grey background marks the periods when the forest inlet tube was opened. The tube was opened first on 04.03.2008 at 11:54 for salt injection and closed again after 44 minutes. On 06.03.2008, the tube was reopened for the rest of the experimental period with a small interruption of 25 minutes (07.03.2008 08:57) where the inlet pipe was cleaned. As rainfall was unusual low resulting in low flow conditions, the average discharge due to the natural hydraulic conditions was only 0.22 L/s. Only by closing the wetland inlet tube, the forest inflow can be increased. For instance, the wetland inlet tube had to be closed on March, 7th because of a mistake in tracer injection which resulted in a higher forest inflow during 09:45 and 16:55 on this day ($Q=1.1$ L/s).

During the experimental period 5.4 mm of the total rainfall contributed to runoff, which equals 19%. Applying the water balance equation yields:

$$29.2 = 5.4 + 23.8 \quad [\text{mm}] \quad (3.4)$$

Thus, the remaining 81% (23.8 mm) were stored in the soil, percolated or evaporated. As rainfall was less in February, the clayey soil had a higher saturation capacity. But even rainfall was less, waterlogged soil was observed.

In total 29.2 mm fell during the experimental period, whereas 42% (12.3 mm) is due to a storm event on March, 10th. At 10 am normal low flow conditions of 0.3 L/s were recorded, but discharge increased to a maximum of 21.4 L/s at 15:15 due to the storm event.

On March, 9th a heavy storm event where trees broke down was observed, but the discharge did not increase even though rainfall was recorded (compare Figure 3.12).

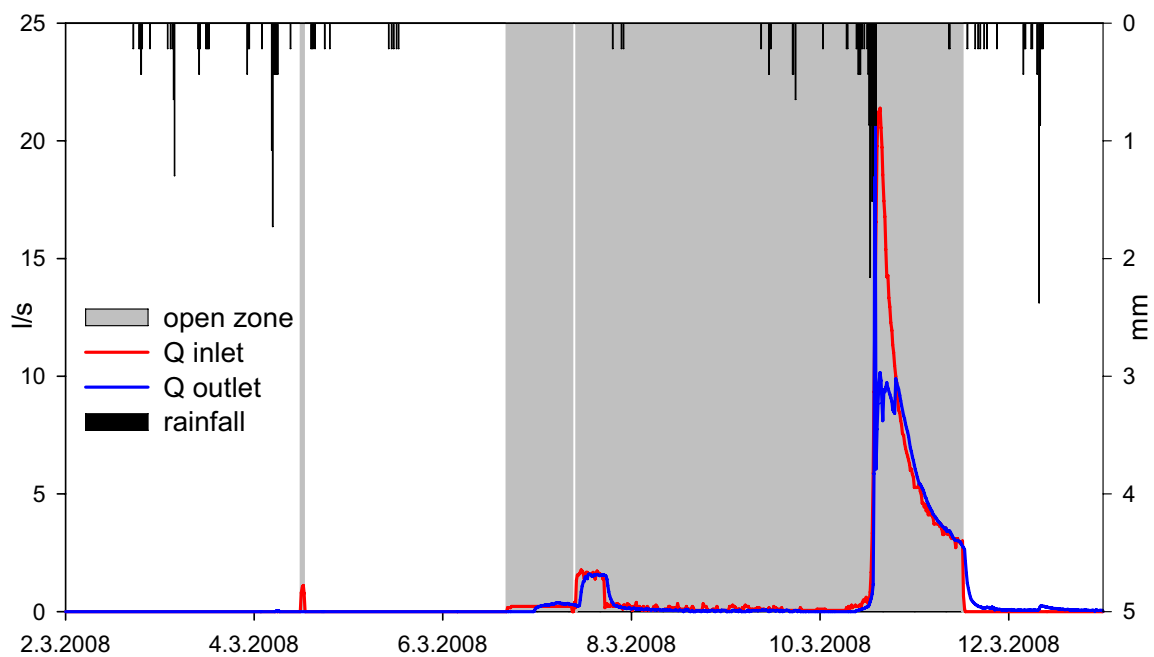


Figure 3.12: Rainfall and runoff during the experimental period

The abrupt decrease in runoff is due to the closing of the inlet tubes. Both buffer zones were closed for revitalisation after the experimental period on March, 11th.

The small increase in runoff at the forest outlet (Figure 3.12) on 12.03.2008 is due to the amount of rain falling on the forest plot (1690 m²) as the inlet tube was already closed. That means that 5.62 mm (cumulative rainfall over 20 h) contributed to a cumulative runoff of 4.13 mm, which corresponds to a runoff coefficient of 73.5%. As the soil in the forest plot was relative saturated due to the prior storm event, the loss of 26.5% is assumed to be evaporation. Transpiration and interception can be neglected as vegetation period has not started.

The groundwater table in the forest plot is not influenced by any drainage pipes.

3.5 Conclusion

The hydrology of the 42 ha agriculturally used watershed is strongly influenced by the drainage system. Drainage of the low permeable clayey soil leads to fast runoff response of rainfall events. Therefore the intense drainage period constitutes the most important one for pesticide transport into the creek Le Calais, for which reason pesticide application is limited during this period. The forested plot with a length of about 71 m acts as an end-of-field buffer zone for pesticide mitigation. Its vegetation and soil organic matter content is essential for sorption processes.

The clay content in the upper 20 cm is 26% and an interface between humus and clay layer does not exist. Even though its hydraulic conductivity is higher ($1.70 \cdot 10^{-6}$ m/s) than in the soil below ($0.77\text{--}1.08 \cdot 10^{-6}$ m/s) the values are still in the same order of magnitude and interflow processes will be difficult to observe.

4 Experimental Design

The forest plot which is described in the previous chapter was investigated regarding varying considerations. Altogether, three different kinds of experiments have been carried out during 03.03.2008-11.03.2008 (Figure 4.1). The first one started one day after the arrival in Bray on March, 4th, including the injection of salt. After the second experiment starting on March, 6th, which resulted in saturation of the forest plot, a multi-tracer experiment was carried out on March, 7th.

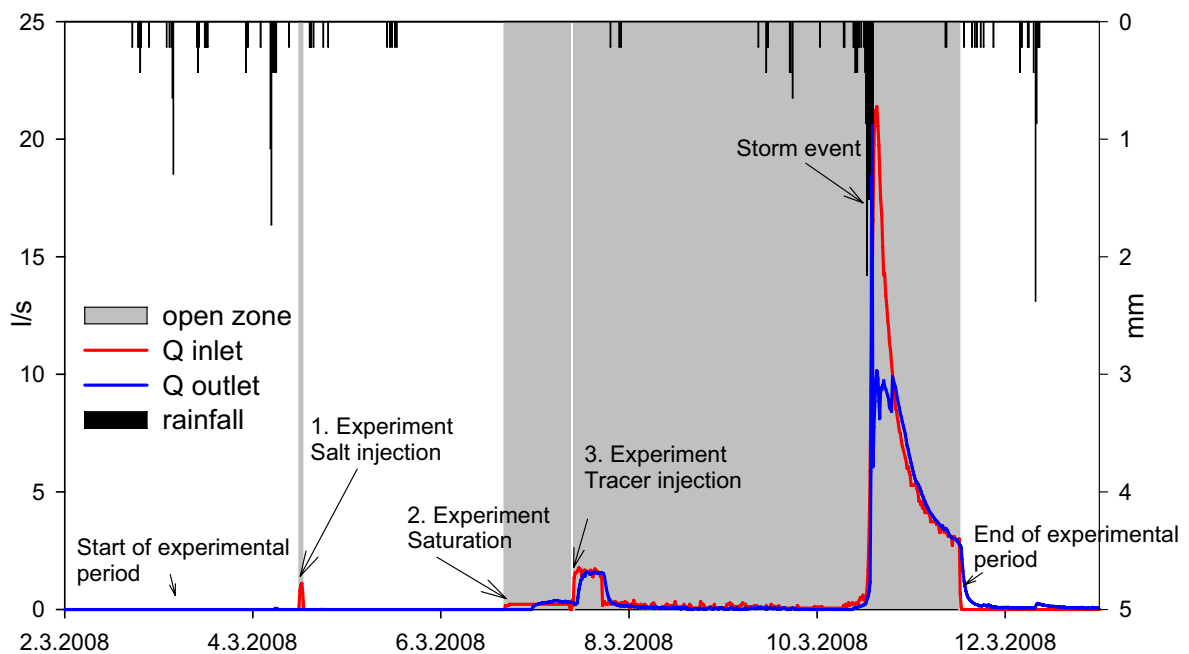


Figure 4.1: Experiment schedule during the experimental period of 03.03.2008-11.03.2008

Due to low flow conditions, the forest plot was reduced to approximately 530 m² for all observations by building a dam after 13 m of the inlet ditch.

For general orientation the map in Figure 4.2 gives an overview about the different locations of the measurement devices installed in the forest plot. The different experiments required different technical equipment depending on the question. The experiments in detail were designed as follows.

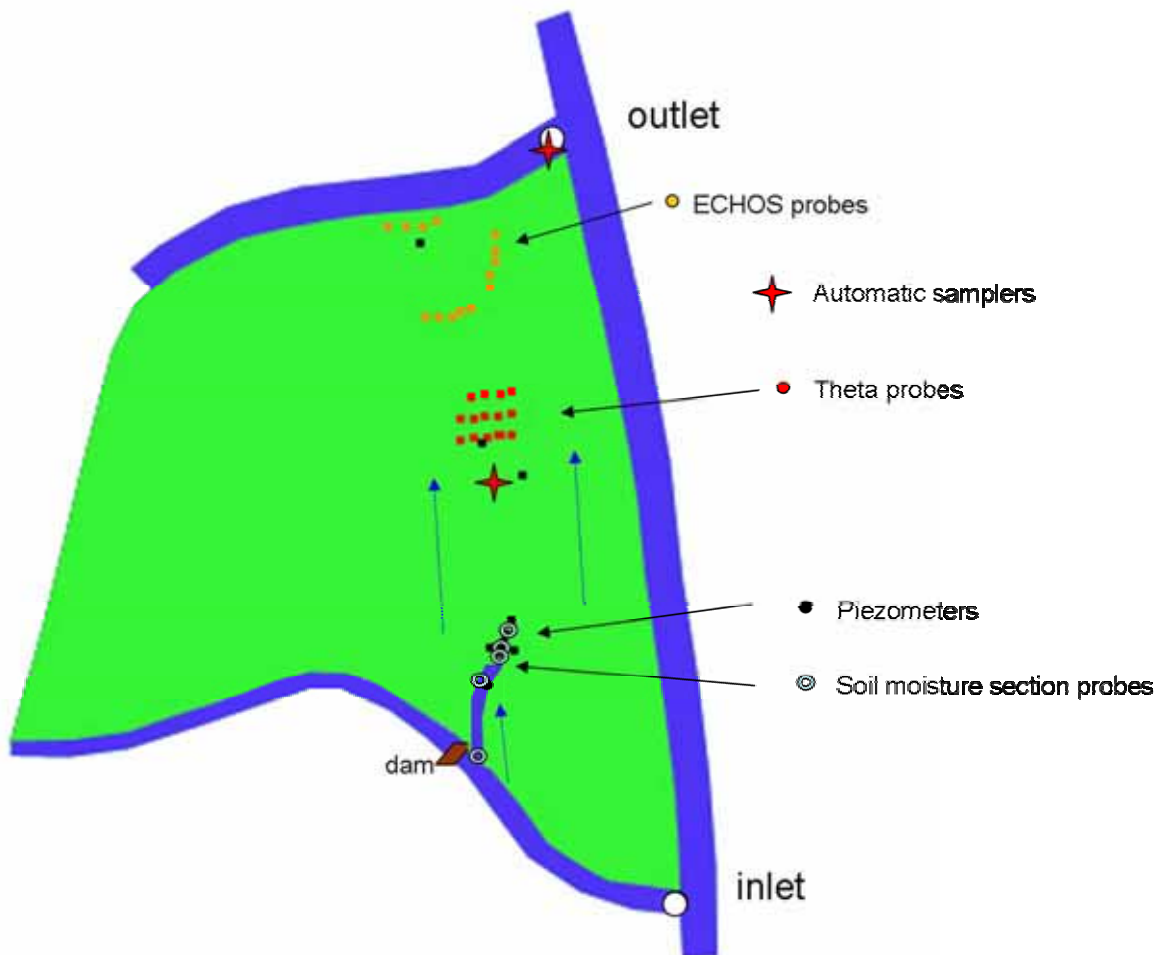


Figure 4.2: Location of the different measurement devices in the forest plot

4.1 Subsurface Flow Experiment

The aim of the first part of this study was to determine subsurface flow in soil and whether there exists interflow on the interface between the humus (O horizon) and the clay (A horizon). Figure 4.3 shows a conceptual model of the expected hydrological processes appearing during the subsurface flow experiment. The salt labelled water is dammed up resulting in a fairly constant water level. The water level dropped only about 2.5 cm within two days. Surface runoff was prevented by the dam, thus the water was enhanced to enter the vadose zone. The wetting front movement of the interflow should be then detectable via the rise in water table and the increase in electric conductivity due to the salt which were both measured by diver devices in the piezometers. Macropores, burrows or cracks are also possible flow paths for preferential flow.

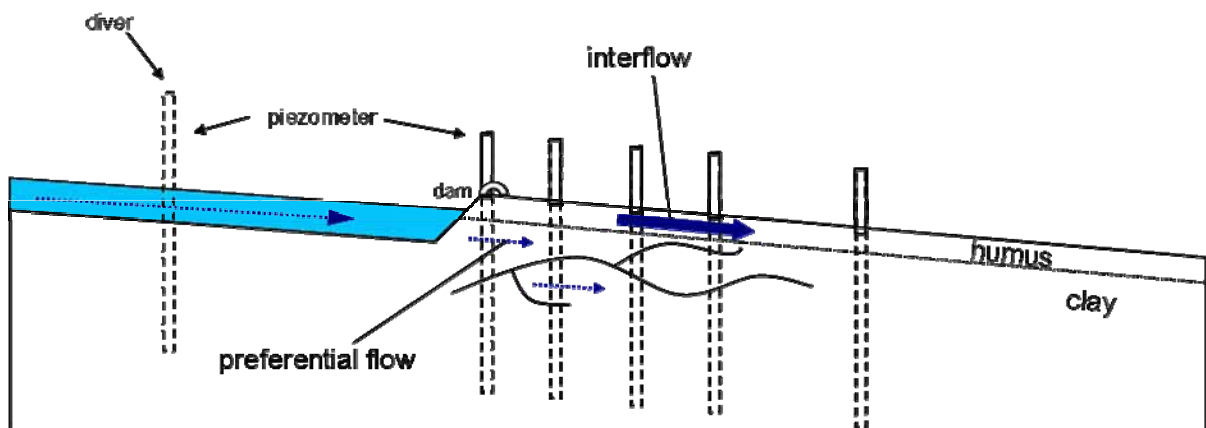


Figure 4.3: Conceptual model of the expected hydrological conditions of the piezometer experiment

The inlet ditch contributes to a smaller-sized trench which was dammed up on a flow distance of 25 m relating to the forest inlet. The experimental plot had a size of 5.5 m · 1.5 m and a slope of approximately 1%. Five access tubes for the soil moisture profile probe (*Profil-Sonde PRI*) were installed at different locations (see “soil moisture section probes” in Figure 4.2). The profile probe uses the dielectric constant of the water in order to find its volumetric water content. Since the dielectric constant of water is higher than that of soil minerals or air, it is a sensitive measure of the water content. The profile probe allows measuring the soil moisture in a vertical section at 10, 20, 30 and 40 cm depth by sending alternating current impulses of a specific frequency which are then reflected depending on the soil capacitivity. The modified and the emitted frequency constitute a standing wave which’s frequency is again different from the emitted one resulting in a voltage change. This voltage change is then displayed on the *HH2 moisture meter (Delta-T devices)*. Ten measurements were manually recorded in different intervals, starting on 04.03.2008 12:29 until 06.03.2008 08:45.

Additionally, eight piezometers were installed with an interspace of 0.5 m to 2.9 m (Figure 4.4). The piezometer “PA” was set up in the inlet ditch, “PB” has been installed in the dam, “PC”-“PH” further downslope. The piezometers were filtered only until surface level. Above surface level, the instruments were clogged with tape to prevent surface water flowing into the piezometers and covered by plastic bags to avoid rainfall input.

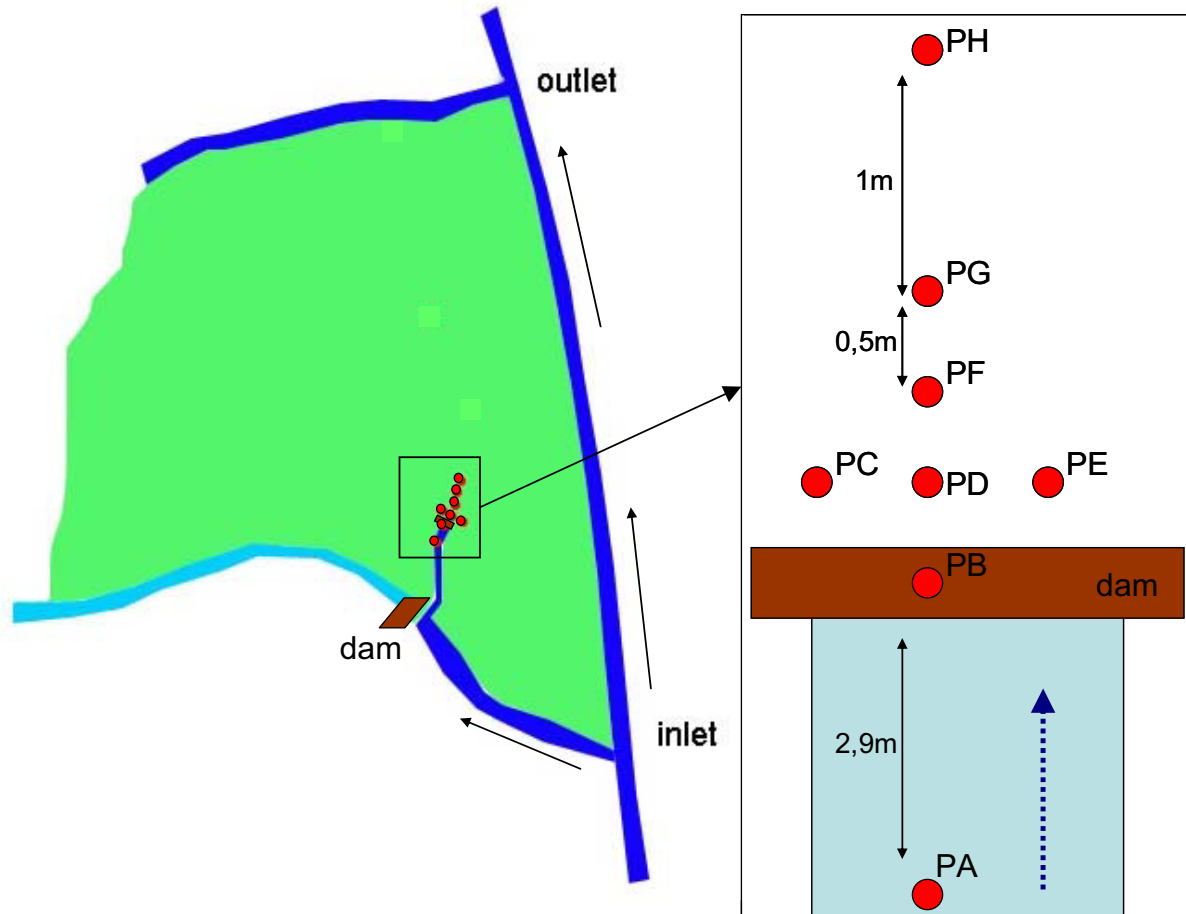


Figure 4.4: Location of the piezometers during the first experiment.

Overall, four *CTD*-divers and one *TD*-diver (*Schlumberger/Van Essen Instruments*) were used in this study. A *CTD*-diver is able to measure electric conductivity, temperature and pressure head and save the data to an integrated logger. This way these parameters were measured continuously in time steps of 15 minutes. The *TD*-diver only records pressure head.

They were installed in the piezometers and they changed their location depending on the water table in the piezometer as there were more piezometers than divers available in this study. Table 4.1 gives the distances between the installed piezometers and the inlet ditch as well as the distances to the built dam. The air pressure head was logged by a *barodiver* installed in a cabin on the forest plot.

The experiment started on March, 4th at 11:54 am with the injection of 5 kg NaCl dissolved in 100 L water. This solution with a concentration of 50 g/L was injected in 44min19 with an

average flow rate of 37 mL/s. The inlet flow during injection was about 1.1 L/s. The total volume of the inflow is only 3.4 m³.

This arrangement was kept unaffected until March, 6th, 16:15 where the forest inlet tube was opened for the next experiment.

The design is presented by the pictures below (Figure 4.5).

Table 4.1: Piezometer locations in m distance from the inlet and the dam

	Distance from inlet [m]	Distance from dam [m]
PA	22.46	
PB	25.41	0
PC	25.81	0.40
PD	25.86	0.45
PE	25.85	0.44
PF	26.33	0.92
PG	26.93	1.52
PH	27.85	2.44



Figure 4.5: Experimental setup of the piezometers and the dammed up water

4.2 Wetting front experiment

For further investigations concerning the determination of interflow and its wetting front velocity, a second experiment was carried out on the forest plot (530 m²). The piezometers were removed and 3 of them and reinstalled, one next to the automatic sampler in the middle of the forest plot (“FM”), one further downslope and the third one near the outlet to observe water level and conductivity (Figure 4.6). Recording by the divers was the same as in the first experiment in time steps of again 15 minutes.

Here, chloride acted as a pre-tracer, also to determine flow paths and travel times under unsaturated conditions and to help defining the automatic sampling intervals for the tracer experiment.

The forest inlet and the dam from the previous experiment were opened at 16:15 on 06.03.2008 and the NaCl from the first experiment was flushed into the forest plot, as conductivity was still exceeding 3000 $\mu\text{S}/\text{cm}$ at the bottom of the inlet ditch.

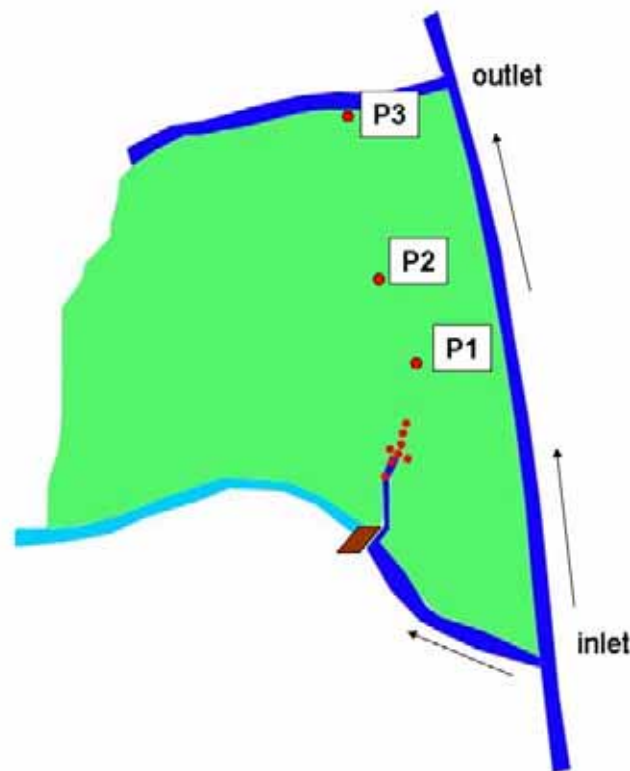


Figure 4.6: Experimental setup of the piezometers P1, P2 and P3

Additionally, a “Theta field” (Figure 4.7) was constructed using 14 frequency-domain-reflectometry (FDR) probes of the type Theta ML2x with 4 metal rods à 6 cm each.

This system obtains the soil dielectric constant by sending a signal in a specific frequency which is transmitted into the soil. The conducted electromagnetic field is dominated by the

water content of the soil as water has a high capacitivity. The volumetric soil water content was recorded by two data logger (*Micromec Multisens*) in time steps of 1 minute (Figure 4.8). The probes use a standard calibration for organic and mineral soils with an accuracy of $\pm 5\%$.

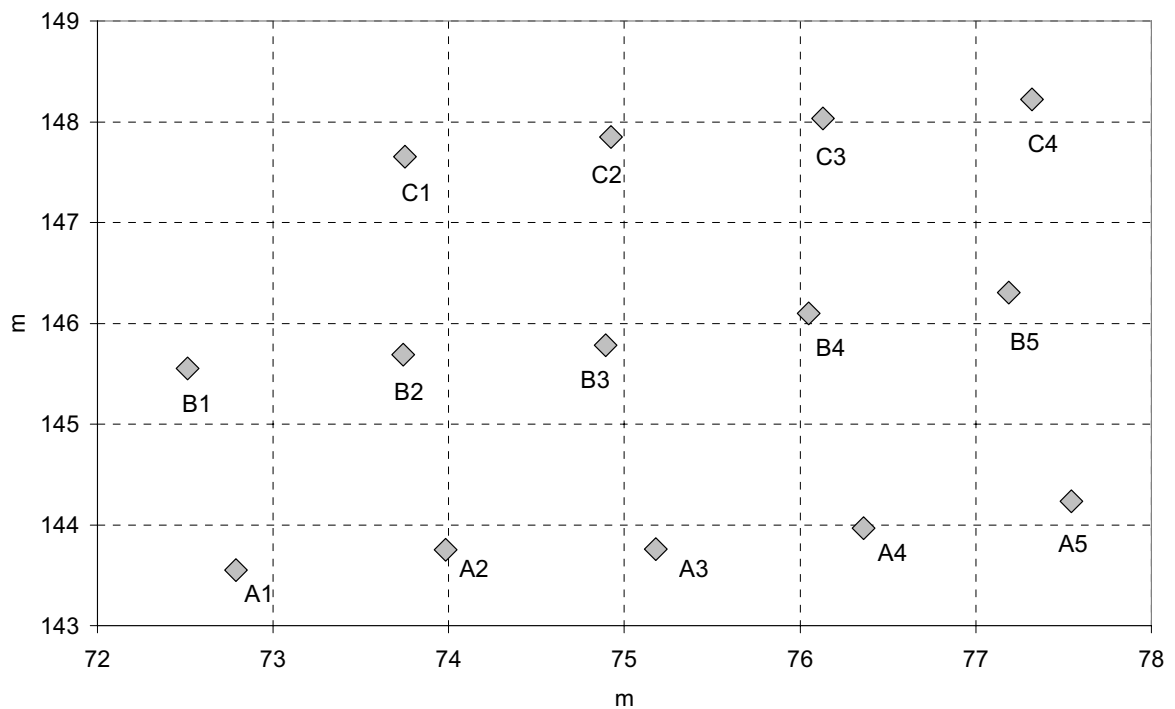


Figure 4.7: Arrangement of the “Theta field” composed of 14 FDR probes



Figure 4.8: Installation of the FDR probes and one of the two data loggers.

Further more, three soil moisture sensor profiles with 5 soil moisture probes (*ECH₂O* Decagon devices) were setup near the outlet (Figure 4.9). ECH₂O probes use also the

dielectric constant to determine the soil moisture, with an accuracy of $\pm 4\%$. Data were stored in time steps of 5 minutes by a data logger for each profile. The arrangement of the probes was chosen to be parallel standing to the suggested flow direction allowing water flow without obstruction.

The experiment resulted in saturation conditions for the tracer experiment.

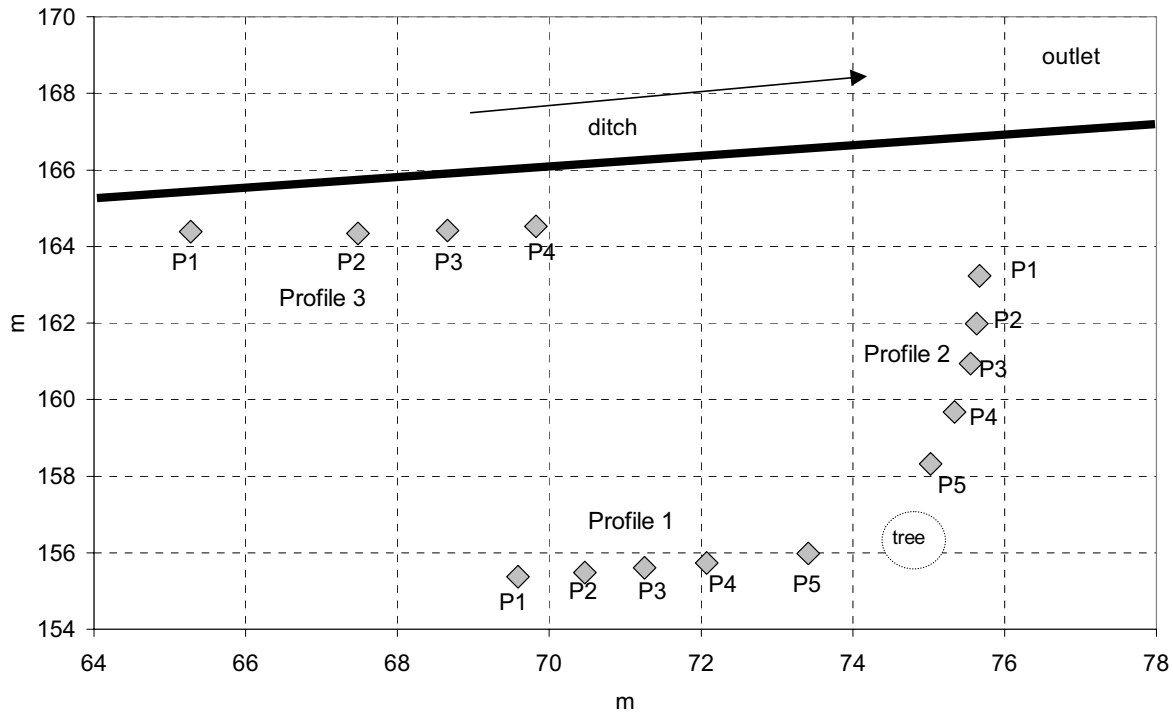


Figure 4.9: Arrangement of the three ECH₂O profiles with 5 moisture probes each for profile 1 and 2, and 4 probes for profile 3.

4.3 Multi-Tracer Experiment

For the tracer experiment, a cocktail of 4 tracers was applied. Uranine was chosen to act as a tracer underlying photo degradation. Sulforhodamine B is sorptive and was used to investigate the efficiency of the forest plot on sorptivity. Sorption is an important process on the mobility of pesticides.

The pesticide Isoproturon was selected because it is often applied on the adjoining cultivated fields. The last application of IPU before the experiment was in November 2007.

Bromide was supposed to act as a conservative ideal tracer and to provide data to compare results with UA, SRB and IPU.

Both fluorescence tracers came from the Institute of Hydrology, Freiburg (IHF); IPU and Bromide were brought by Cemagref, Antony. Unfortunately, not Bromide has been injected, but Nitrate. Therefore, comparable results of an ideal tracer could not be recorded.

Samples were taken in brown glass bottles to pretend photo degradation. Sampling was done by automatic samplers at two locations, one approximately in the centre of the forest plot ("FM") and another one at the outlet of the forest ("FO") (see Figure 4.2).

At the outlet a filter fluorimeter (*GGun Fl-30*) was additionally installed in combination with a data logger (Figure 4.10) to record the fluorescence intensities of Uranine and Sulforhodamine B in time steps of 15 minutes. Online devices have a high temporal resolution and unexpectedly fast arriving breakthroughs are not missed out, but the quality of results does not compare to the analytical methods applied in laboratories (WGSHS 2003).

During the rainfall event on March, 10th, twelve additional hand samples were taken.



Figure 4.10: Filter fluorimeter ("Fluo") installed in the outlet ditch of the forest. The automatic sampler "FO" took samples through the little tube fixed in the PVC pipe, where the EC was also recorded (black cable). Low flow conditions obvious.

The tracer experiment started on March, 7th. At 08:57 the forest inlet tube was closed for 25 minutes for the cleaning of the pipe. This cleaning included the injection of dish liquid which should be avoided because of fluorescent substances in such cleaning liquids. At 09:20, the forest was reopened and at 09:45 started the injection of the tracers through the inlet pipe (Figure 4.11). The first 20 L of the injection solution contained 2g Uranine and 5g Sulforhodamine whereas the injection last 1min48. 50g of the pesticide Isoproturon was mixed with the accidentally taken 3 kg potassium nitrate in 60 L water and instantly injected. This injection took 5min24. The injection equipment was then rinsed with 40 L additional water. The injection of tracers can be regarded as a Dirac impulse.

Due to the low flow conditions, the tracer injected in the forest inlet tube flow back into the middle channel. Therefore, the wetland inlet tube had to be closed to avoid tracer flow into the wetland. Thus, to not disturb the wetland tracer experiments the wetland was closed from 09:45 to 16:55.



Figure 4.11: Injection of the tracer cocktail.

5 Results

5.1 Subsurface Flow Experiment results

5.1.1 Profile probe

The results of the profile probe measurements do not show anything suspicious. Figure 5.1 displays the signal in voltage expressed in mV, which is directly linked to the volumetric soil moisture content, versus time. At each site measurements were recorded in different depths, at least three. Usually, a calibration should be conducted which was missed out in this study. Thus, a correct relationship between the voltage and the soil moisture content is not given. In general, it can be seen that the soil moisture is affected by the opening of the forest inlet tube and by rainfall on March, 5th in which the upper soil reacts first (except “A” and “C”).

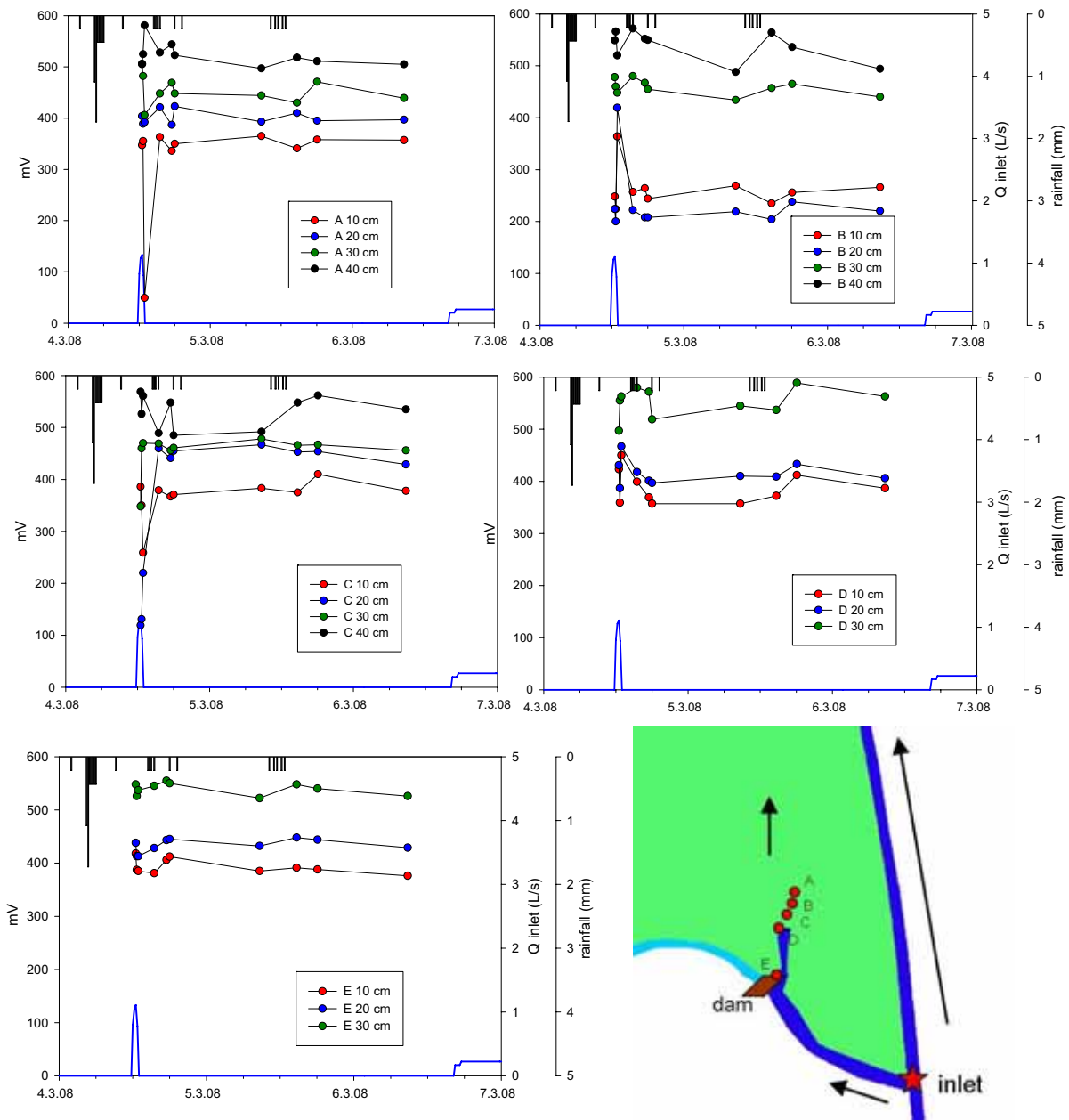


Figure 5.1: Results of the section probe device

5.1.2 Piezometers

The five divers recorded electric conductivity and the pressure head continuously. They changed their location several times during the experiment as piezometers stayed dry. Movements were noted for tracing back the data to the referring piezometers.

There are no data for the piezometers “PD” and “PG” because they stayed dry. The TD diver was placed in “PF”, thus there exist only water table data for this piezometer.

Figure 5.3 shows the electric conductivity data during the experiment lasting from March, 4th to March, 12th, but the experiment itself stopped when the forest inlet tube was opened for the next experiment on March, 6th, 16:15.

Even though “PA” was located in the inlet ditch it does not show any reaction before March, 6th, 03:30. Then its conductivity increases rapidly to values higher than 7 mS/cm which is above the measurable range of the diver (5mS/cm). Conductivity stays high also after the opening on March, 6th, 16:15.

“PB” does not show any reaction before 06.03.2008 03:05 but has a constant value after 06.03.2008 12:40 of about 790 μ S/cm.

It can be seen that “PC” was dry during 04.-05.03.2008, but on a constant electric conductivity level of 420 μ S/cm during 09:25-15:35 on March, 6th. Unfortunately, the data for the rise in conductivity are missing.

“PE” measurements start on 05.03.2008 09:00 and show a highly variable curve progression. Multiple peaks in conductivity were also observed in “PH” but there was already water in “PH” before the injection of the salt labelled water into the ditch.

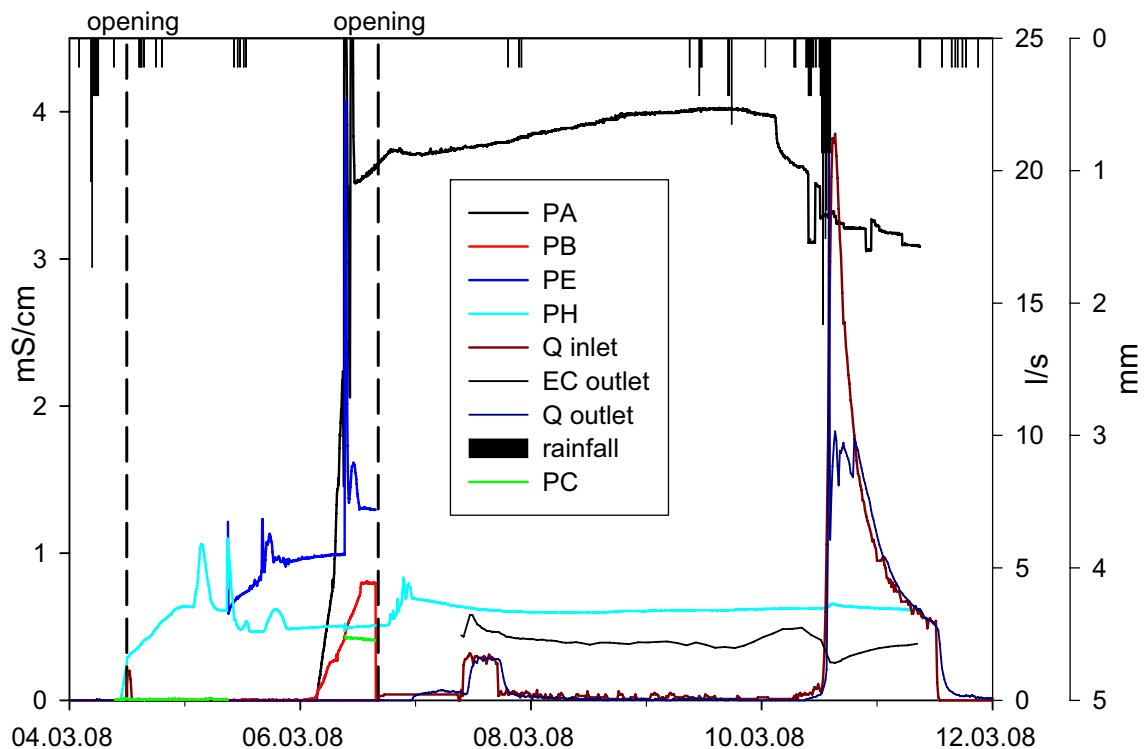


Figure 5.2: Electric conductivity in each piezometer recorded by the divers

Water table data were calculated by subtracting the air pressure recorded by the barodiver from the pressure head recorded by the CTD divers. The results expressed in [cm below

surface] are shown in Figure 5.3. Significant rises in water table were only observable in “PH” and “PE”. After the experiment, the opening of the forest inlet tube resulted in saturation and the water table rose above surface level as noticed in “PA” and “PH”.

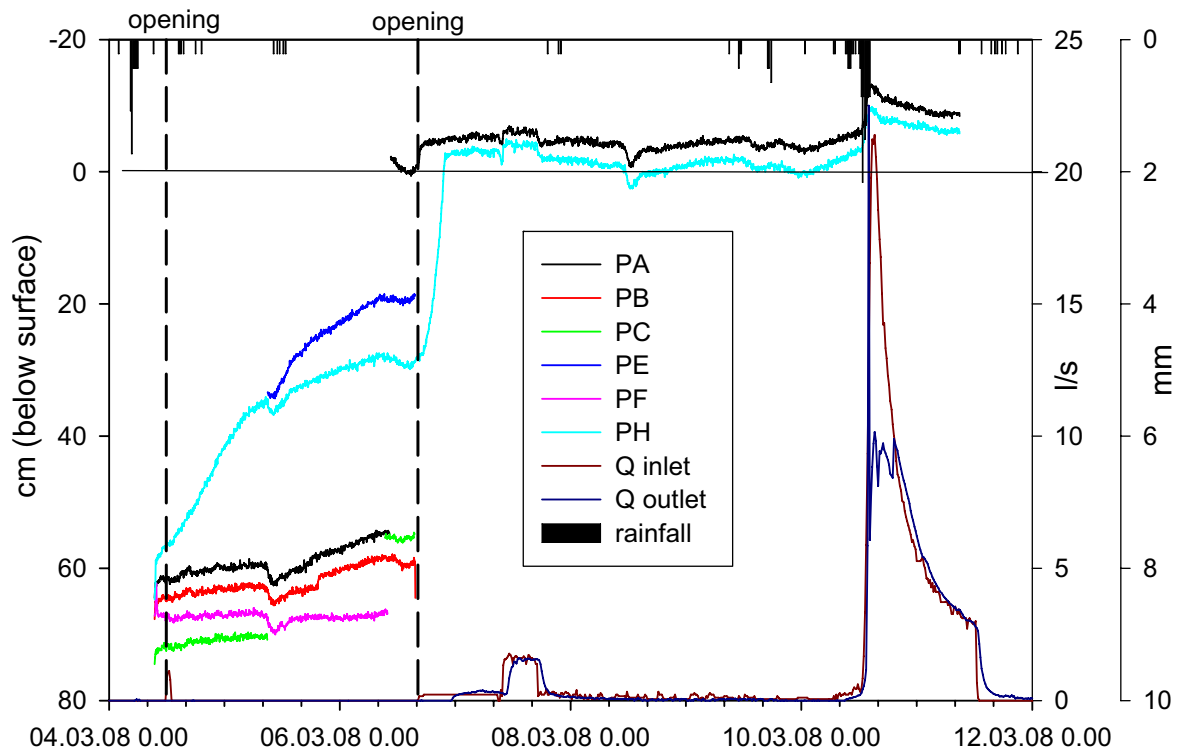


Figure 5.3: Water table in the piezometers.

5.1.3 Discussion

If there existed an interface between humus and clay layer, interflow would have been expected leading to a response in electric conductivity and water table faster than the hydraulic conductivity suggests. A linear relationship between the distance of the piezometers from the dam and the time of first reaction was assumed.

The data obtained in this experiment should be regarded censoriously. For instance “PA” gives conductivity values higher than 7mS/cm which must be an error in measurement. The maximum conductivity in the inlet ditch exceeded 4mS/cm, thus concentration of the injected solution (50g/L) was probably too high. KÄSS (1998) recommends much lower concentrations to avoid tracer sinking. The high conductivity values in “PA” could therefore be related to a salt sinking in the piezometers, but values are still high even after the storm event on March, 10th. The peak in conductivity in “PH” on 05.03.2008 03:30 could be caused by salt tracer arrival, but there is no explanation for the immediate decrease afterwards.

The temporary decrease in water table in all piezometers on March, 5th is also not explainable.

Another doubt exists regarding the functioning of the piezometers. “PA” was directly installed in the saturated area of the inlet ditch and “PB” close to the end of the inlet ditch. Thus one would expect them to react first, but it took almost 40 h to detect the first water in these piezometers. That indicates that the available piezometers do not work well in clayey soils as they are recommended to be used in sandy soils (e.g. OBBINK 1969). The piezometers could have been clogged by the clay and the field capacity of clay is usually high resulting in less phreatic water.

For velocity calculations only data obtained in “PE” and “PH” can be considered as other piezometers stayed dry or the ascending branch was missed out. Table 5.1 gives the subsurface flow velocities based on the first significant increase in electric conductivity exceeding the average background concentration (in the range of $\sim 400 \mu\text{S/cm}$).

Table 5.1: Subsurface velocities based on electric conductivity detection in "PE" and "PH".

Piezometer	Date	Distance [m]	Velocity [m/s]
PE	05.03.2008 09:00	0.44	$5.79 \cdot 10^{-6}$
PH	05.03.2008 03:30	2.44	$4.34 \cdot 10^{-6}$

With the hydraulic conductivities (k_f) calculated in section 3.3 one can apply Darcy's Law which is

$$v_f = k_f \cdot i \quad (5.1)$$

where v_f is the filter velocity and i the slope (1%). Assuming an effective porosity of 0.44 allows the calculation of the flow velocity v_a :

$$v_a = \frac{v_f}{n_{eff}} \quad (5.2)$$

leading to the following data in Table 5.2:

Table 5.2: Flow velocities, according to the two k_f -estimation-methods

	COSBY ET AL. (1984)	SAXTON ET AL. (1986)
k_f [m/s]	$2.64 \cdot 10^{-6}$	$1.03 \cdot 10^{-6}$
v_f [m/s]	$2.64 \cdot 10^{-8}$	$1.03 \cdot 10^{-8}$
v_a [m/s]	$6.0 \cdot 10^{-8}$	$2.34 \cdot 10^{-8}$

Both calculated flow velocities according to the different k_f -estimation-methods are two orders of magnitude smaller than the maximum tracer velocities given in Table 5.1 which are

$5.79 \cdot 10^{-6}$ m/s in “PE” and $4.34 \cdot 10^{-6}$ m/s in “PH”. This could be either due to a permeability of the clayey soil higher than assumed or to any kind of preferential flow. It is also questionable why “PH” reacted prior to “PE” even though it was more distant from the dam. This fact is amplifying the hypothesis of preferential flow through macropores. Interflow can be excepted as there was no humus horizon existent (compare Figure 4.5). But these assumptions still remain arguable as all parameters are extremely inaccurate.

5.1.4 Conclusion

In general, this experiment was unsuccessful concerning interflow observations. As the study site was not visited prior the experimental period the system was supposed to exist of a distinct humus horizon. Interflow at the boundary of organic and mineral horizon is possible as reported in DEEKS ET AL. (2008) where the amount of interflow constituted about 44% of the water input.

Unfortunately, the experimental plot presented only a thin litter layer and no distinct humus accumulation for which reason the hydraulic conductivity values do not vary with depth. Thus, among other things interflow could not be identified.

Interflow is usually investigated as a hillslope runoff process. For example, MOSLEY (1982) could determine interflow velocities on a steep slope of 55-70%. Lateral flow was also observed on rather gentle slopes by LEHMANN & AHUJA (1985) (6-8% slope) and recently by DEEKS ET AL. (2008) (10% slope), but the slope in the forest plot is down to only 1% and it remains questionable if interflow might occur.

5.2 Wetting front results

5.2.1 FDR probes

From the 14 FDR probes, unfortunately one of them (B3) was not connected to the data logger. The other 13 FDR probes recorded the volumetric soil moisture content presented in Figure 5.4. During this experiment no rainfall occurred.

It can be seen that all FDR probes reacted to the water front on the same day of the opening. Table 5.3 gives the wetting front velocities at each FDR probe in order to their reaction after the opening of the forest inlet tube. The topographic situation of their elevation is shown in Figure 5.5.

Table 5.3: Velocities of the wetting front at the FDR probes according to their time of first reaction

FDR probe	v [m/s]
A2	$1.96 \cdot 10^{-2}$
A3	$1.62 \cdot 10^{-2}$
C3	$6.24 \cdot 10^{-3}$
B4	$5.92 \cdot 10^{-3}$
C2	$6.02 \cdot 10^{-3}$
A5	$5.06 \cdot 10^{-3}$
C4	$5.28 \cdot 10^{-3}$
A4	$4.77 \cdot 10^{-3}$
C1	$3.89 \cdot 10^{-3}$
B1	$3.49 \cdot 10^{-3}$

After 7h15min, the runoff at the outlet reacted on the forest opening, leading to a flow velocity of $2.73 \cdot 10^{-3}$ m/s.

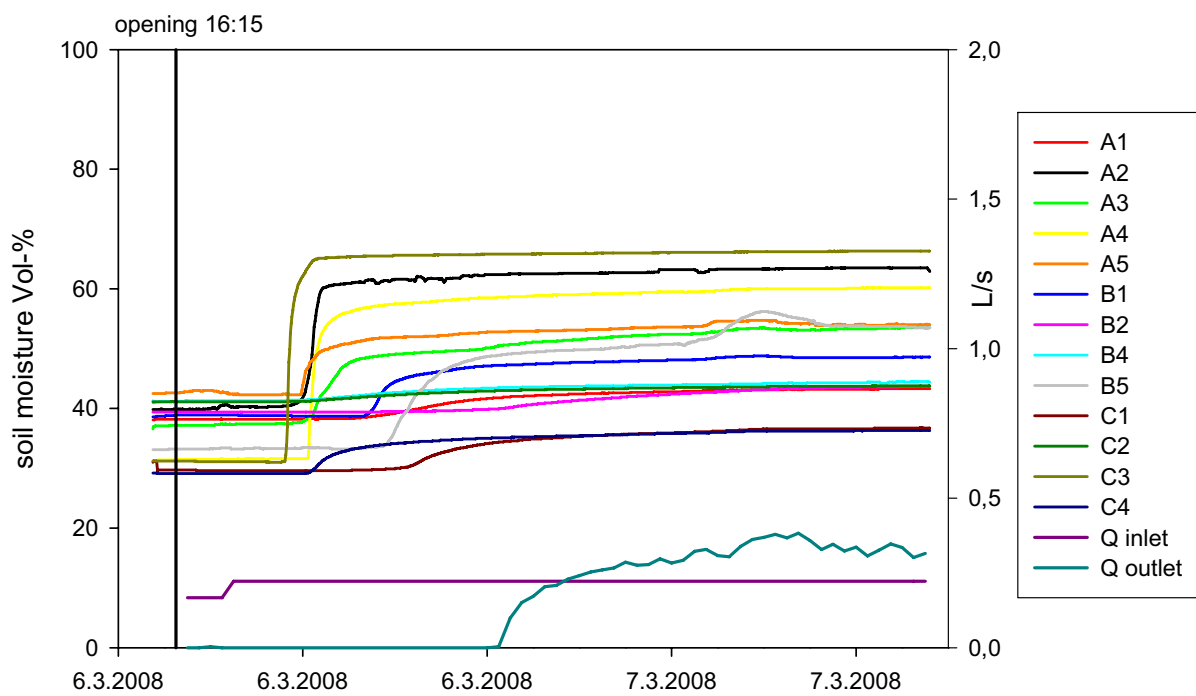


Figure 5.4: Soil moisture recorded by the FDR probes

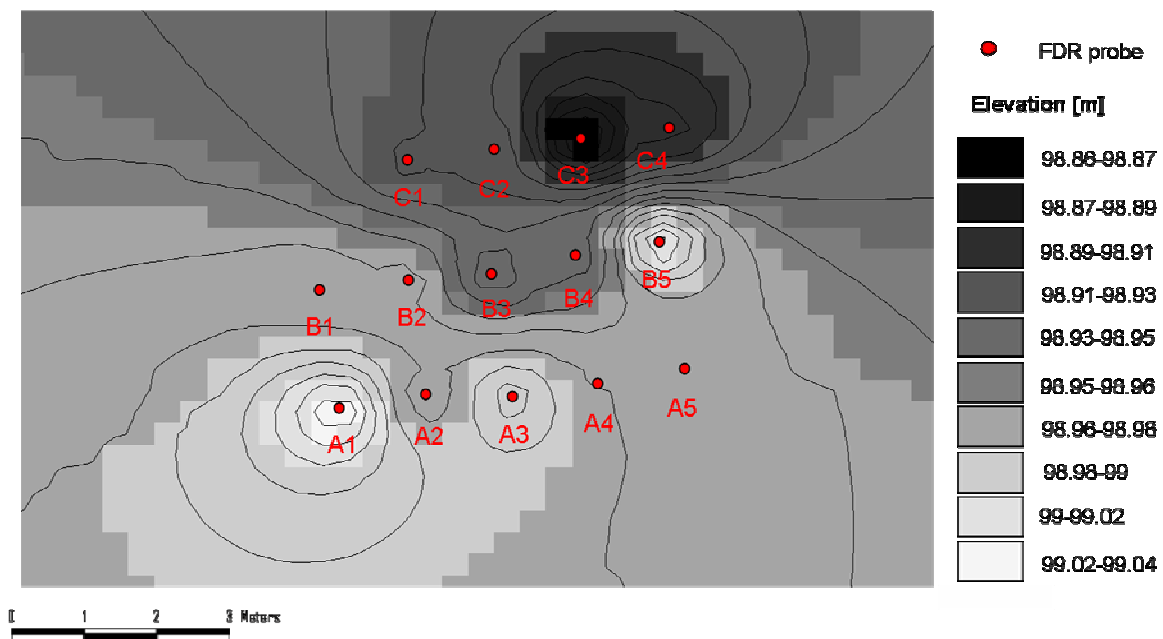


Figure 5.5: ArcView image showing the elevation distribution of the experimental plot. Dots represent the FDR probes.

5.2.2 ECH₂O probes

In three sections using five ECH₂O probes each the volumetric soil moisture content was recorded by data logger whereas one data logger did not work. Thus, data for only two of the sections, Profile 1 and Profile 2, are available. Additionally, the ECH₂O probe P3 in Profile 2 did not work.

The result of the volumetric soil moisture content versus time is shown in Figure 5.6 and Figure 5.7.

In Profile 1, all ECH₂O probes exhibit a similar answer to the wetting front, only P3 shows almost no reaction. In contrast the devices P4 and P5 in Profile 2 reacted different than P1 and P2 Figure 5.7, showing a fast increase of the soil moisture content. The accordant maximum velocities of the wetting front measured by each device are presented in Table 5.4 and Table 5.5.

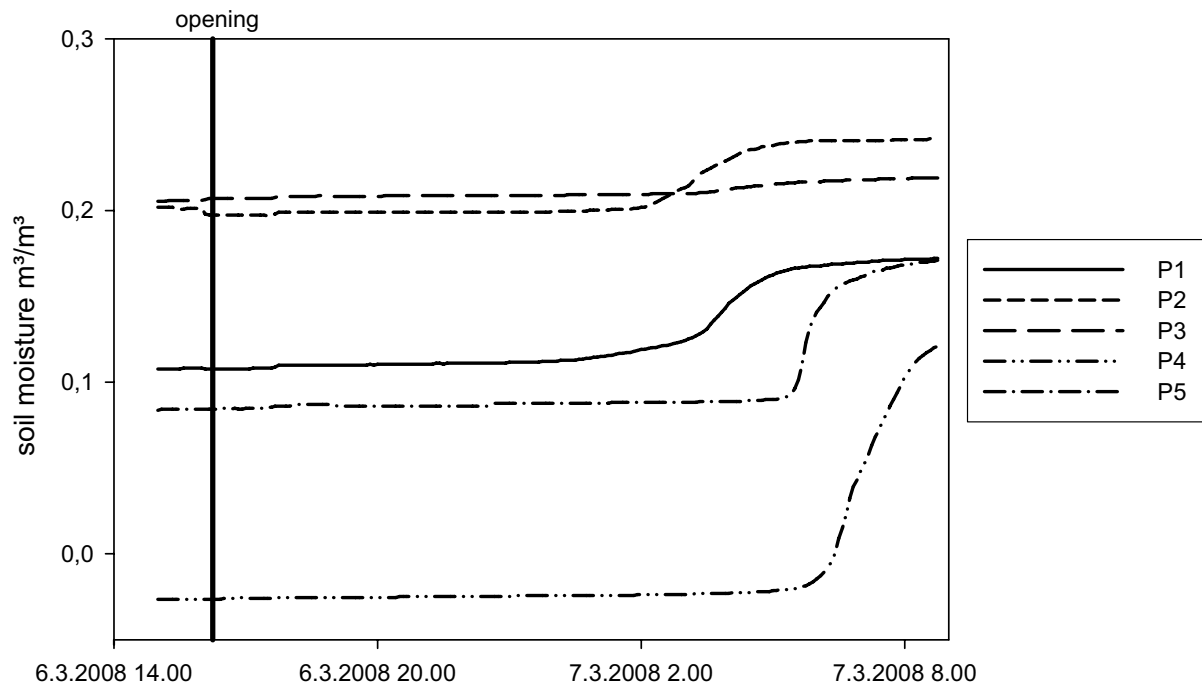


Figure 5.6: Profile 1, soil moisture recorded by the ECH₂O_s.

Table 5.4: Maximum velocities at Profile 1

ECH ₂ O probe	v [m/s]
P1	$1.13 \cdot 10^{-2}$
P2	$1.87 \cdot 10^{-3}$
P3	$1.69 \cdot 10^{-3}$
P4	$1.54 \cdot 10^{-3}$
P5	$1.53 \cdot 10^{-3}$

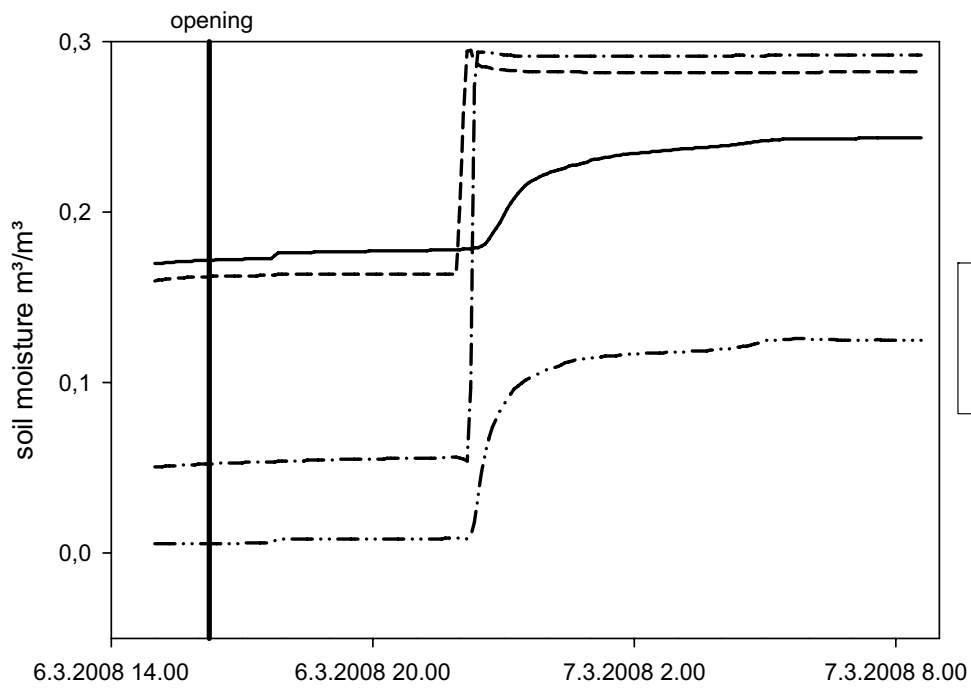


Figure 5.7: Profile 2, soil moisture recorded by the ECH₂Os

Table 5.5: Maximum velocities at Profile 2

ECH ₂ O probe	v [m/s]
P1	$1.27 \cdot 10^{-2}$
P2	$2.49 \cdot 10^{-2}$
P3	-
P4	$1.54 \cdot 10^{-2}$
P5	$7.04 \cdot 10^{-2}$

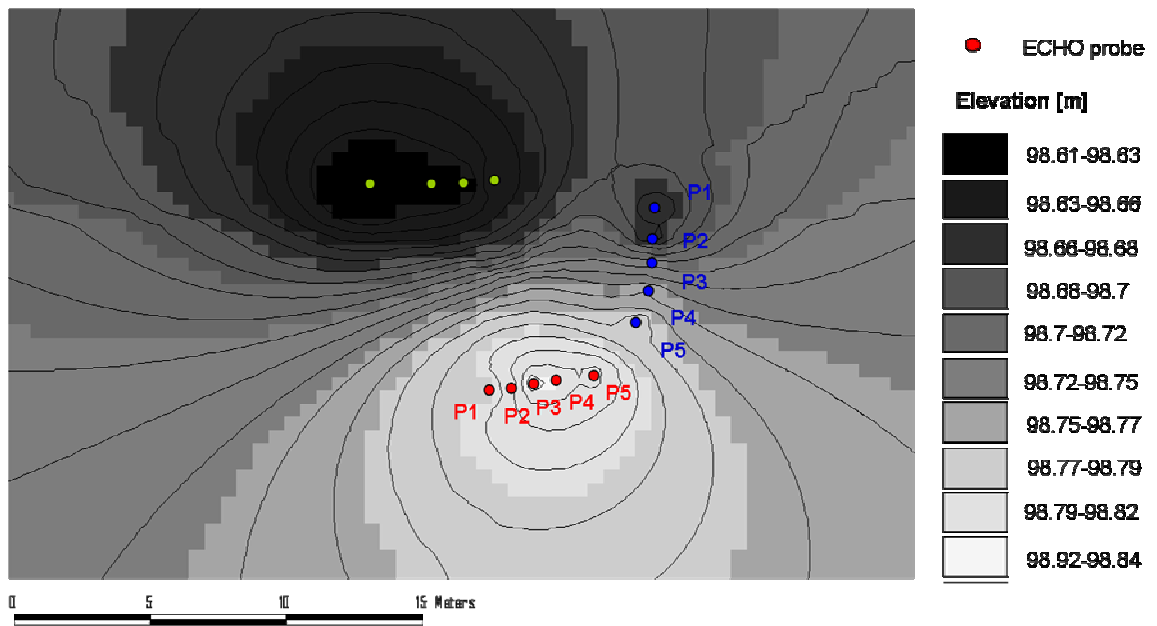


Figure 5.8: ArcView image showing the elevation of the ECH₂O devices (red: Profile 1; blue: Profile 2).

5.2.3 Piezometers

Figure 5.9 shows the electric conductivity in the three piezometers and at the outlet after opening of the forest inlet tube on March, 6th, 16:15. In general, there are several peaks in conductivity at all locations. High EC values are reached immediately after opening as the salt labelled water from the previous experiment was flushed. They react according to their distance: P1 after 75 minutes, P2 after 130 minutes and P3 after 620 minutes, leading to flow velocities of 0.9, 0.6 and 0.2 cm/s, respectively. P2 exhibits a first peak after 680 minutes, its second peak comes along with the first peaks in EC of P1 and P3, according to the injection of the tracers and nitrate.

Another longer-lasting increase in conductivity is then observable for P1, P3 and the outlet, but not in P2.

The accordant water tables measured by the divers in the piezometers are shown in Figure 5.10. Water table rises above surface level with opening of the inlet tube and due to the storm event. Figure 5.11 displays the elevation of the piezometer locations.

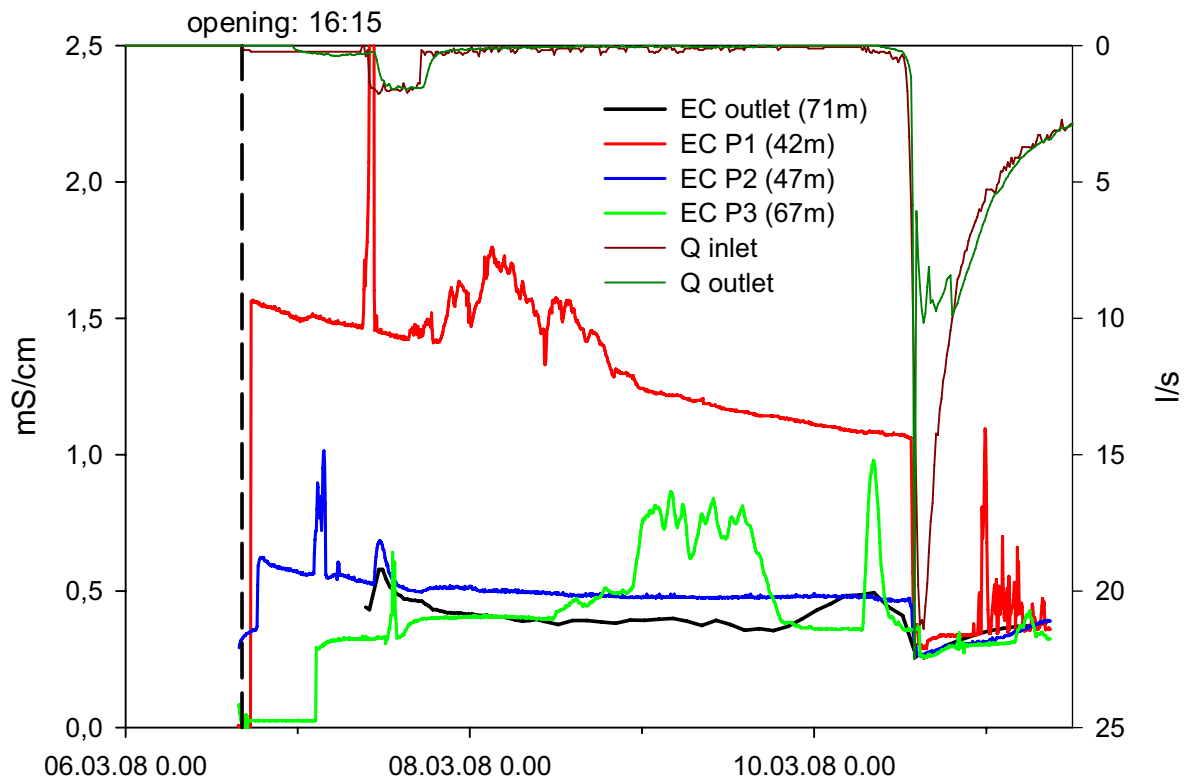


Figure 5.9: Electric conductivity (EC) recorded by the divers in the piezometers 1, 2 and 3

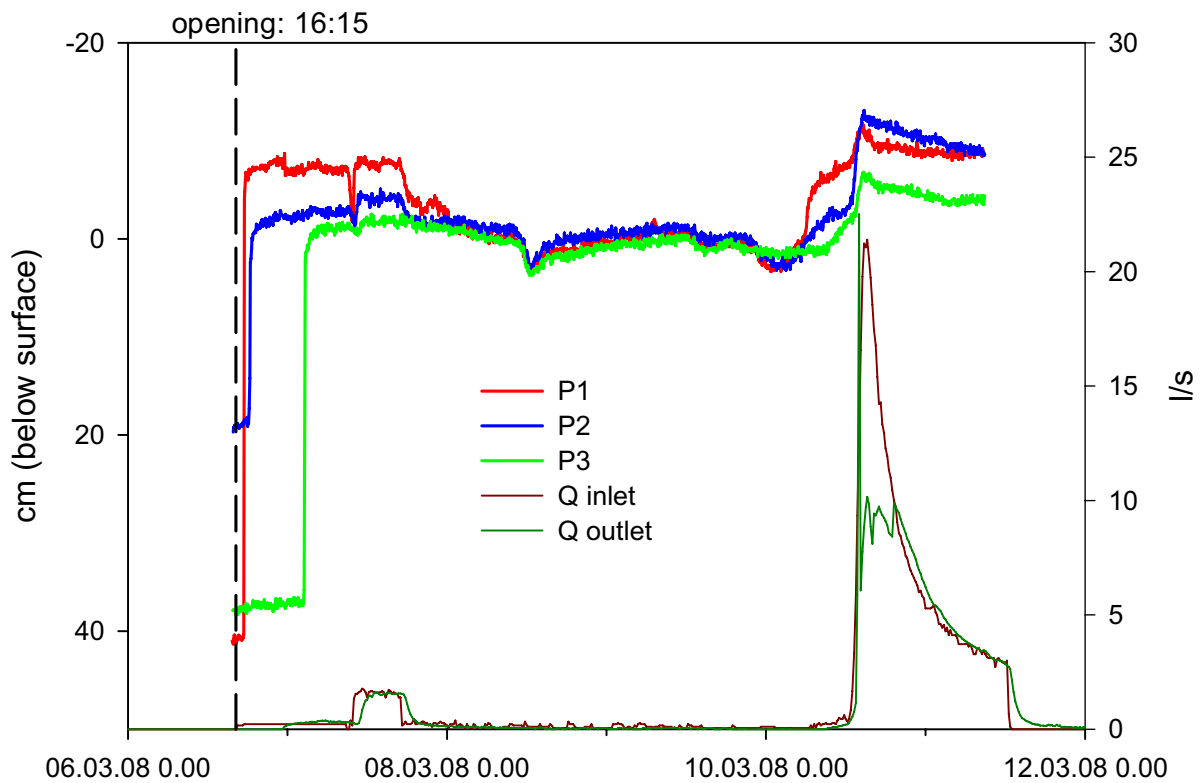


Figure 5.10: Water tables recorded by the divers in the piezometers P1, P2 and P3

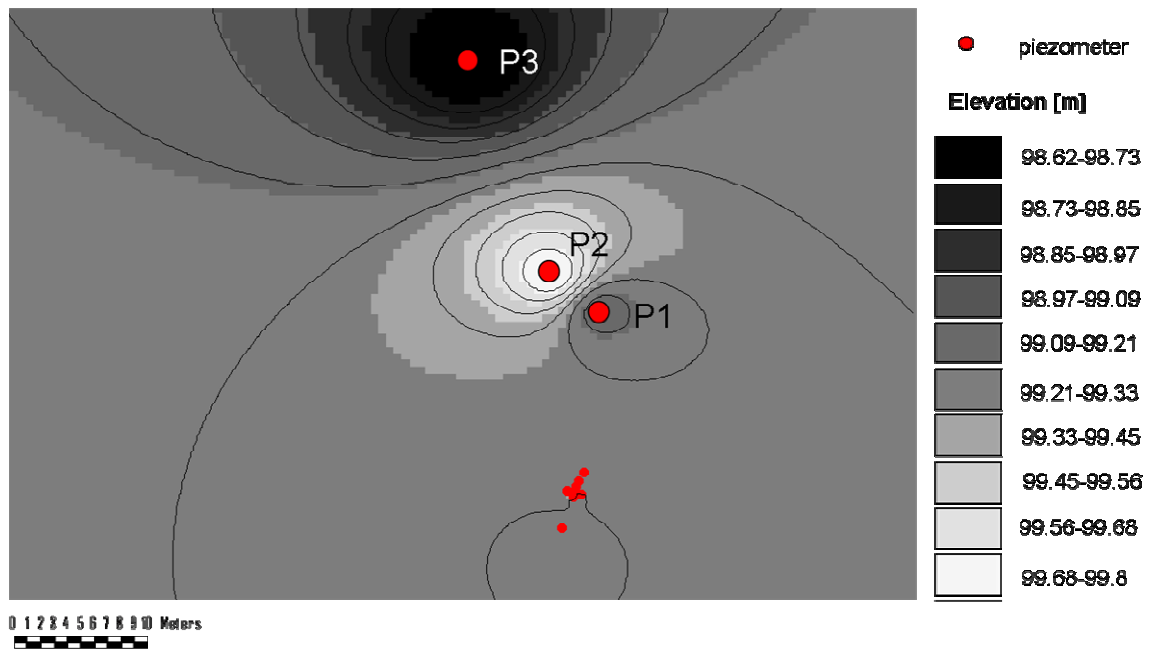


Figure 5.11: ArcView image showing the elevation of the piezometers

5.2.4 Discussion

The runoff at the forest outlet reacted to the opening of the forest inlet tube after 7h15min. It is conspicuous that Q_{out} exceeded Q_{in} , despite the fact that no rainfall occurred within this experiment, but overall, cumulated Q_{in} is higher than cumulated runoff at the outlet. The fill and spill hypothesis by TROMP-VAN MEERFELD & MCDONNELL (2006) says that retention depressions can be first filled and afterwards the water is spilled in delay, hence depending on the micro topography.

It is obvious that the soil moisture devices react according to the surface elevation, if their reaction times are compared to the topographic analysis. The initial reactions of the FDR probes show that not a homogeneous wetting front reached the devices, indicating that the micro topography differs from the local slope of 1%. Hence, different gradients lead to differences in flow velocity and the fact that a sharp interface between humus and clay layer does not exist inhibit a consistent subsurface flow.

FEYEN ET AL. (1999) also reported the influence of micro topography on runoff generation; and observed a high spatial and temporal variability of soil chemicals and hydrological processes even in small catchment of 1500m². Therefore they decided to investigate plots of 13 m² by conducting tracer experiments, in which the interflow component was

distinguishable. Their existent heavy clayey sub-soils were permeable as well, although having a low conductivity.

In general, it remains questionable why the soil water content of 100% is not obtained even though the soil was obviously totally saturated. According to DALTON & VAN GENUCHTEN (1986), a conducting medium such as a saline soil may influence the capacitivity leading to false conclusions in soil moisture measurements. Hence, a calibration should have been done for accurate soil moisture measurements as salt was used in the previous experiment. Therefore, the displayed graphs of the soil water contents rather show the relative behaviour of saturation processes.

The EC results of the piezometers should be regarded censoriously. Disturbances in EC measurements are assured, hence leading to false peaks which remain unexplainable. It is difficult to interpret why such peaks disappear again leading to the question for which reason the EC should decrease that rapidly.

“P1” might react faster because surface flow along ditch is the main occurring runoff process. The first peak in “P2” is also not explainable. The EC level in “P1” is extremely high, so maybe there is salt on the bottom of piezometers because of its higher density. The next EC-increase in “P1”, “P3” and at the outlet could present a second flow path as velocities are the same of 0.01 cm/s if assumed that the increase in EC is affected by the same input. Then, “P2” does not show this reaction because its location is higher elevated as the topographic map shows, but the depression storage theory due to the micro topography is also possible.

5.2.5 Conclusion

Overall, similar problems as in the first experiment show up. The forest plot at Bray is not a suitable site for interflow observations, as there is no sharp interface between a permeable layer overlying an impermeable one enhancing interflow processes. Macropore flow would be a more realistic flow path as they occur in clayey soils.

In general, calculated flow velocities exceeds the assumed ones in several orders of magnitudes, and flow through the litter and surface flow is supposed to be the dominant runoff component as it was observable anyway.

5.3 Tracer Experiment Results

5.3.1 Dye Tracer

5.3.1.1 Analysis

The analysis of the dye tracer concentrations of the “FM” and “FO” samples has been carried out at the IHF, using the *Perkin Elmer* LS 50 B Luminescence Spectrometer. All UA concentrations of the samples taken prior the storm event were calculated via the relationship:

$$y = 0.02 \cdot x - 0.6853 \quad (5.3)$$

and SRB concentrations by applying:

$$y = 0.3419 \cdot x - 1.4643 \quad (5.4)$$

where y =concentration and x =intensity of fluorescence with $R^2=1$ for both calibration lines.

Applying the synchroscan method, problems with high fluorescence background occurred for all samples taken as from the storm event, which started on 10.03.2008 about 13 pm. Thus, the UA and SRB peaks could not be distinguished clearly (Figure 5.12).

The high fluorescence background has been tried to be eliminated by filtration using 0.45 μm and 0.2 μm filters. Figure 5.12 shows the effect of filtration on a blank sample (10.03.2008 15:10) taken upstream of the inlet ditch and on the sample “FO64” (10.03.2008 16:20) which was taken at the forest outlet. After filtration with 0.45 μm filters, the fluorescence background was still too high. Therefore, all samples as from the storm event were filtered with 0.2 μm filters. The fact that tracer remains in the filter requires a new calibration, thus a new calibration was made obtaining:

$$y = 0.2945 \cdot x + 0.2712 \quad (5.5)$$

for SRB with $R^2=0.932$, whereupon between 11 and 30% of the tracer remained in the filter. UA concentrations were not calculated because no clear UA peaks in fluorescence could be observed (see Figure 5.12). Even without high fluorescence background, UA would probably not be detectable anyway as it is assumed to be degraded after 5 days due to photochemical decay.

Before the storm event the pH value was quite stable, ranging between 6.75 and 7.30. UA fluorescence is only about 80% and less for those pH values. Due to acid rainfall, the pH decreased rapidly during the storm event to 6.20 at 14:15 down to 5.27 at 15:00. The low pH values indicate that UA fluorescence is less than 40%. Even alkalisation did not lead to better results. Thus, concentrations of UA are probably underestimated.

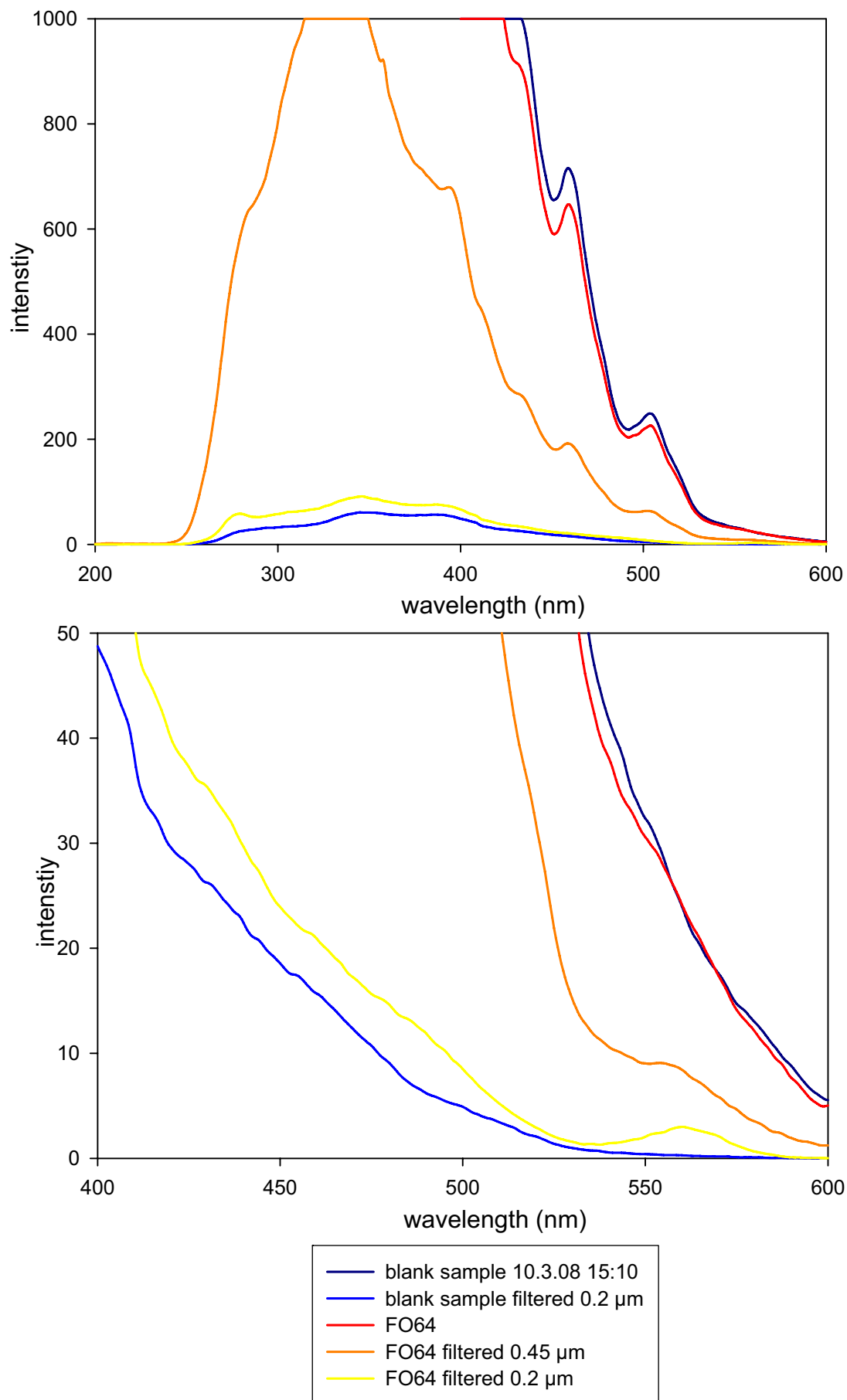


Figure 5.12: Comparison of synchroscans of unfiltered and filtered samples

5.3.1.2 Breakthrough curves

Figure 5.13 shows the resulting dye tracer concentrations measured in the samples taken by the automatic sampler at the outlet of the forest plot. The tracer cocktail was injected through the forest inlet tube at 09:45 on March, 7th. As the flow rate was very low (0.2 L/s), tracer flow back into the main ditch. To avoid tracer input into the wetland, the wetland inlet tube was closed resulting in increasing discharge in the forest plot (1.4 L/s). After reopening of the wetland inlet tube the discharge again decreased to 0.2 L/s at 17:15. Thus it can be assumed that during the first 7.5 hours of the tracer experiment steady state conditions were obtained with an average flow rate of 1.6 L/s.

The first detection of both dye tracers at the forest outlet was at 11:20, only 95 minutes after injection, yielding to a maximum velocity of 1.25 cm/s. Peak concentrations were observed at 11:50 for UA and at 12:20 for SRB, leading to flow velocities of 0.95 cm/s and 0.77 cm/s, respectively. Mean velocities can be calculated by taking the time when 50% of the injected tracer mass is recovered, leading to 0.55 cm/s for UA and 0.48 cm/s for SRB

On March, 9th a heavy storm event started where trees broke down, but there was still SRB amounts visible in the entrance ditch. These dye tracer amounts were probably washed out by the rainfall event on March, 10th, resulting in a second increase in SRB concentrations. Thus, the recovery rates for SRB can be separated regarding the conditions existing between 07.03.2008 and 10.03.2008 and the rainfall event conditions starting at noon on March, 10th.

Figure 5.14 presents the recovery curves for SRB and UA. Overall, calculation of the tracer recovery yield 39.0% for SRB including the storm event and 26.1% excluding the storm event. For UA, the total tracer recovery is 33.1%, excluding the storm event as data are not available after March, 10th, 12:20.

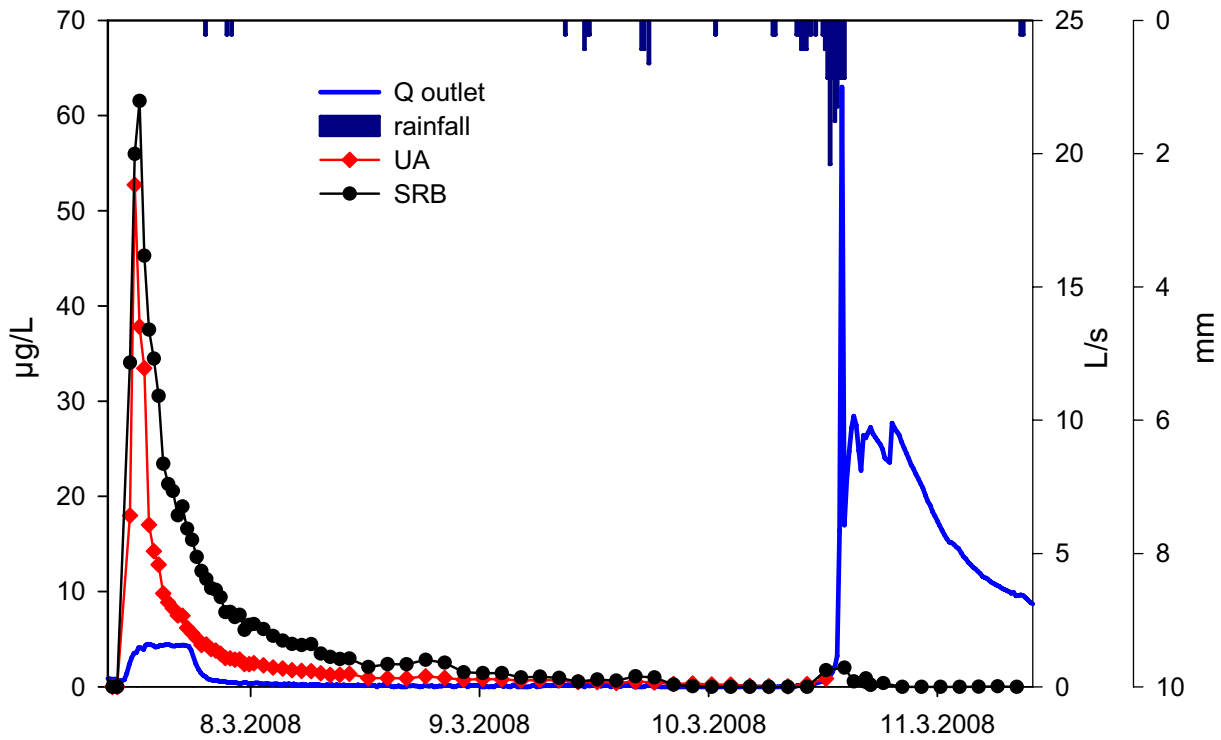


Figure 5.13: UA and SRB breakthrough curves at "forest outlet" ("FO")

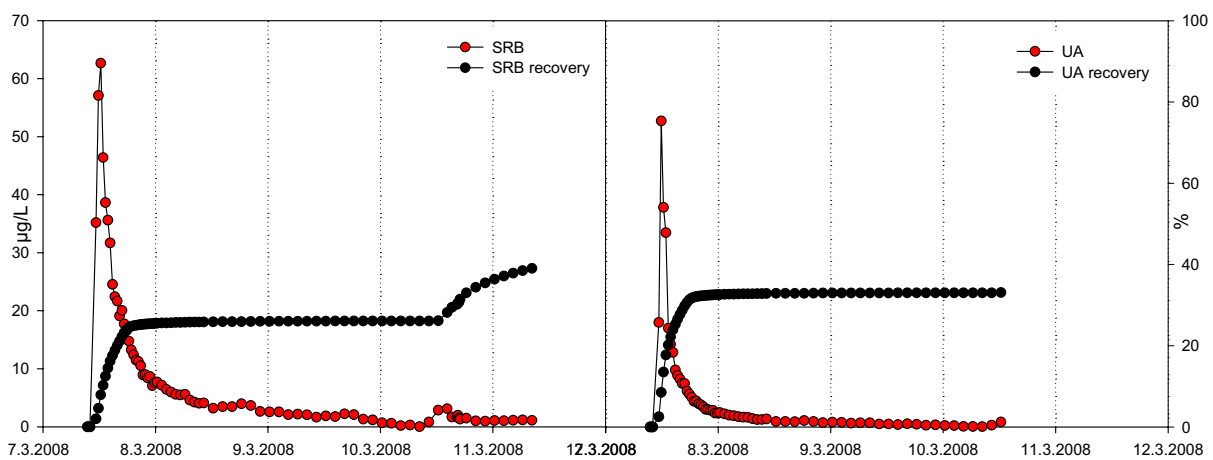


Figure 5.14: Tracer recovery curves for SRB and UA

The tracer breakthrough curves at the "forest middle" station shows a variable progression (Figure 5.15). No samples were taken in the inlet ditch, thus varying input concentrations are not known. Due to the low flow rate after reopening of the wetland inlet tube, there is a range of missing values when the automatic sampler fell dry overnight from March, 7th, to 8th. The intake tube of the automatic samples was then moved to a water filled area, but the discharge remained low (0.2 L/s). Recovery rates are 56.3% for UA and 68.1% and 50.0% for SRB including and excluding the storm event, respectively.

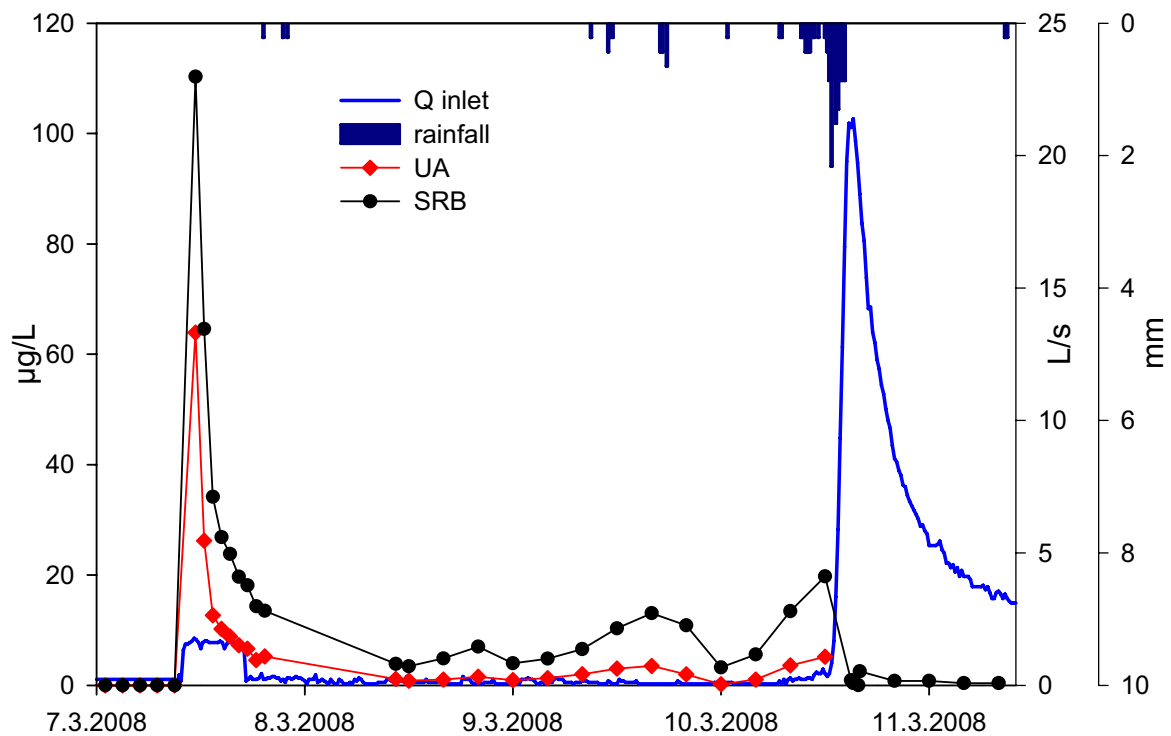


Figure 5.15: SRB and UA breakthrough curves at "forest middle" ("FM")

The filter fluorimeter installed at the outlet of the forest recorded the SRB and UA concentrations continuously. Figure 5.16 shows the UA and the SRB concentrations compared to the results from laboratory equipment. The behaviour of the breakthrough curves is similar. UA even shows a little increase in concentration for the storm event. But the SRB curve progression shows that some material or turbidity disturbed the measurements. During low flow periods, the instrument had to be installed again in deeper parts of the ditch. This movement resulted also in increasing turbidity which is responsible for the first artificial peak on 10.03.2008. The next peak starting on 10.03.2008 13:00 is due by the turbidity caused by the stormy rainfall event. In general, the concentrations do not trace back to zero because the calibration of the filter fluorimeter was made in the laboratory prior the field experiments. For calibration, distilled water has been used instead of blank sample as there was no blank sample available prior experiment. Unfortunately, the pH of the used distilled water is only 5.5 which diminish the dye tracer concentrations.

For further investigations, the laboratory analysis results are taken, because the quality of filter fluorimeter is less as there are not sensitive enough (WGSHS 2003). Even though there is a good correlation between concentrations measured by the filter fluorimeter and the *Perkin Elmer* results (Figure 5.17).

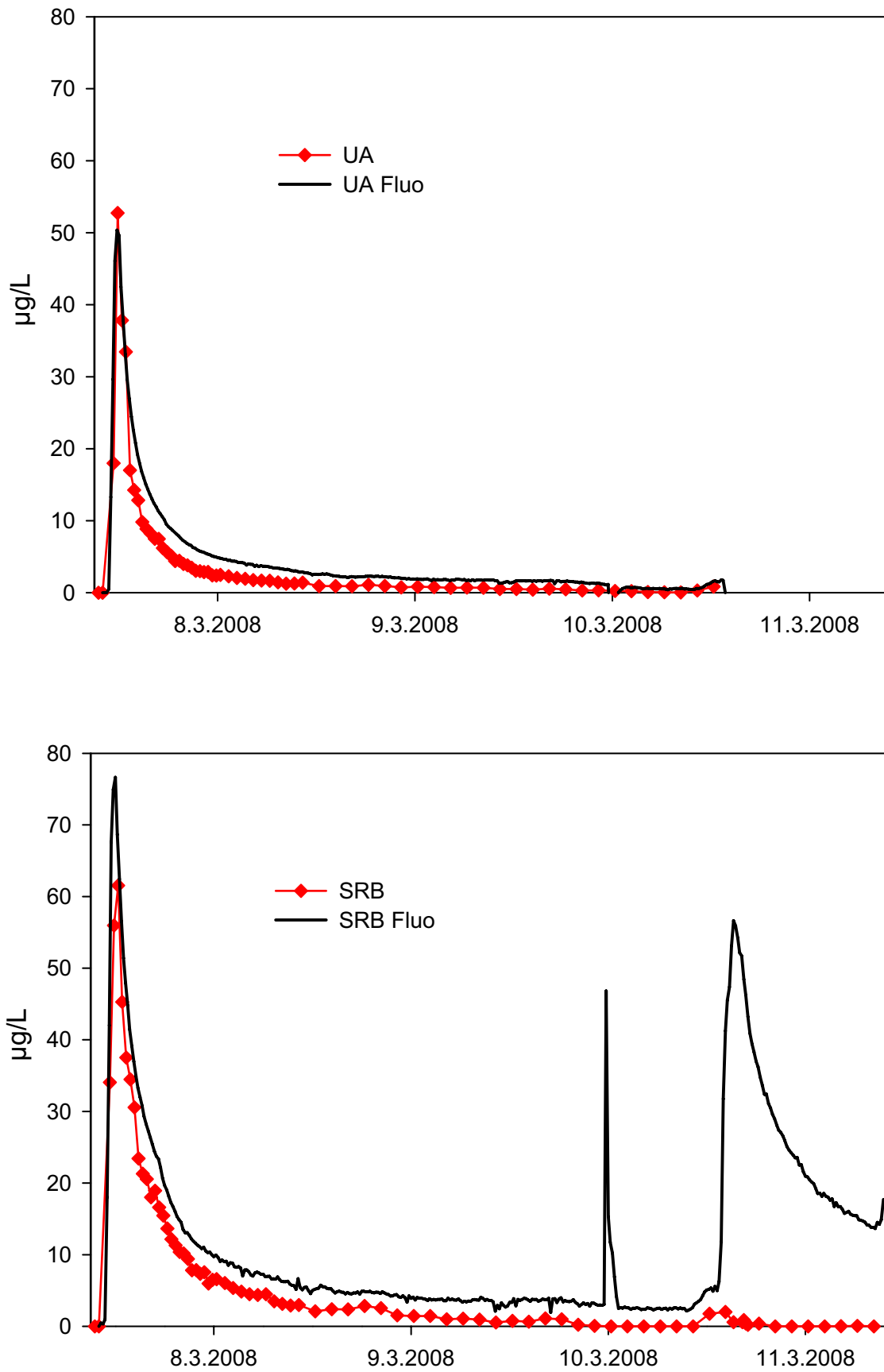


Figure 5.16: UA and SRB breakthrough curves compared to the UA and SRB breakthrough curves recorded by the filter fluorimeter ("Fluo")

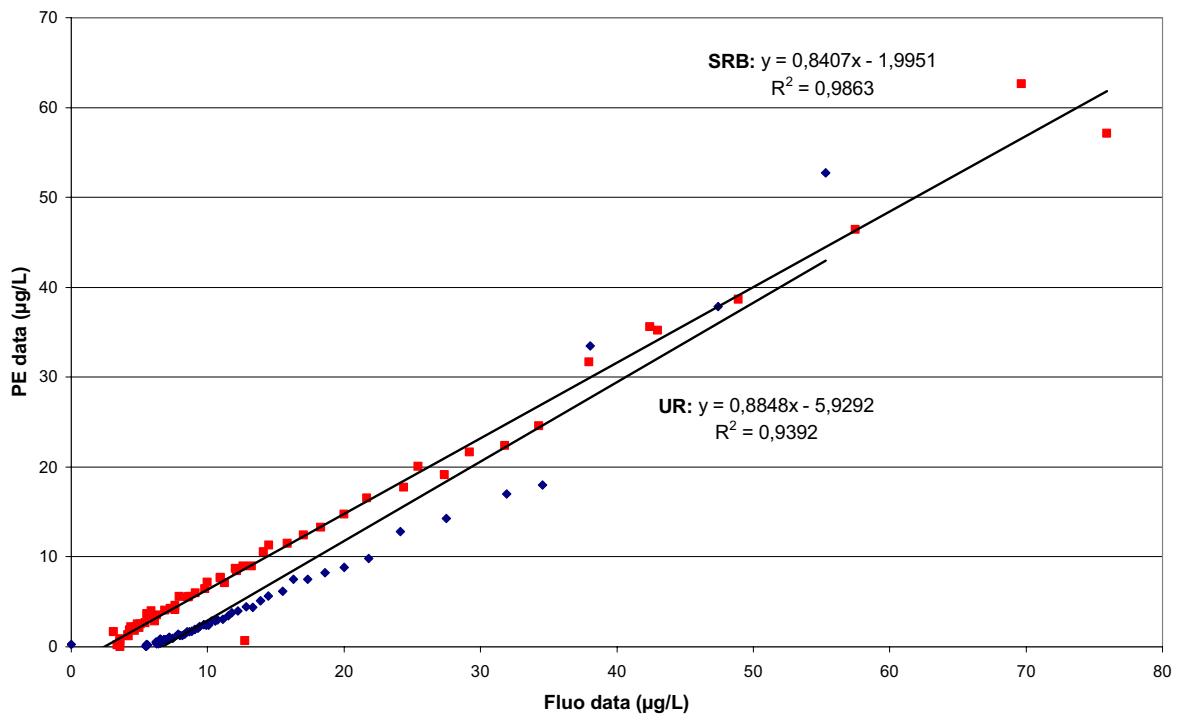


Figure 5.17: Correlation between the continuous data ("Fluo data") and the laboratory results ("PE data"). Storm event excluded.

5.3.1.3 Mathematical Modelling using the Dispersion Model

The dispersion model can be applied for the Uranine and the Sulforhodamine B breakthrough curve. Due to unsteady state conditions not concentrations but mass fluxes are simulated. The best visual fit to the measured data is shown in Figure 5.18. A good fitting for the SRB breakthrough curve is obtained by assuming one flow path. The UA curve is better simulated by superposition of two flow paths, but as UA and SRB were in the same solution taking the same flow path, it was also fitted by simulating one single flow path. Applying the usual dispersion model SRB data are underestimated but UA data overestimated. Thus, a term for photo degradation was additional included in the dispersion model for the UA data, but simulated mass fluxes are still higher than the measured data. Peak concentrations were hard to fit.

The fitting parameters for simulations are the dispersion parameter $P_D = 0.18$ (for UA, for SRB=2.5) and the mean velocity $v = 0.003$ m/s leading to a mean residence time of 6.6 h.

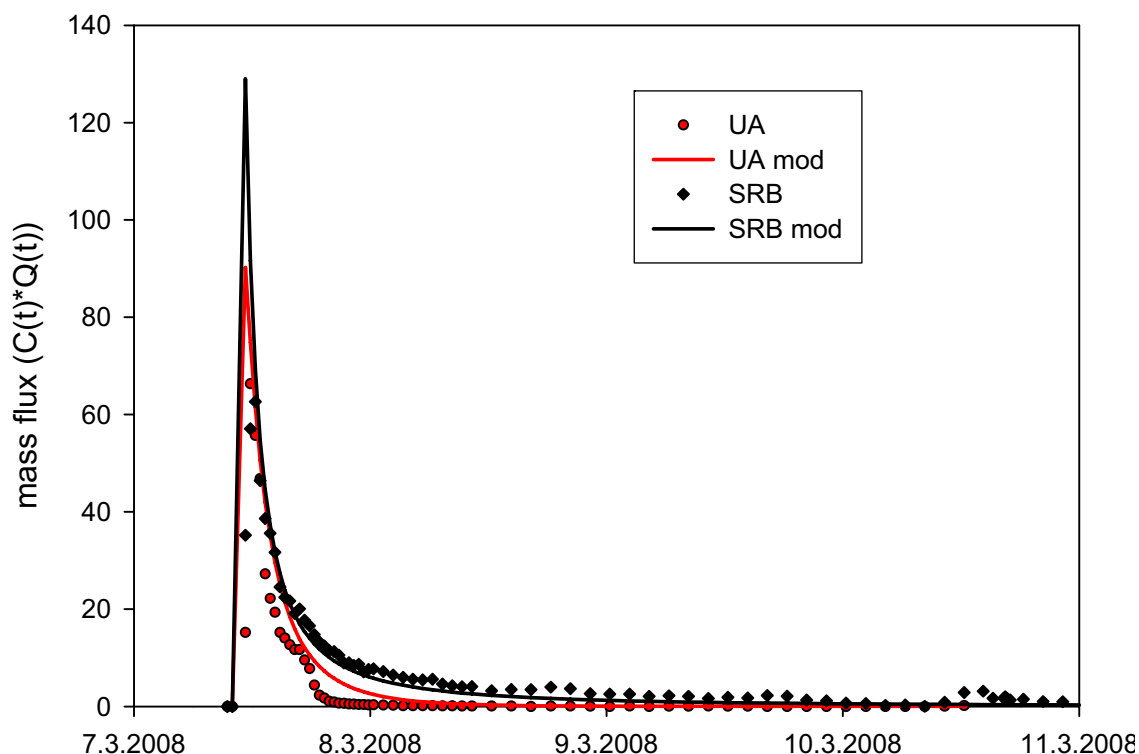


Figure 5.18: Simulated breakthrough curves using the dispersion model

5.3.1.4 Discussion

The results in dye tracer concentrations constitute to instructive tracer breakthrough curves despite the fact that the analysis was difficult for the storm event samples as the fluorescence background was high due to disturbances. Many natural occurring matters like humic substances and other macromolecules can disturb fluorometric analysis, resulting in false conclusions (FRANKE ET AL. 1997). Also SMART & LAIDLAW (1977) reported high backgrounds caused by natural fluorescence and suspended sediment. FRANKE ET AL. (1997) could separate compounds causing background fluorescence by solid-phase extraction at a pH of 3, because the molecules were then uncharged and retained by the sorbent. But fluorescence of organic matter, e.g. dissolved organic matter can also be useful as a tracer, as represented in the work of MARIOT ET AL. (2007).

By using the dispersion model, the two meaningful characteristics which are the mean transit time and the dispersion parameter could be determined.

The dispersion parameter P_D is very small which indicates that, according to the relationship

$$P_D = \frac{D_L}{v \cdot x},$$

convection is the main process for transporting the dye tracers. Even though the

mean transit time of both tracers is only 6.6 h for the whole system (530 m²), the forest plot show a respectable retention capacity. After a flow distance of 71 m, only 39.0% of SRB was recovered. As no data are available for UA during the storm event, the recovery of UA is 33.1% and probably underestimated. The fact that the fitting of the dispersion model including a term for photo degradation leads to a better fit on the UA mass flux, confirms that UA is sensitive to light and recovery rates are lower due to photo degradation. But half-times allow only a rough estimation of this degradation because they are usually determined under laboratory conditions which differ from field conditions, e.g. the intensity of radiation varies in time and space as well as the shadowing of trees influences (LEIBUNDGUT ET AL., unpublished). Thus, the low recovery of UA should be regarded censoriously.

All recoveries for “FO” were calculated with the runoff data from the outlet (Q_{out}). It is obvious that Q_{out} is different from Q_{in} . During the storm event, runoff was too high to leave the forest plot through the outlet. Thus, outflow was also observed at the other end of the outlet ditch and via the adjacent path leading to lower runoff data at “FO”. Mass balance calculations yield that about 17% of the inflow during the storm event was not recorded at the outlet. As saturation was reached, these 17% are suggested to be runoff losses. Therefore, all recoveries calculated for “FO” are underestimated. Recoveries for “FM” were calculated by using Q_{in} because the inlet ditch contributes directly towards the automatic sampler “FM” after a flow distance of approximately 40 m, leading to higher values e.g. of 68.1% for SRB. Table 5.6 shows the differences in recoveries of the dye tracers depending on the experimental period (if the storm event is included or not).

Table 5.6: Recoveries of dye tracers depending on the runoff data and the experimental period

Tracer	Sampling site	Q	Excl. storm	Incl. storm
UA	FM	Q_{in}	56.3%	-
	FO	Q_{out}	33.1%	-
SRB	FM	Q_{in}	50.0%	68.1%
	FO	Q_{out}	26.1%	39.0%

The dye tracers have been applied after a salt experiment. According to SMART & LAIDLAW (1977), dye tracers may be affected if used in saline environments. Fluorescence of SRB might decrease with increasing salinity. Therefore, dye losses must not only be attributed to adsorption. For reference, a conservative tracer should also be injected conducting tracer experiments. Numerous field studies have been carried out using KBr as a conservative tracer (e.g. VELLIDIS ET AL. 2002) leading to comparable data sets.

The tracer breakthrough curves of UA and SRB are both comparable to the ideal breakthrough curve in Figure 5.19 with little dispersion, hence $v_{water} = v_{tracer}$. The high runoff coefficients calculated in chapter 3 also implement that the breakthrough curve is mainly influenced by convection, thus surface flow is supposed to be the major flow path.

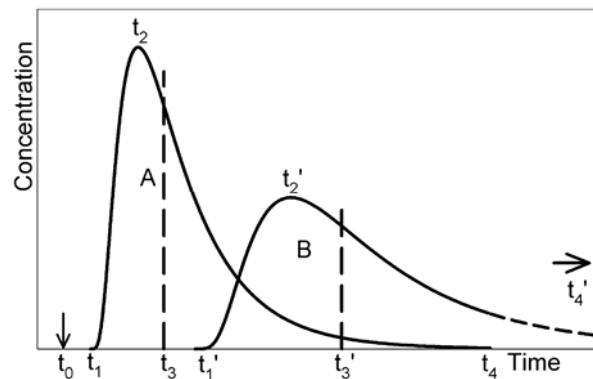


Figure 5.19: Tracer breakthrough curves (curve A: ideal tracer; curve B: reversible sorption) (LEIBUNDGUT ET AL. unpublished)

The second peak in SRB concentration during the storm event is caused by the fact that there were still SRB amounts visible in the inlet ditch (Figure 5.20). It is apparent that the tracer remained at the bottom due to the low flow rate and higher density as salt has also been used in concentrations higher than recommended by KÄSS (1998). These amounts were then flushed out by the increased discharge. Also WAUCHOPE ET AL. (2002) reported that remaining deposits will eventually be washed out by rain. This “first flush effect” usually occurs within the first major rainfall after application or injection (e.g. DÖRFLER ET AL. 2006) and will be also discussed in chapter 5.3.2.2.



Figure 5.20: SRB residues in the inlet ditch still on March, 10th prior the storm event.

5.3.2 Isoproturon

5.3.2.1 Results

Isoproturon was measured in 16 samples of “FO” and in six samples of “FM” which have been filtered instantly on the field. They were analyzed by Cemagref Antony after the experimental period by using *ELISA* immunoassay tests. Figure 5.21 and Figure 5.22 presents the non-uniform curves of Isoproturon concentrations versus time. Both curves show a highly variable behaviour possessing several peaks in concentration.

The first peak in Isoproturon concentration at “FO” due to the injection of 50 g IPU diluted in 60 L is not completely documented. The first analyzed sample (07.03.2008 11:20) already exhibits a maximum in concentration of 535 $\mu\text{g/L}$. A second peak of 372 $\mu\text{g/L}$ is recorded in the sample of 08.03.2008 03:20. After a minimum of 13.2 $\mu\text{g/L}$ (08.03.2008 16:20), concentration increases and the sample taken during the storm event is even again higher concentrated (61 $\mu\text{g/L}$).

The maximum peak at “FM” is measured in the sample of 07.03.2008 19:24 with 434.5 $\mu\text{g/L}$ which is delayed compared to the maximum concentration of “FO” despite the fact that “FM” is closer to the injection station. After a minimum of 75.7 $\mu\text{g/L}$ which is also on March, 8th, concentration rises again. After the storm event, both concentration curves end up in low values of about 14 $\mu\text{g/L}$.

The calculation of the dominant IPU velocities based on the main peak leads to 1.25 cm/s at “FO” and 0.2 cm/s at “FM”.

Accounting the recovery rates depending on the implemented runoff data and whether the storm event is included or not leads to the results shown in Table 5.7.

Table 5.7: Recoveries of IPU depending on the runoff data and the experimental period

Sampling site:	Q	Excl. storm event	Incl. storm event
FO	Q_{out}	20.5%	42.5%
FM	Q_{in}	27.5%	35.3%

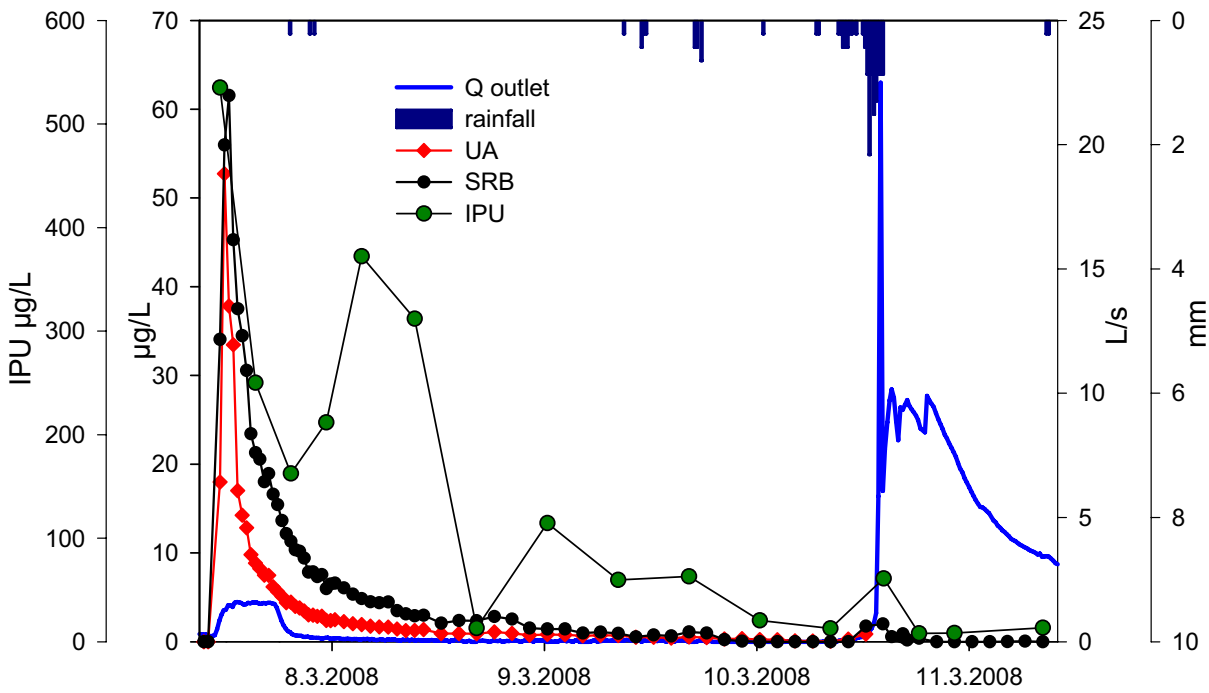


Figure 5.21: UA, SRB and IPU breakthrough curves at "FO"

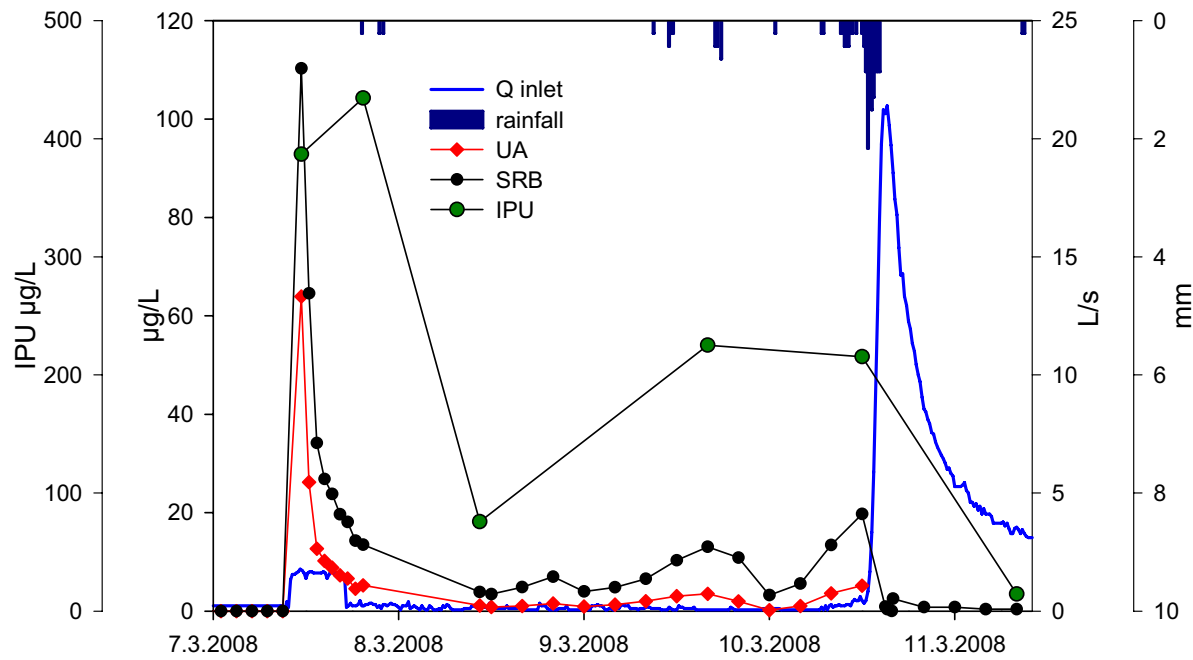


Figure 5.22: UA, SRB and IPU breakthrough curves at "FM"

5.3.2.2 Discussion

Overall, IPU shows diversifying values in concentration at both sampling sites. This non-uniform behaviour of the pesticide IPU was also observed e.g. by Worrall et al. (1997) or Harris et al. (1994). They conducted batch experiments regarding sorption processes over time. After the injection, a first fast initial sorption to the solid phase took place, leading to a maximum in sorbed concentration. The next process occurring was desorption, after what the sorbed concentration increased again to its equilibrium value due to diffusion between the aqueous phase, soil surface and colloidal matter, shown in Figure 5.23. These processes could be an explanation for the varying IPU concentrations. The first peak is caused by the injection, then concentrations decrease as the pesticide is sorbed or flush out, and increase again due to desorption processes, accordingly. The next minimum in concentration is documented only by one single sample, which could be an error in analysis. Otherwise it is hard to interpret why another sorption process should take place. The IPU concentrations at “FM” are also difficult to discuss as only very few samples were analyzed. According to Worrall et al. (1997), again the concentration sequence could be maximum (injection) – minimum (sorption) – maximum (desorption) – equilibrium.

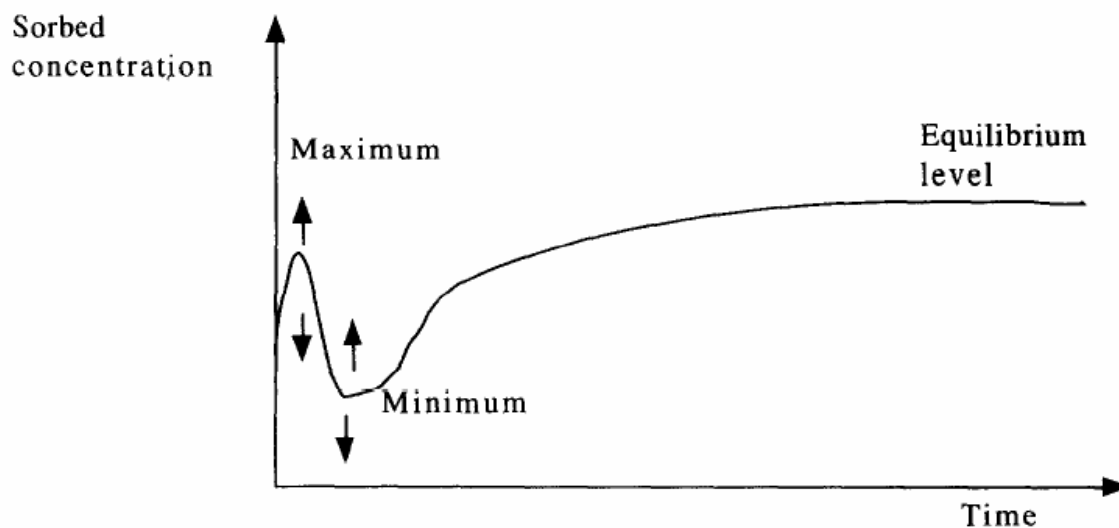


Figure 5.23: Sorbed concentration versus time observed in batch experiments (Worrall et al. 1997).

That indicates that sorption processes are an important factor influencing the concentrations of pesticides in aqueous environments, resulting in low recovery rates of 42.5% at “FO” and 35.3% at “FM”. Hence, the recovery rate at “FM” is lower than at “FO”, even though “FO” is more distant. The fact that the peak in IPU concentration at “FM” is later than at “FO”

confirms additionally that the series of data at “FM” is questionable as temporal resolution is low.

Especially organic matter is an important sorbent, as well as clay minerals offer preferred sorption sites (WAUCHOPE ET AL. 2002) due to their excess of imbalanced negative charges (FETTER 2001). The soil at the experimental site has clay contents ranging from 26% up to 36.6% depending on the soil depth, thus adsorption on clay is possible. Also dissolved organic matter can play a role in sorption, as reported by ERTLI ET AL. (2004) and WORRALL ET AL. (1997). NEMETH-KONDA ET AL. (2002) conducted several experiments on an agricultural Luvisol with 15.4% clay regarding the sorption behaviour of several pesticides. There, it has been shown that particularly soil organic matter influences adsorption and desorption processes, enhancing a time delayed release of the pesticide. Therefore, the K_{OC} value provides a reasonable parameter for the interpretation of pesticide compartment, but it is directly related to the partition coefficient K_d which is soil dependent. Thus, additional batch experiments are required.

HARRIS ET AL. (1994) reported that IPU was rather persistent and degraded slowly with 35% of applied amount persisting after 4 month.

Another important process which can be observed is the washout effect caused by the storm event. The recovery rates including the data obtained during the storm event are significantly higher than those excluding it. At the forest outlet, the recovery until March, 10th, 12:00 is only 20.5%, but afterwards 42.5% of the injected pesticide is recovered. This can be explained by the first flush hypothesis. The first major rainfall after pesticide application is the most important for the transport of pesticides, as remaining deposits are washed out (WAUCHOPE ET AL. 2002, DÖRFLER ET AL. 2006, HARRIS ET AL. 1994).

Also VELLIDIS ET AL. (2002) reported that the movement of the two examined herbicides Atrazine and Alachlor in surface runoff took place primarily in events within short period after their application. High pesticide loads in surface runoff and their occurrence in few events after application was already observed by WU ET AL. (1983).

5.3.3 Electric Conductivity, Anions and Cations

5.3.3.1 Results

Electric Conductivity

The electric conductivity was measured continuously in time steps of 5 minutes at the forest outlet. There occurred problems with the measurement device during the storm event, probably because of disturbances due to high turbidity in the discharge. Therefore, electric conductivity was also measured in the sample bottles at the IHF later on April, 8th. Those values differ from the continuous data as it can be seen in Figure 5.24. Precipitation processes of substances in the sample bottles could be a possible explanation for lower values in conductivity. Figure 5.24 shows an increase in EC prior the storm event, whereas the continuous data are fairly constant about 500 $\mu\text{S}/\text{cm}$.

All conductivity curves exhibit peaks on March, 7th, 11:20 which is only 95 minutes after the injection of the tracer cocktail due to the injected nitrate, leading to a flow velocity of 1.25 cm/s. The remarkable decrease on March, 10th, is caused by the storm event leading to dilution.

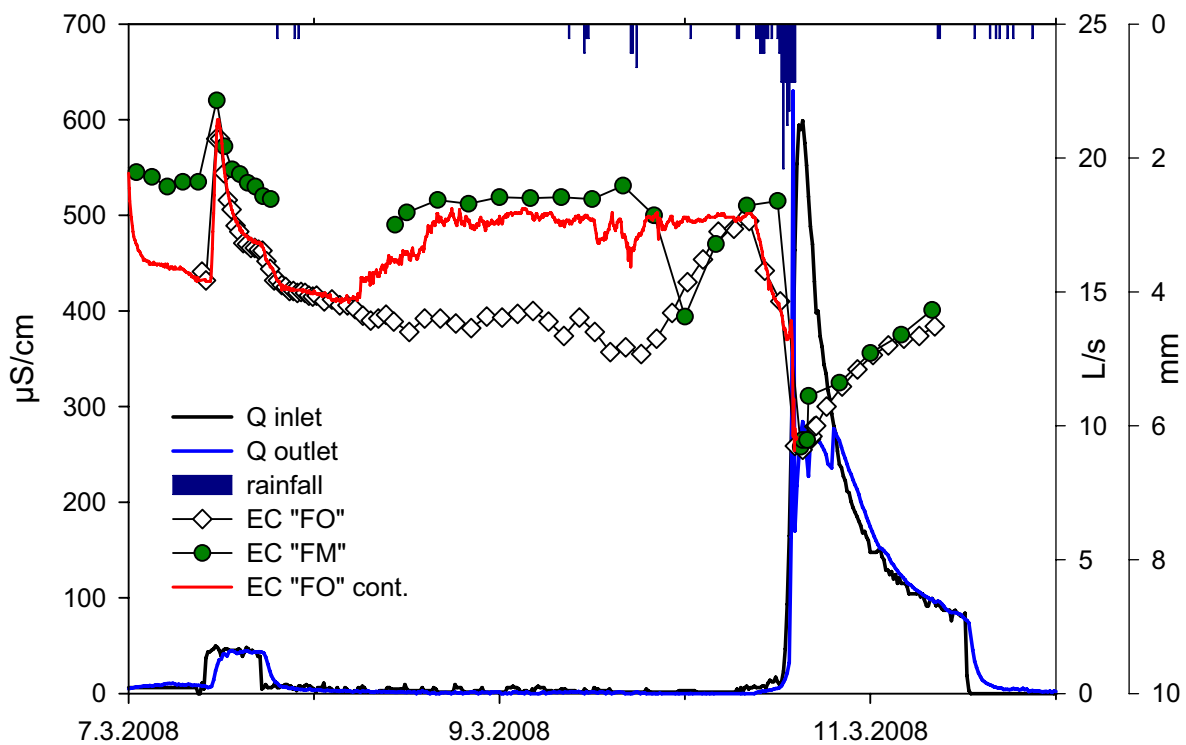


Figure 5.24: Electric conductivity at "FM" and "FO".

Anions

Figure 5.25 and Figure 5.26 show the behaviour of the concentrations of chloride, nitrate and sulphate analyzed by Cemagref Antony. The 16 samples analyzed for “FO” show interesting concentration progressions (Figure 5.25), whereas for “FM” again only six samples were analyzed showing fairly constant values (Figure 5.26).

All species except SO_4 are higher concentrated with the start of the tracer experiment, whereas the first analyzed sample is already during peak tracer concentrations.

At “FO”, NO_3 shows high concentrations due to the injection of KNO_3 with a maximum of 72.33 mg/L (07.03.2008 11:20) which is only 95 minutes after the injection (09:45). The concentration then decreases to a minimum of 2.92 mg/L (10.03.2008 08:20). With the beginning of the storm event on March, 10th, again concentration increases to 23.52 mg/L on 10.03.2008 18:20, rising up even afterwards to 64.8 mg/L on March, 11th.

For chloride, only one sample documents a peak of 58.95 mg/L only 95 minutes after tracer injection. A second slight increase is observed prior the storm event. The distinct decrease in Cl concentration is caused by dilution due to storm event (minimum of 14.46 mg/L at 10.03.2008 18:20).

In contrast, sulphate concentrations behave fairly constant. Only a slight increase immediately after injection and another one with increasing discharge (up to 23.52 mg/L 10.03.2008 18:20) appear.

For “FM”, no interesting variations in concentrations of the anions are observable. NO_3 concentrations are higher due to the KNO_3 injection, but as only few samples were analyzed, the peak is again not completely documented.

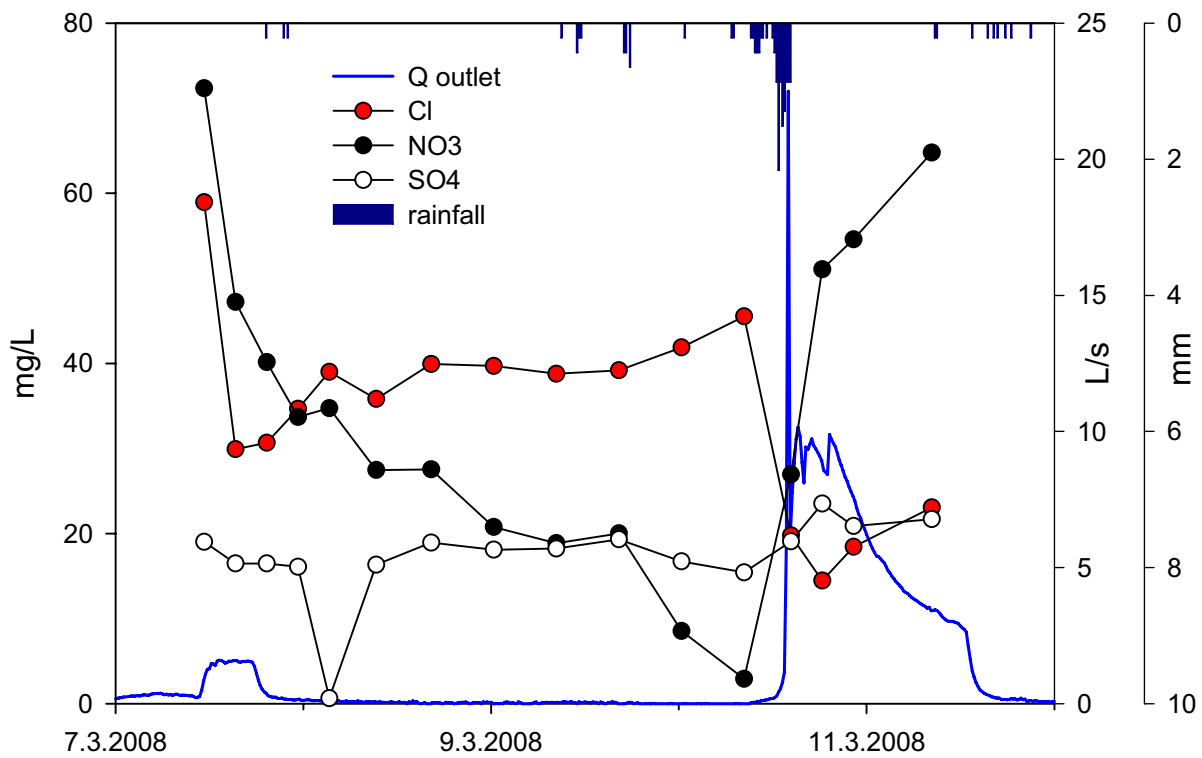


Figure 5.25: Anion analysis of selected "FO" samples

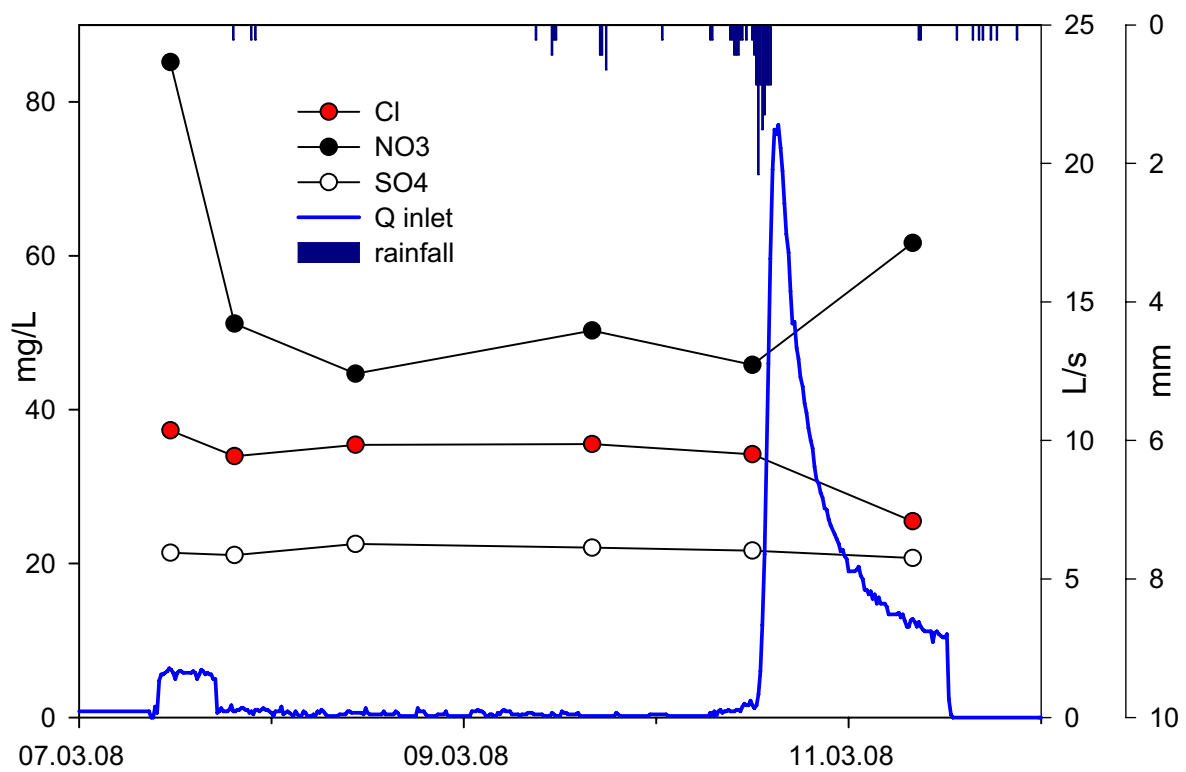


Figure 5.26: Anion analysis of selected "FM" samples

Cations

Additionally, the cations Na, K, Mg, and Ca were analyzed using an ionic chromatograph (*LC20 Chromatography, Dionex*) at the IHF. Samples for analysis were picked out of the “FO” samples only.

Figure 5.27 shows the result of their cation concentrations. All species show a peak immediately after the tracer injection (when exactly?). Na has been injected directly insofar as amounts are incorporated in UA and SRB. Prior the storm event, the sodium concentration increases slightly as well as magnesium and calcium do so.

Potassium was injected via nitrate as KNO_3 has been applied. Its curve is similar to the one of a tracer breakthrough curve, with one peak due to injection and a second one describing a second input of K during the storm event on March, 10th. Calculating the recovery of K yields 56.2% including the storm event and 54.5% excluding it.

Dilution effects over the hydrograph are obvious during the storm event for Na, Mg, Ca as well as the electric conductivity. The curve for Calcium concentration is close to the progression of the electric conductivity.

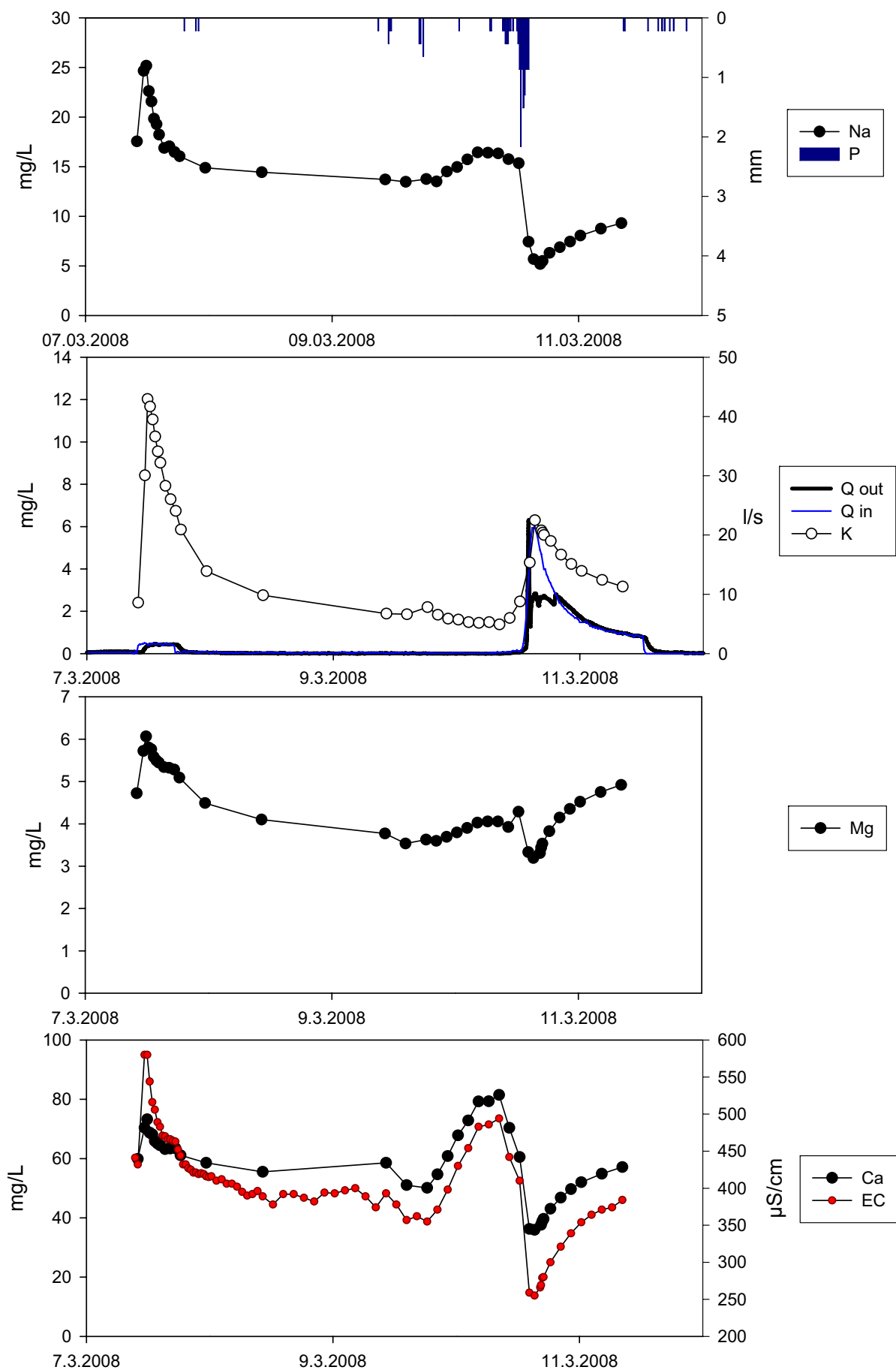


Figure 5.27: Result of cation analysis of selected FO samples

5.3.3.2 Discussion

Ion concentrations in water are influenced by multiple processes. All analyzed ions show high concentrations after the tracer injection, either due to opening and hence flushing of the forest plot or due to direct injection by tracer application.

In investigations by FEYEN ET AL. (1999), the flushing hypothesis could be confirmed. In their study, the upper soil layer was enriched in nitrogen which was then flushed by intense rainfall. Thus, nitrate losses during high flow conditions could be observed. In general, FEYEN ET AL. (1999) suggested two important rapid processes controlling the runoff chemistry during high flow periods which are ion exchange and leaching. Slow processes are usually mineral dissolution and uptake of nutrients by plants and micro organisms controlled by diffusion processes in the rhizosphere. But during fast flow processes like in this study, the residence time in the vadose zone is too short to allow such uptake.

Despite the flushing hypothesis, the concentration of nitrate increases during the storm event. HYER ET AL. (2001) investigated the variation of several substances during runoff processes. They also observed an increase in NO_3 during heavy rainfall as it was injected as ammonium nitrate applied on fields. The elevated nitrate signal lagged several hours behind the other elevated constituents, which is similar to the behaviour of nitrate in this study. Thus, a second anthropogenic input flushed from the fields is also possible. Nitrate is usually used as a contaminant tracer already being in the environment. In a former study of JOB & ZÖTL (1969) sodium nitrate was injected and easily recovered due to lower sorptivity.

Forests act as nitrogen sinks and infiltration was discovered to be a key factor controlling N pollutant removal from surface runoff (LOWRANCE & SHERIDAN 2005), but clayey soils are not effective referring to this (VERCHOT ET AL. 1997).

The peak in chloride concentration could be also due to flushing of the inlet ditch, as there was still NaCl of the applied salt tracer from the previous experiment. The second increase prior the storm event is questionable. This increase is also observable for Mg, Na, Ca and therefore EC. As there was some rainfall during March, 9th, this increase could be either due to remobilization and exchange processes or to a time delayed flow path.

Sulphate increases after injection probably because of the sulphur content in SRB. There is one sample with a concentration of almost zero which seems to be an error in analysis as the other analyzed samples show fairly constant concentrations.

SCHOEN ET AL. (1999) reported that anions behaved faster than other tracers due to anion exclusion. Cations undergo cation exchange, e.g. K preferably substitutes Ca and Mg. In their study, anions acted conservative with a recovery close to 100% but they also noted that in

clayey soils anions might not be good tracers. If a reactive anion (e.g. nitrate) is used, it should be associated with a conservative tracer (e.g. bromide), which was missed out in this study.

Recoveries for anions and cations are not reliable as too many processes influence their concentration in the aqueous phase. E.g., aluminium (Al^{3+}) occurring in clay minerals is replaceable by magnesium (Mg^{2+}), leading to a negative charge which can be filled by potassium (K^+). Hence, the recovery of potassium in this study is rather low, both including and excluding the storm event, because it has already gone to sorption processes. Thus, they should be regarded censoriously. For instance, LEITE (1985) observed highest potassium losses in soil indicating that this element is most leachable and mobile. The cation exchange capacity at the study site ranges between 17-23.6 cmol/kg depending on the depth as the CEC is directly linked to clay content and organic matter.

Peaks for all analyzed cations can be observed after opening, but their input cannot be estimated as input due to tracer injection as well as other sources are possible.

5.3.4 Discussion and Conclusion

In this multi tracer approach, the calculation of the recovery rates of UA, SRB and IPU is reasonable. Figure 5.28 and Figure 5.29 show the recovery rates for the two dye tracers and the pesticide at “FO” and “FM”, respectively.

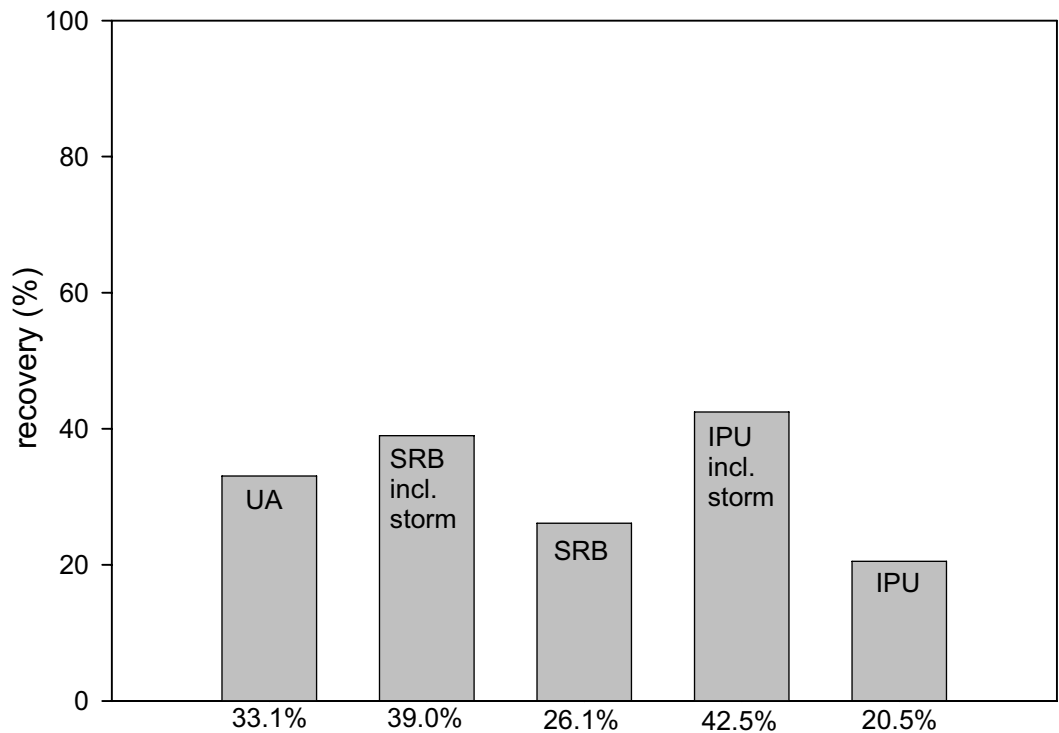


Figure 5.28: Tracer recoveries at "FO"

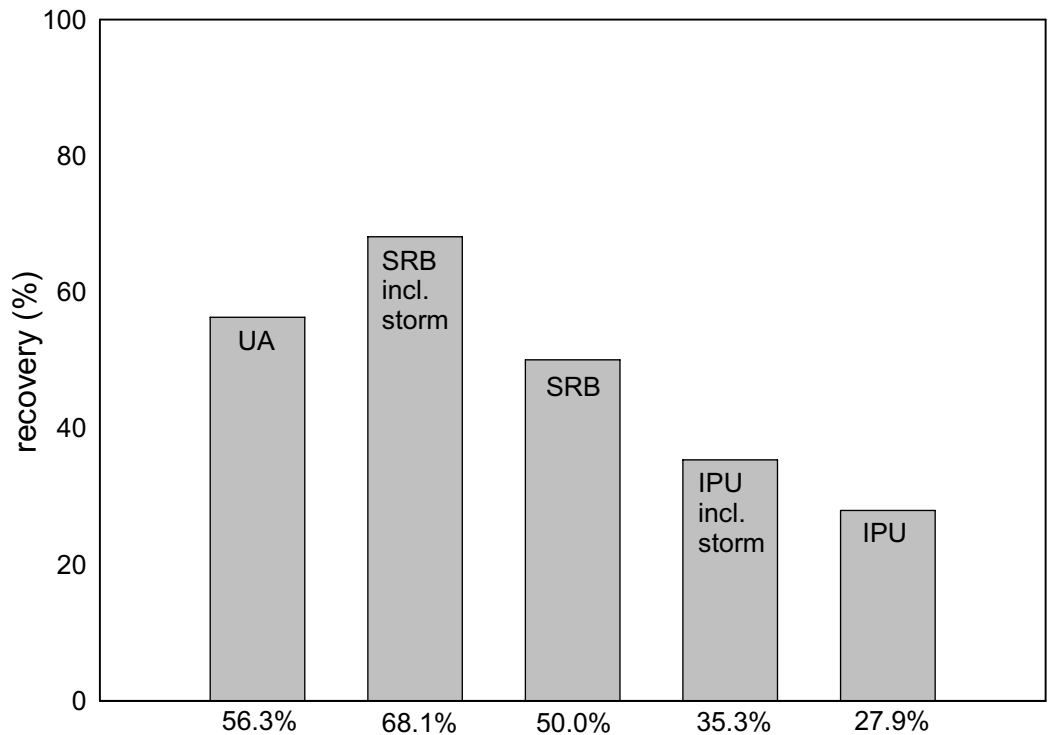


Figure 5.29: Tracer recoveries for "FM"

In general, the forest plot seems to provide an adoptable retention capacity of the dye tracers and the pesticide, leading to fairly small recovery rates.

It can be seen that the recoveries at “FM” are smaller than at “FO”, because “FM” was located directly after the inlet ditch. Especially the part of the forest plot between “FM” and “FO” is efficient for retention as it was the most untouched part showing litter cover and partially humus accumulation.

During the storm event, runoff was observed in all downslope directions of the forest plot. In total, 17% of the inflow did not reach the outlet and was not detected by the electromagnetic flowmeter. As saturation was reached the loss is assumed to be surface flow. Hence, all recoveries are underestimated.

It is obvious that IPU behaves different compared to the breakthrough curves of UA and SRB, event though it was injected at the same time. But data has to be regarded censoriously as the peak is not totally documented and only few samples were analyzed leading to a smaller temporal resolution than the for dye tracers. Its recovery of 42.5% indicates that sorption is an important occurring process. As the recovery of SRB is 39% and hence similar to IPU it is assumed to be sorbed, too, despite the fact that it was in the ditch in visible concentrations until the storm event. Only 33.1% of UA was recovered, but it is assumed to be destroyed by light as the experiment lasted from 07.03.2008-11.03.2008. UA concentrations could not be determined for the storm event, probably because its concentration was lower than the detection limit. By comparison, the recovery of potassium is higher due to leaching or exchange processes. Anyway, cations do not suit as tracer.

Retention is expected to be higher if tracer experiment had been carried out on an unsaturated forest plot due to infiltration capacity. VERCHOT ET AL. 1997 reported that the investigated forest buffers were ineffective during the winter and spring when the waterfilled pore space exceeded 25 to 35% and infiltration was low. Thus, infiltration is a key factor controlling pollutant removal from surface runoff, indicating that buffers in clayey soils may not be as effective as sandy coastal plain soils (VERCHOT ET AL. 1997).

DANIELS AND GILLIAM (1996) report that the combination of grass and riparian forest filters could reduce nutrient runoff loads by 50 to 80% (depending on nutrient and its characteristics, 50% for nitrate).

Velocities between the dye tracers and IPU cannot be discussed as the peak in IPU concentration is not completely documented.

Overall, the hydraulic retention time of 6.6 h is too short to allow mitigation due to plant uptake, diffusion or mineralization. The influence of common oak on pesticide mitigation is not yet studied and probably low, but vegetation was little in March, anyway.

The low dispersion coefficient suggests that the transport of chemical compounds mainly takes place by surface flow. Especially during the storm event surface flow led to washout of the injected tracers UA, SRB, IPU and NO₃. SCHULZ (2004) describes this effect as a hydrological dilemma: Heavy rainfall constitutes storm runoff, leading to a large water volume within a short time. This water volume may not be retained by any sort of buffer strip resulting in unavoidable pesticide contaminations of surface water. This flush out has been reported in numerous studies (e.g. VELLIDIS ET AL. 2002, WU ET AL. 1983). Hence, the tracer experiment results presented in this study are comparable to the functioning of the forest plot under natural conditions, including the possibility of heavy rainfall after pesticide application.



Figure 5.30: Locations forest outlet ("FO") and forest middle ("FM") on March, 10th, after the rainfall event.

6 Conclusion and Outlook

To determine the pesticide mitigation efficiency of the forest plot, a multi-tracer experiment was carried out. Only 39% and 42.5% of the two sorbend compounds SRB and IPU were recovered. UA was photo degraded and only 33.1% of the applied amount reached the forest outlet, but conservative tracers should be additionally used in further experiments. Despite these low recoveries and the fact that the mean residence time of the tracers was only 6.6 h, the first flush effect remains a serious problem. Desorption of IPU is also possible, hence it is not degraded leading to a time delayed risk.

Concerning the objective of the interflow investigations, the piezometer and soil moisture results did not bring up evaluable data. A further experiment has been planned regarding interflow processes on a micro-plot scale by isolating a soil block as this method was established in previous studies. Finally, this experiment was cancelled as the soil system at Bray is not suitable for interflow processes. Due to the heavy clayey soils, surface flow is expected to be the major runoff component if soils are not drained anyway.

The data obtained in the first experiment affirm overland flow during the tracer experiment as the water level recorded by the divers in “PA” and “PH” was above surface elevation.

Additionally, the dye tracer breakthrough curves do not indicate different flow paths as interpretable from EC data at the outlet. Also the other peaks in EC remain unexplained. Calculations of the peak velocities did not lead to specific conclusions. Only few studies have directly investigated the importance of different catchment flow paths and there is a lack of catchment-scale studies regarding the individual transportation of components (NG & CLEGG 1997, HYER ET AL. 2001, FEYEN ET AL. 1999, FENELON & MOORE 1998).

Overall, the forest plot demonstrates an inexpensive and easy manageable facility to mitigate pesticide transport into surface water, but the use of forest plots is restricted because they are not as easily constructed as artificial wetlands.

In this case dug trenches were found in the forest plot enforcing surface runoff through channels. This should be avoided because channelized flow is not conducive to sediment deposition. Sediments adsorb pesticides, thus sedimentation as well as subsurface flow through the vadose zone should be enhanced (LOWRANCE 1998). The residence time should be as long as possible to allow the uptake by plants and micro organisms (FEYEN ET AL. 1999).

This study corroborates the importance of runoff events soon after application as already reported in various studies (e.g. VELLIDIS ET AL. 2002, ARORA ET AL. 1996, LOWRANCE & SHERIDAN 2005).

VELLIDIS ET AL. (2002) observed that the variability in the retention is due to variability among events in amount of infiltration. Thus, infiltration is a key process and should be considered in prospective studies. The infiltration capacity of the forest plot at Bray is assumed to be low. This is indicated by high runoff coefficients caused by the low permeable clayey soil. Also VERCHOT ET AL. (1997) noted that infiltration controls the pollutant removal from surface runoff and that clayey soils counter this process.

Sorption of pesticides depends primarily on organic matter and clay. FARENHORST (2006) claims that organic matter is even the single most important soil constituent which affects the sorption of pesticides. Hence, the soil organic carbon coefficient K_{OC} is essential for estimating the mobility of a chemical compound and its prevalence of leaching from soil. The K_{OC} is directly related to the dimensionless partition constant K_d which is directly measurable by conducting batch experiments. In further investigations, such batch experiments should be considered. Carrying out tracer experiments regarding a system's mitigation efficiency, it would be expedient to use tracers with a similar K_{OC} . A good understanding of the interaction between soil organic matter and pesticides is important and could be helpful in risk assessment at a large scale. Transport from agricultural fields into the broader environment is typically performed at large scales such as across soil series, agricultural fields, watersheds, or regions. Furthermore, sorption partition coefficients are among the most sensitive parameters in models (e.g. PRZM (pesticide root zone model), LEACHM (leaching estimation and chemistry model), TOXSWA) (FARENHORST 2006). Even though lots of modelling is done to estimate pesticide leaching and transport, field studies are not compensable. There are only few reports about such measurements and the behaviour of IPU in watersheds is still not understood.

According to the review of SCHULZ (2004) small catchments are more susceptible for pesticide pollution. Thus, future monitoring programs should include catchments of small size and long-term monitoring could help avoiding unexpected long-term ecosystem effects. An idea to investigate different flow paths in catchment-scale regarding their pesticide transport could be long-term monitoring of different components which are also useful for an end-member-mixing-analysis (EMMA) (HYER ET AL. 2001). Another idea for further investigations could be taking samples in piezometers to see whether there is pesticide

transport in shallow groundwater, but still the use of piezometers in clayey soil remains difficult.

LOWRANCE AND SHERIDAN (2005) reported that the combination of a grass buffer and a managed forest was the most effective mitigation system encouraging the combination of buffer zones, but establishing recommendations and guidelines for the construction and management of buffer zones still poses a challenge.

Bibliography

AHUJA, L.R., ROSS, J.D. (1983): Effect of subsoil conductivity and thickness on interflow pathways, rates and sources areas for chemicals in a sloping layered soil with seepage face. *Journal of Hydrology*, Vol. 64, 189-204.

ALCAYDE, G., BROSSE, R., LORENZ, C. AND J., RASPLUS, L. (1980): Val de Loire: Anjou, Touraine, Orléanais, Berry. Guides géologiques régionaux. Eds.: C. Pomerol. Masson, Paris, New York, Barcelona, Milan, 199 p.

ANBUMOZHI, V., RADHAKRISHNAN, J., YAMAJI, E. (2005): Impact of riparian buffer zones on water quality and associated management considerations. *Ecological Engineering*, Vol. 24, 517-523.

APPELO, C.A.J., POSTMA, D. (2005): *Geochemistry, Groundwater and Pollution*. 2nd edition, Balkema Publishers, Leiden, Netherlands, 649 pp.

ARORA, K., MICKELSON, S.K., BAKER, J.L., TIERNEY, D.P., PETERS, C.J. (1996): Herbicide retention by vegetative buffer strips from runoff under natural rainfall. *Transactions of the ASEA*, Vol. 39, 2155-2162.

ARTWET (2008):

<http://www.artwet.fr/pages.jsp?idTheme=4011&idRub=1244&rubSel=1244&idsite=592>

Research site description on the official ARTwet website, 20.6.2008, 15:09

BEVEN, K. AND GERMANN, P. (1982): Macropores and Water Flow in Soils. *Water Resources Research*, Vol. 18, 1311-1325.

BLOEMEN, W. (1980): Calculation of hydraulic conductivities of soils from texture and organic matter content. *Z. Pflanzenernähr. Bodenk.*, 43, 581-605.

BOULDIN, J.L., FARRIS, J.L., MOORE, M.T., COOPER, C.M. (2004): Vegetative and structural characteristics of agricultural drainages in the Mississippi Delta landscapes. *Environmental Pollution*, Vol. 132, 403-411.

BOULDIN, J.L., FARRIS, J.L., MOORE, M.T., SMITH JR., S., COOPER C.M. (2006): Hydroponic Uptake of Atrazin and Lambda-cyhalothrin in *Juncus effuses* and *Ludwigia peploides*. *Chemosphere*, Vol. 66, 1049-1057.

BOULDIN, J.L., FARRIS, J.L., MOORE, M.T., SMITH JR., S., STEPHENS, W.W., COOPER, C.M. (2005): Evaluated fate and effects of atrazine in lambda-cyhalothrin in vegetated and unvegetated microcosms. *Environmental Toxicology*, Vol. 20, 487-498.

BRGM (2008): <http://infoterre.brgm.fr/MainTileForward.do>, BRGM France, 24.06.2008, 14:30

BURKEN, J.G., SCHNOOR, J.L. (1996): Phytoremediation: plant uptake of atrazine and role of root exudates. *Journal of Environmental Engineering*. Vol. 122, 958-963.

CEMAGREF: Data and pictures by courtesy of Cemagref, Le Centre d'Antony, Parc du Tourvoie, BP 44, F 92163, Antony Cedex.

COSBY, B.J., HORNBERGER, G.M., CLAPP, R.B., GINN, T.R. (1984): A statistical exploration of the relationships of soil moisture characteristics to the physical properties of soils. *Water Resources Research*, Vol. 20, 682-690.

DABROWSKI, J.M., BENNETT, E.R., BOLLEN, A., SCHULZ, R. (2006): Mitigation of azinphos-methyl in a vegetated stream: Comparison of runoff- and spray-drift. *Chemosphere*, Vol. 62, 204-212.

DABROWSKI, J.M., BOLLEN, A., BENNETT, E.R., SCHULZ, R. (2005): Pesticide Interception by Emergent Aquatic Macrophytes: Potential to Mitigate Spray-drift Input in Agricultural Streams. *Agriculture, Ecosystems & Environment*, Vol. 111, 340-348.

DALTON, F.N., VAN GENUCHTEN, M.TH. (1986): The time-domain reflectometry method for measuring soil water content and salinity. *Geoderma*, Vol. 38, 237-250.

DANIELS, R.B., & GILLIAM, J.W. (1996): Sediment and chemical load reduction by grass and riparian filters. *Soil. Sci. Soc. Am. J.*, Vol. 60, 246-251.

DEEKS, L.K., BENGOUGH, A.G., STUTTER, M.I., YOUNG, I.M., ZHANG, X.X. (2008): Characterisation of flow paths and saturated conductivity in a soil block in relation to chloride breakthrough. *Journal of Hydrology*, Vol. 348, 431-441.

DÖRFLER, U., CAO, G., GRUNDMANN, S., SCHROLL, R. (2006): Influence of a heavy rainfall event on the leaching of [¹⁴C]isoproturon and its degradation products in outdoor lysimeters. *Environmental Pollution*, Vol. 144, 695-702.

ERTLI, T., MARTON, A., FÖLDÉNYI, R. (2004): Effect of pH and the role of organic matter in the adsorption of Isoproturon on soils. *Chemosphere*, Vol. 57, 771-779.

ESIS (2008): European Chemical Substances Information System. <http://ecb.jrc.it/esis/> (01.07.2008, 17:23).

EUROPEAN PARLIAMENT (2008): Neue EU-Politik für Einsatz von Pestiziden. Pressebericht zur Abstimmung – Plenarsitzung vom 23.10.2007, Straßbourg. www.europarl.de/presse/pressemitteilungen (29.07.2008 14:00)

FARENHORST, A. (2006): Importance of Soil Organic Matter Fractions in Soil-Landscape and Regional Assessments of Pesticide Sorption and Leaching in Soil. *Soil Sci. Soc. Am. J.*, Vol. 70, 1005-1012.

Fenelon, J.M., Moore, R.C. (1998): Transport of Agrichemicals to Ground and Surface Water in a Small Central Indiana Watershed. *Journal of Environmental Quality*, Vol. 27, 884-894.

FETTER, C.W. (2001): *Applied Hydrogeology*. Prentice Hall, Upper Saddle River, New Jersey. 4th edition, 598 pp.

- FEURTET-MAZEL, A., GROLLIER, T., GROUSELLE, M., RIBEYRE, F., BOUDOU, A. (1996): Experimental study of bioaccumulation and effects of the herbicide isoproturon on freshwater rooted macrophytes. *Chemosphere*, Vol. 32, 1499-1512.
- FEYEN, H., WUNDERLI, H., WYDLER, H., PAPRITZ, A. (1999): A tracer experiment to study flow paths of water in a forest soil. *Journal of Hydrology*, Vol. 225, 155-167.
- FRANKE, C., WESTERHOLM, H., NIESSNER, R. (1997): Solid-phase extraction (SPE) of the fluorescence tracers Uranine and Sulphorhodamine B. *Water Resources Research*, Vol. 31, 2633-2637.
- FREEZE, R.A., CHERRY, J.A. (1979): *Groundwater*. Prentice Hall, Englewood Cliffs, 604 S.
- FRIESEN-PANKRATZ, B., DOEBEL, C., FARENHORST, A., GOLDSBOROUGH, L.G. (2003): Interactions between Algae (*Selenastrum capricornutum*) and Pesticides: Implications for Managing Constructed Wetlands for Pesticide Removal. *Journal of Environmental Science and Health, Part B-Pesticides, Food Contaminants, and Agricultural Wastes*, Vol. 38, 147-155.
- HAARSTAD, K., BRASKERUD, B.C. (2005): Pesticide Retention in the Watershed and in a Small Constructed Wetland Treating Diffuse Pollution. *Water Science & Technology*, Vol. 51, 143-150.
- HAMMER, D.A. (1992): Designing constructed wetlands systems to treat agricultural nonpoint source pollution. *Ecological Engineering*, Vol. 1, 49-82.
- HARRIS, G.L., NICHOLLS, P.H., BAILEY, S.W., HOWSE, K.R., MASON, D.J. (1994): Factors influencing the loss of pesticides in drainage from a cracking clay soil. *Journal of Hydrology*, Vol. 159, 235-253.
- HORNBERGER, G.M., GERMANN, P.F., BEVEN, K.J. (1991): Throughflow and solute transport in an isolated sloping soil block in a forested catchment. *Journal of Hydrology*, Vol. 124, 81-99.

HYER, K.E., HORNBERGER, G.M., HERMAN, J.S. (2001): Process controlling the episodic streamwater transport of atrazine and other agrichemicals in an agricultural watershed. *Journal of Hydrology*, Vol. 254, 47-66.

ISSA, S., WOOD, M., PUSSEMIER, L., VANDERHEYDEN, V., DOUKA, C., VIZANTINOPOULOS, S., GYORI, Z., BORBELY, M., KATAI, J. (1997): Potential Dissipation of Atrazine in the soil unsaturated zone: a comparative study in four European countries. *Pesticide Science*, Vol. 50, 99-103.

JOB, C., ZÖTL, J. (1969): Zur Frage der Herkunft des Gasteiner Thermalwassers. *Steir. Beitr. Hydrogeol.*, Graz 1969, 51-115.

KÄSS, W. (1998): *Tracing Technique in Geohydrology*. Brookfield, A.A. Balkema, 581 pp., 1998.

LEHMANN, O.R., AHUJA, L.R. (1985): Interflow of water and tracer chemical on sloping field plots with exposed seepage faces. *Journal of Hydrology*, Vol. 76, 307-317.

LEIBUNDGUT, CH., MALOSZEWSKI, P., KÜLLS, C. (UNPUBLISHED): *Tracers in Hydrology and Water Research*. Wiley, in preparation.

LEITE, J. DE O. (1985): Interflow, overland flow and leaching of natural nutrients on an alfisol slope of Southern Bahia, Brazil. *Journal of Hydrology*, Vol. 80, 77-92.

LI, Q.X., ALCANTARA-LICUDINE, J.P. (1999): Environmental analysis and fate of photoactive xanthene insecticides. *Recent Research Developments in Agricultural & Food Chemistry*, Vol. 3, 181-190.

LOWRANCE, R. (1998): Riparian Forest Ecosystems as Filters for Nonpoint-Source Pollution. In: *Successes, Limitations, and Frontiers in Ecosystem Science*. Eds.: Pace, M.L., Groffmann, P.M., Springer 1998, New York, 113-141.

LOWRANCE, R., ALTIER, L.S., NEWBOLD, J.D., SCHNABEL, R.R., GROFFMAN, P.M., DENVER, J.M., CORRELL, D.L., GILLIAM, J.W., ROBINSON, J.L., BRINSFIELD, R.B., STAVES, K.W., LUCAS, W., TODD, A.H. (1997): Water Quality Functions of Riparian Forest Buffers in Chesapeake Bay Watersheds. *Environmental Management*, Vol. 21, 687-712.

LOWRANCE, R. & SHERIDAN, J.M. (2005): Surface Runoff Water Quality in a Managed Three Zone Riparian Buffer. *Journal of Environmental Quality*, Vol. 34, 1851-1859.

LOWRANCE, R., TODD, R., FAIL, J., HENDRICKSON, O., LEONARD, R., ASMUSSEN, L. (1984): Riparian Forests as Nutrient Filters in Agricultural watersheds. *BioScience*, Vol. 34, 374-377.

LUCIANI, M.-A. (2007): Fonctionnement d'une zone humide construite: aspects hydrauliques et dimensionnement. Memoire de travail de fin d'étude. Pour l'obtention du diplôme d'ingénieur de l'Ecole Nationale du Génie de l'Eau et de l'Environnement de Strasbourg

MALOSZEWSKI, P. (1994): Mathematical modelling of tracer experiments in fissured aquifers. *Freiburger Schriften zur Hydrologie*, Band 2. Eds.: Leibundgut, Ch., Professur für Hydrologie, 107 pp.

MARIOT, M., DUDAL, Y., FURIAN, S., SAKAMOTO, A., VALLÈS, V., FORT, M., BARBIERO, L. (2007): Dissolved organic matter fluorescence as a water-flow tracer in the tropical wetland of Pantanal of Nhecolândia, Brazil. *Science of the Total Environment*, Vol. 388, 184-193.

MCKINLAY, R.G., KASPEREK, K. (1999): Observations on Decontamination of Herbicide-Polluted Water by Marsh Plant Systems. *Water Research*, Vol. 33, 505-511.

METEOFRANCE (2008):

http://www.meteofrance.com/FR/climat/dpt_tempsdumois.jsp?LIEUID=DEPT37

MeteoFrance, 21.06.2008, 16:00

MON, J. (2004): Sorption and its effects on transport of organic dyes and cesium in soils. Dissertation, Washington State University, Department of Crop and Soil Sciences, 159 pp.

MOORE, M.T., BENNETT, E.R., COOPER, C.M., SMITH JR., S., FARRIS, J.L., DROUILLARD, K.G., SCHULZ, R. (2006): Influence of vegetation in mitigation of methyl parathion runoff. *Environmental Pollution*, Vol. 142, 288-294.

MOSLEY, M.P. (1982): Subsurface flow velocities through selected forest soils, South Island, New Zealand. *Journal of Hydrology*, Vol. 55, 65-92.

NEMETH-KONDA, L., FÜLEKY, G., MOROVJAN, G., CSOKAN, P. (2002): Sorption behaviour of acetochlor, atrazine, carbendazim, diazinon, imidacloprid and isoproturon on Hungarian agricultural soil. *Chemosphere*, Vol. 48, 545-552.

NG, H.Y.F., AND CLEGG, S.B. (1997): Atrazine and metolachlor losses in runoff events from an agricultural watershed: the importance of runoff components. *Science of the total Environment*, Vol. 193, 215-228.

OBBINK, J.G. (1969): Construction of piezometers, and method of installation for ground water observations in aquifers. *Journal of Hydrology*, Vol. 7, 434-443.

POMEROL, C. (1980): *Geology of France. Guides géologiques régionales*. Eds.: C. Pomerol. Masson, Paris, New York, Barcelona, Milan, 256 pp.

REICHENBERGER, S., BACH, M., SKITSCHAK, A., FREDE, H.-G. (2007): Mitigation strategies to reduce pesticide inputs into ground- and surface water and their effectiveness; A review. *Science of the total Environment*, Vol. 384, 1-35.

RENAUD, F.G., BROWN, C.D., FRYER, C.J., WALKER, A. (2004): A lysimeter experiment to investigate temporal changes in the availability of pesticide residues for leaching. *Environmental Pollution*, Vol. 131, 81-91.

ROUSSEAU, D.P.L., VANROLLEGHEM, P.A., DE PAUW, N. (2004): Model-based design of horizontal subsurface flow constructed treatment wetlands: a review. *Water Research*, Vol. 38, 1484-1493.

SAXTON, K.E., RAWLS, W.J., ROMBERGER, J.S., PAPENDICK, R.I. (1986): Estimating generalized soil-water characteristics from texture. *Soil Sci. Soc. Am. J.*, Vol. 50, 1031-1036.

SCHOEN, R., GAUDET, J.P., BARIAC, T. (1999): Preferential flow and solute transport in a large lysimeter, under controlled boundary conditions. *Journal of Hydrology*, Vol. 215, 70-81.

SCHULZ, R. (2004): Field studies on exposure, effects, and risk mitigation of aquatic nonpoint-source insecticide pollution: a review. *Journal of Environmental Quality*. Vol. 33, 419-448.

SCHULZ, R., HAHN, C., BENNETT, E.R., DABROWSKI, J.M., THIERS, G., PEALL, S.K.C. (2003): Fate and Effects of Azinphos-methyl in a Flow-Through Wetland in South Africa. *Environmental Science & Technology*, Vol. 37, 2139-2144.

SMART, P.L., LAIDLAW, I.M.S. (1977): An Evaluation of Some Fluorescent Dyes for Water Tracing. *Water Resources Research*, Vol. 13, 15-33.

SPITZ, K., MORENO, J. (1996): A practical guide to groundwater and solute transport modelling. Wiley, 461 pp.

SUDO, M., NISHINO, M., OKUBO, T. (2006): Decrease in herbicide concentrations and affected factors in lagoons located around Lake Biwa. *Water Science & Technology*, Vol. 53, 131-138.

TIETJE, O., HENNINGS, V. (1996): Accuracy of the saturated hydraulic conductivity prediction by pedo-transfer functions compared to the variability within FAO textural classes. *Geoderma*, Vol. 69, 71-84.

TROMP-VAN MEERVELD, H.J., McDONNELL, J.J. (2006): Threshold relations in subsurface stormflow: 2. The fill and spill hypothesis. *Water Resources Research*, Vol. 42, W02411, doi:10.1029/2004WR003800.

URL1:<http://www.biophysica.com/conductivity.htm> Measuring water conductivity. 02.07.2008, 10:10

URL2:

www.mygeo.info/landkarten/frankreich/Frankreich_Landkarte_Topographie_Staedte.png

05.07.2008, 16:03

VAN GENUCHTEN, M.TH., KAVEH, F., RUSSELL, W.B., YATES, S.R. (1989): Direct and indirect methods for estimating the hydraulic properties of unsaturated soils. In: Land Qualities in Space and Time. Eds.: Bouma, J., Bregt, A.; Proc. Symp. ISSS, 1988, Wageningen.

VELLIDIS, G., LOWRANCE, R., GAY, P., WAUCHOPE, R.D. (2002): Herbicide Transport in a restored Riparian Forest Buffer System. Transactions of the ASEA, Vol. 45, 89-97.

VELLIDIS, G., LOWRANCE, R., GAY, P., HUBBARD, R.K. (2003): Nutrient Transport in a Restored Riparian Wetland. Journal of Environmental Quality, Vol. 32, 711-726.

VERCHOT, L.V., FRANKLIN, E.C., GILLIAM, J.W. (1997): Nitrogen Cycling in Piedmont Vegetated Filter Zones: I. Surface Soil Processes. Journal of Environmental Quality, Vol. 26, 327-336.

WAUCHOPE, R.D., YEH, S., LIDERS, J.B.H.J., KLOSKOWSKI, R., TANAKA, K., RUBIN, B., KATAYAMA, A., KÖRDEL, W., GERSTL, Z., LANE, M., UNSWORTH, J.B. (2002): Review. Pesticide soil sorption parameters: theory, measurement, uses, limitations and reliability. Pest Management Science, Vol. 58, 419-445.

WERNLI, H.R. (2003): Einführung in die Tracerhydrologie. Geographisches Institut der Universität Bern, Labor. Script, 120 pp.

WGSHS (2003): Working Group of the Swiss Hydrogeological Society: Application of artificial tracers in hydrogeology – Guideline. Bulletin d'Hydrogéologie, N° 20.

WORRALL, F., PARKER, A., RAE, J.E., JOHNSON, A.C. (1997): A study of the sorption kinetics of Isoproturon on soil and subsoil: the role of dissolved organic carbon. Chemosphere, Vol. 34, 87-97.

WU, T.L., CORRELL, D.L., REMENAPP, H.E.H. (1983): Herbicide runoff from experimental watersheds. *Journal of Environmental Quality*, Vol. 12, 330-336.

ZEHE, E., FLÜHLER, H. (2001): Preferential transport of isoproturon at a plot scale and a field scale tile-drained site. *Journal of Hydrology*, Vol. 247, 100-115.

Appendix



Figure A 1: The inlet ditch of the forest plot prior injection and after injection of the tracer cocktail.



Figure A 2: Surface flow in the forest plot after the storm event.



Figure A 3: Surface flow in the forest plot.



Figure A 4: Surface flow on the adjacent field and at the outlet of the forest.



Figure A 5: Functioning of the forest plot in July 2008 (CEMAGREF).

Ehrenwörtliche Erklärung

Hiermit erkläre ich, dass ich die Arbeit selbständig und nur unter Verwendung der angegebenen Hilfsmittel angefertigt habe.

Datum, Unterschrift